David Tinarwo

Design of Village Power and Micro-Grids for Rural Areas of Zimbabwe with Specific Attention to Voltage Regulation on Low Voltage Meshed Distribution Grids

kassel university press

This work has been accepted by the faculty of Electrical Engineering and Computer Science of the University of Kassel as a thesis for acquiring the academic degree of Doktor der Ingenieurwissenschaften (Dr.-Ing.).

Supervisers:

Prof. Dr.-Ing. Jürgen Schmid
Dr. rer. nat. Thomas Degner

Defense day: 10th November 2008

Bibliographic information published by Deutsche Nationalbibliothek
The Deutsche Nationalbibliothek lists this publication in the Deutsche Nationalbibliografie; detailed bibliographic data is available in the Internet at http://dnb.d-nb.de.

Zugl.: Kassel, Univ., Diss. 2008
ISBN print: 978-3-89958-636-7
ISBN online: 978-3-89958-637-4
URN: urn:nbn:de:0002-6371

Printed by: Unidruckerei, University of Kassel
Printed in Germany

Vorwort

Diese Arbeit beinhaltet die Machbarkeitsstudie für den Einsatz von erneuerbaren Energiequellen in Bauernhöfen in Zimbabwedie habe gemacht und meiner Tätigkeit als wissenschaftlicher Mitarbeiter am Institut für Solare Energieversorgungstechnik (ISET) e. V., Kassel. Sie wurde durch das Projekt "More Micro-Grids" (Contract No: SES6-019864) gefördert. Mein herzlichster Dank gebührt dem Leiter des Instituts für Solare Energieversorgungstechnik (ISET), Herrn Prof. Dr.-Ing. J. Schmid, für die mir gegebene Möglichkeit, meine Promotion beim ISET durchzuführen und für die hilfreiche Betreuung, und DAAD und UniKassel für die Financierung von mein studim. Mein besonderer Dank gilt Herrn Dr. rer.nat. T. Degner für die hilfreiche Betreuung, nützliche Hinweise und Anregungen bei der Abfassung dieser Arbeit.

Herren Dr.-Ing. B.M. Valov, Dr. M. Vandenberg und Dipl. Ing. D. Geipel möchte ich recht herzlich für die Hilfe mit Experimenten im Labor (DeMoTec), seinen gute Zusammenarbeit sowie einen Beistand danken. Von Zimbabwe möchte ich recht herzlich für die Information von Ländliche Elektrifizierung die hat mir gegeben Herr E. Midzi (C.E.O. Rural Electrification Agency), Herr Thole der Manager von Rosenwald Milchwirschaft / Viehfarm, Dr. Edward Chikuni und Dr. Zivayi Chiguvare von University of Zimbabwe und Frau J. Muguti von Department of Energy Zimbabwe, und allen die haben mir in eine weg oder andere.

Weiterhin danke ich allen Mitarbeitern des Instituts ISET für die hervorragende Zusammenarbeit, insbesondere mein spezieller Dank geht zu Herrn Dipl. Ing. P. Funtan, für seine brüderliche Sorgfalt wärend der Zeit, die ich in Deutchland gewesen bin.

Nicht zuletzt möchte ich meiner späten Mutter für ihre anspornenermutigung, meine Frau Oripar sowie meinen Söhne David, Donewell und Dowell, und mein Vater für ihren Geduld und Unterstützung danken. Der familiäre Rückhalt war notwendig für das Gelingendieser Arbeit.

Kassel, im 14. October 2008

David Tinarwo

Dedication

First and for most I dedicate this work to my late mother Mrs Eunice Tinarwo who passed away on 17th of August 2008 during my final days of the thesis. I say to her, “May your soul rest in peace and you inspired me to continue working to promote the use of sustainable energy in the poor rural communities”. To my beloved sons, David (jnr), Donewell and Dowell, my wife Oripar, and my father, I thank you for your encouragement.

Abstract

This work constitutes a feasibility study of the use of renewable energy resources in rural farming villages in Zimbabwe. A case study was done for a farming village consisting of a dairy farm called Rosenwald with 627 dairy cows and surrounded by local villagers offering manpower labour for the dairy activities. The village setup presents great opportunities for a sustainable power supply system in the form of village power system using the powerful microgrid concept since the farm is already connected to the national grid but with great problems of reliability, which is already a national problem if not regional due to the worst economics crisis facing the country coupled with the present regional power shortage experiencing the whole Southern Africa region. With the intended on-farm energy generation, the energy services are to be extended to the surrounding villages. Thus the study aims to stimulate better focus to the use of locally available renewable energy resources at bigger scales starting from the disadvantaged communities in the rural areas. The focus is put to these rural farming communities because these could be a strong force in the speedy electrification of the poor communities surrounding them. This could be more viable given the already existing business activities in these farms. So in this thesis the study of the on-farm energy generation using the farm and animal waste has shown that such communities can be totally independent from the electric grid by using the locally available resources. Here the technologies assessed are the biogas and solar and all the evaluation of the designs, choice of components and their suitable sizes was done with the help of a micropower optimization model HOMER simulation programme from National Renewable Energy Laboratory available at their website www.nrel.gov/homer. From the assessment done for the case study farm, it was shown that an electricity price of EUR 0.26/kWh is possible from the on – farm energy generation scheme. The results of the simulations showed that the biogas without solar could be most cost effective. In the studied case a great potential of self reliance in terms of energy for the community has been demonstrated. The thesis also looks at some technical aspect of such systems especially when interconnected in different topologies, for example when parallel connected via medium voltage system and also when these are connected in mesh topology in the low voltage. Aspects such as active power sharing, reactive power exchange among these microgrids voltage regulation were studied. Particular attention was given to the study of voltage regulation in low voltage meshed networks using the method of reactive power injection. The method was demonstrated both experimentally and by simulation in ATP - EMTP (Alternative Transient Programme – Electromagnetic Transient Programme). Also the dynamic operation of a biogas fired microturbine was studied to have a clear knowledge of the operation of this since it is the main generating/conversion component of the proposed system.

Zusamenfassung

Diese Arbeit beinhaltet die Machbarkeitsstudie für den Einsatz von erneuerbaren Energiequellen in Bauernhöfen in Zimbabwe. Die Studie beschäftigt sich mit einem Bauernhof, der eine Molkerei betreibt. Das Anwesen heißt Rosenwald, hat 627 Kühe und beschäftigt die lokalen Dorfbewohner. Rosenwald ist an das nationalen Stromversorgungsnetz angeschlossen und hat mit großen Zuverlässigkeitsproblemen in Bezug auf die Stromversorgungssicherheit zu tun. Der Grund ist die schlechte wirtschaftliche Lage in Zimbabwe, wie auch auf dem im gesamten südafrikanischen Bereich. Trotzdem bietet Rosenwald eine großartige Gelegenheit zum Betreib von erneuerbaren Energiesystemen auf der Basis von Microgridkonzepten. Der Vorteil von Microgridkonzepten liegt darin, auch umliegende Dörfer mit Strom zu versorgen. Ziel dieser Studie ist es, den Einsatz von lokalen erneuerbaren Energiequellen zu fördern und die armen umliegenden Gemeinden mit Strom zu versorgen. Auf Grund des genannten Konzeptes kann die Molkerei besser funktionieren. Diese Arbeit hat die Unabhängigkeit des Bauernhofes vom regionalen Stromnetz untersucht. Die Technologien die zur dieser Untersuchung gedient haben, sind Biogas- und Solarenergiesysteme. Die Auswahl der Komponenten sowie der Entwurf des gesamten Systems wurden mit dem Optimierungsprogramm “HOMMER” durchgeführt, das von dem National Renewable Energy Laboratory zur Verfügung gestellt wird. Die hier vorgestellten Untersuchungen zeigen, dass ein Strompreis von EUR 0,26/kWh möglich ist. Darüber hinaus haben die Ergebnisse der Simulationen gezeigt, dass die Biogasstromerzeugung ohne den Solarbeitrag kostengünstiger wäre. Inhalt dieser Arbeit ist auch der technische Aspekt zum Einsatz von verschiedenen Netzstrukturen auf Niederspannungsniveau. Austausch von Wirkleistung zwischen Microgrids und Spannungsregelung sind andere Aspekte, die in dieser Arbeit untersucht wurden. Ein besonderer Schwerpunkt bildete die Untersuchung der Spannungsregelung in vermaschten Niederspannungsnetzen durch Anwendung des Blindleistungseinspeiseverfahrens. Die Ergebnisse dieses Verfahrens wurden experimentell und durch Simulationen anhand des Programms ATP-EMTP geprüft. Außerdem wurde der dynamische Betrieb einer Biogasturbine untersucht. Dies mit dem Ziel tiefere Kenntnisse über deren Betrieb zu erhalten, da es die Hauptenergiequelle von diesem vorgeschlagenen System ist.

Table of Contents

Chapter 1 **Introduction**

1.1 **Background**

According to IEA - Energy outlook 2004 some 1.6 billion people, about one quarter of the world's population, have no access to electricity today. Eighty percent of these people live in rural areas of the developing world, mainly in South Asia and sub-Saharan Africa where rapid urban migration and population growth will occur over the next several decades [1]. Without adequate supplies of affordable energy, it is virtually impossible to carry out productive economic activity or improve health and education. Poverty becomes inescapable.

The continuing prohibitively high cost of grid extension coupled with the general increase in electricity demand without corresponding increase in generation capacity presently experienced by many developing countries will be the most cohesive factors to the increased future use of locally available renewable energy resources. Although most of these renewable energy technologies are well proven, it is my opinion that their adoption mostly in poor countries has not been accorded their deserving merits. Unlike in developed countries where the use of renewable energy has reached relatively high commercial levels, in the poor developing countries these are still used as an option to supply energy to the remote and low energy demand locations without access to the utility grid. However, due to still relatively high capital costs involved in these technologies the donor or government dependence of the intended end users - poor communities is inevitable.

Among many reasons, the slow market response of the renewable energy sector in the developing countries could, on one side be attributed to lack of complete and active involvement and lack of basic technical preparation for the operation and maintenance of the installed systems on the part of the end-users resulting in high system failures. On the other hand government policies on renewable energy and other socio-economic factors related to customs and culture play a significant role.

In other cases wrong designs and wrong component sizing of the systems have also lead to unsatisfactory performance and hence confidence in these technologies badly eroded. However, with

some concerted efforts put to address the mentioned issues and others, the potential to electrify a significant percentage, if not the whole of the remaining approximately one quarter of the world population through these technologies is still enormous.

Due to the intermittent nature of most renewable energy sources, as has already been demonstrated, hybrid power systems may constitute the most economically feasible solution that provides a more reliable supply of electricity in this context. These can be in the form of island grids or grid connected systems. The systems can even be more affordable if communities could come together in coordinated groups and mobilise resources towards funding community power projects such as forming the so-called *village power systems.* These systems may even be more viable if the villages practise some economic activities like farming. In many African countries like Zimbabwe most commercial farmers are grid connected, but, however, in most cases the villages surrounding the farms or even the farm workers have no access to electricity. The author thus strongly believes such communities may serve as starting points of fast and sustainable rural electrification. Here the villagers can be motivated to form some organized groups to mobilise resources for the purpose of village power system formation.

The widespread and combined application of the concept of these village power systems and the recently emerged Micro-Grids concept to the remote village electrification schemes will bring together all their individual advantages and accelerate the move to achieve the goals of clean and sustainable energy to all in the near future.

1.2 **Motivation and statement of the problem**

The motivation to this work are the difficulties poor communities have in accessing clean energy in the present environment of exorbitantly high prices for fossil fuels coupled with tremendous increase in power demand worldwide leaving many developing countries in a very difficulty situation. For example in the southern part of Africa, the regional giant power producer, South Africa has started cutting power supply to its neighbouring countries due to the acute domestic shortages [2]. The scenario is expected to worsen unless the respective governments take alternative strategies to deal with the problem. In this scenario a country like landlocked Zimbabwe, going through the worst

economic crisis characterised by more than seven-digit inflation rate and has to import more than 35 % of its electricity [3] and 100 % of its petroleum needs would be worst affected. In response to this the Zimbabwe government has embarked on such projects like the National Bio-diesel Project aimed at significantly cutting down the foreign currency expenditures on natural diesel. On electricity, there are a number of PV projects scattered around the country, but, due to their high initial capital requirement the questions of affordability and sustainability are still hindering the progress and replication of such project. So, it is my feeling that the country has big and still unexploited potential from other renewable energy resources that can be relatively better affordable and more sustainable. The farming sectors produce vast quantities of animal and plant waste that can be converted to energy in form of heat and electricity and in some cases the by-products from these generation processes can substitute the much needed chemical fertilizers for the crop farming. Sewage treatment in the cities, food processing industries and even the boarding schools can contribute highly to cover the electricity deficit the country is having. These technologies have not yet received the deserved merits in the country's energy sector, especially for the purpose of generating electricity at relatively as high a level as covering the respective farm's energy demand, or feeding excess to the national grid and extending to surrounding villages. The reason to this unpopularity may be due to lack of clear demonstration of the technical feasibility and economical viability of these technologies. Thus this work aims to answer the following questions:

1. Is it economically viable to use the available agricultural wastes in the farms in rural Zimbabwe to generate the electricity?
2. Which technologies are appropriate and cost effective for these purposes?
3. Are the systems technically feasible?
4. Finally of what social benefit could these systems be?

This way the thesis demonstrates the enormous potential some communities have of producing enough power for their use and even contribute to the national demand in a sustainable manner. So in this way the work will assess the economic viability and technical feasibility of farming village power systems in the form of Micro-Grid as could be applied to rural villages in Zimbabwe. The available resources are assessed and a design of a suitable power system is presented. Some technical aspects concerning their interaction when interconnected in simple parallel and mesh topology are assessed. In particular reactive power exchange and active power sharing is assessed for the Micro-Grids connected via a medium voltage system. A new method of voltage regulation by reactive

power injection in low voltage grids with droop controlled inverters is practically tested in laboratory. It is hoped that this work would save as a reference to interested stakeholders in the common fight to increase the country's electricity generation capacity.

1.3 Main focus and scope of the thesis

This thesis aims at evaluating the possibility to generate electricity from biogas in a profitable way in a case study dairy farm in Zimbabwe. The objectives of this are:

1. To calculate the costs and benefits of running an on-farm biogas plant

After evaluating the electricity production I then calculate the money that the farmer can earn and save by selling the energy and reducing the bill.

The other aspect looked at in this work is interaction of similar power systems when connected in different topologies. Here the objectives are:

2. To study power sharing among Micro-Grids via medium voltage lines

More than two Micro-Grids are connected via medium voltage system, reactive power exchange and active power sharing among the Micro-Grids is assessed during the operation of the system. The aim here is to see how this sharing depends on the line parameters.

3. To regulate voltage in meshed low voltage networks by a method of injecting reactive power

Here three microsources (droop controlled battery inverters) are connected in a triangular form to represent the simplest form of mesh network and voltage at two of the generator nodes are regulated by injecting reactive power from the third microsource.

4. To measure the start-up and shutdown time of a grid tied biogas fired microturbine

Lastly the start-up and shutdown process for a biogas fired microturbine were tested. This test was aimed at obtaining this information to see its suitability in backup function where uninterruptible power supply is needed.

1.4 Methodology

Due to the nature of this study, I started by reviewing literature related to the energy situation in Zimbabwe. During the field work study I collected recent and unpublished information from the different government departments of the country that include Department of Energy in the Ministry of Energy and Power Development, Ministry of Science and Technology, Rural Electrification Agency (REA), Zimbabwe Electricity Regulatory Commission (ZERC), Agricultural Research And Extension Services (*Arex*), and from farmers and some of their unions. I interviewed three farm managers and a number of the farm workers from the three farms from which I collected data on the farming activities, number of animals and energy demand. To bring awareness and involve the different stakeholders, I organized a three-universities joint seminar of Bindura University of Science Education (my university and host), University of Zimbabwe and Chinhoyi University of Technology to which farmers, Department of Energy in the Ministry of Energy and Power Development, Ministry of Science and Technology, Rural Electrification Agency (REA), Zimbabwe Electricity Regulatory Commission (ZERC), Agricultural Research And Extension Services (Arex), and from farmers and some of their unions were represented.

The data collected from the field work was then analyzed and a power system designed. For the evaluation of the designs, choice of components and their suitable sizes a micropower optimization model HOMER from National Renewable Energy Laboratory available at their website www.nrel.gov/homer was utilised. The study involved a lot of practical testing of some power system configurations in the Design-Centre for Modular Supply Technology (DeMoTec) and the common microsources. The microsources measured are the CHP working on rape seed oil and a biogas fired microturbine.

1.5 Outline of the thesis

The thesis has several chapters. In Chapter 1 the background to the study is outlined and leading to the motivation and statement of the research problem. Here the main focus and scope of the thesis are laid out leading to the outlining of the objectives of the study. The chapter concludes with the presentation of the methodologies employed and the outline of the thesis. Chapter 2 reviews the

country – Zimbabwe energy situation. This starts with a brief country introduction and an overview of the history of the power sector. Reviewed also in this chapter is the renewable energy resource in the country. Chapter 3 is dedicated to the Micro-Grid concept, the droop control mechanism of the voltage source inverters and the voltage and frequency control in both high and low voltage grids. Also closely reviewed here are the two Micro-Grids control strategies, that is, the Single Master Operation (SMO) and Multi Master Operation (MMO) in island mode of operation. Chapter 4 presents the results of the experimental studies of load sharing among Micro-Grids via medium voltage system. In chapter 5 the results of the experimental study of the voltage regulation by injecting reactive power to the generator nodes are presented. Chapter 6 presents the case study of a rural farming village in Zimbabwe. The chapter presents the socio-economic aspects, energy demand and resource data of the village. Designs of power systems are presented and their feasibility assessed using an optimising computer simulation in Homer designing software. Finally the most optimal design is proposed and its operation strategy described. In this chapter technical aspects of the microturbine technology are also presented, in particular the test measurement done on the microturbine in operation at an Agricultural Training Institute at Eichhof is presented. Here of major focus was the dynamic operation of the microturbine, start up, shut down, ramp up and ramp down times. Then the thesis concludes with chapter 7 which summarises the results of the study.

Chapter 2 **Energy situation in Zimbabwe**

2.1 **Country introduction**

Zimbabwe is a landlocked Sub-Saharan country with a total area of 390 757 km^2, comprising 386 670 km^2 of land and 4 087 km^2 of water with a population of about 13,3 million inhabitants according to Population Reference Bureau mid-2007 statistics (see PRB website[1]). For 2007 (according to CIA – World Fact Book last update 24 July 2008, see website[2]), the per capita gross domestic product was US$200 based on 2007 purchasing power parity estimates. The country is surrounded by Mozambique to the east, South Africa to the south, Zambia to the north and Botswana and Namibia to the west (see Figure 2-1). The country is endowed with abundant mineral resource, agriculture, tourism natural resources and a highly skilled workforce. The economy is agro – based and has magnificent and well – diversified infrastructure.

Zimbabwe is endowed vast mineral resources like coal, gold, platinum, copper, nickel, tin, clay, and numerous metallic and non-metallic ores (see Figure 2-2) with coal reserves estimated at 26 billion tons, but have no oil reserves. Coal – bed methane was recently discovered and the deposits are believed to be the largest natural gas fields in Eastern and Southern Africa estimated at 500 million cubic metres of gas. There are many uses of coal - bed methane, which include electricity generation, which should come in handy considering the forecast regional electricity shortage by 2007. The hydroelectric potential on the Zambezi River is estimated at 37 TWh per annum. Fuel wood resources cover about 20% of the land area. The solar potential is relatively high with an average radiation of 2 100 kWh/m^2/year, but wind potential is negligible.

[1] http://www.prb.org/Countries/zimbabwe.aspx

[2] https://www.cia.gov/library/publications/the-world-factbook/geos/zi.html

Figure 2-1 The map of Zimbabwe showing its neighbouring countries [4]

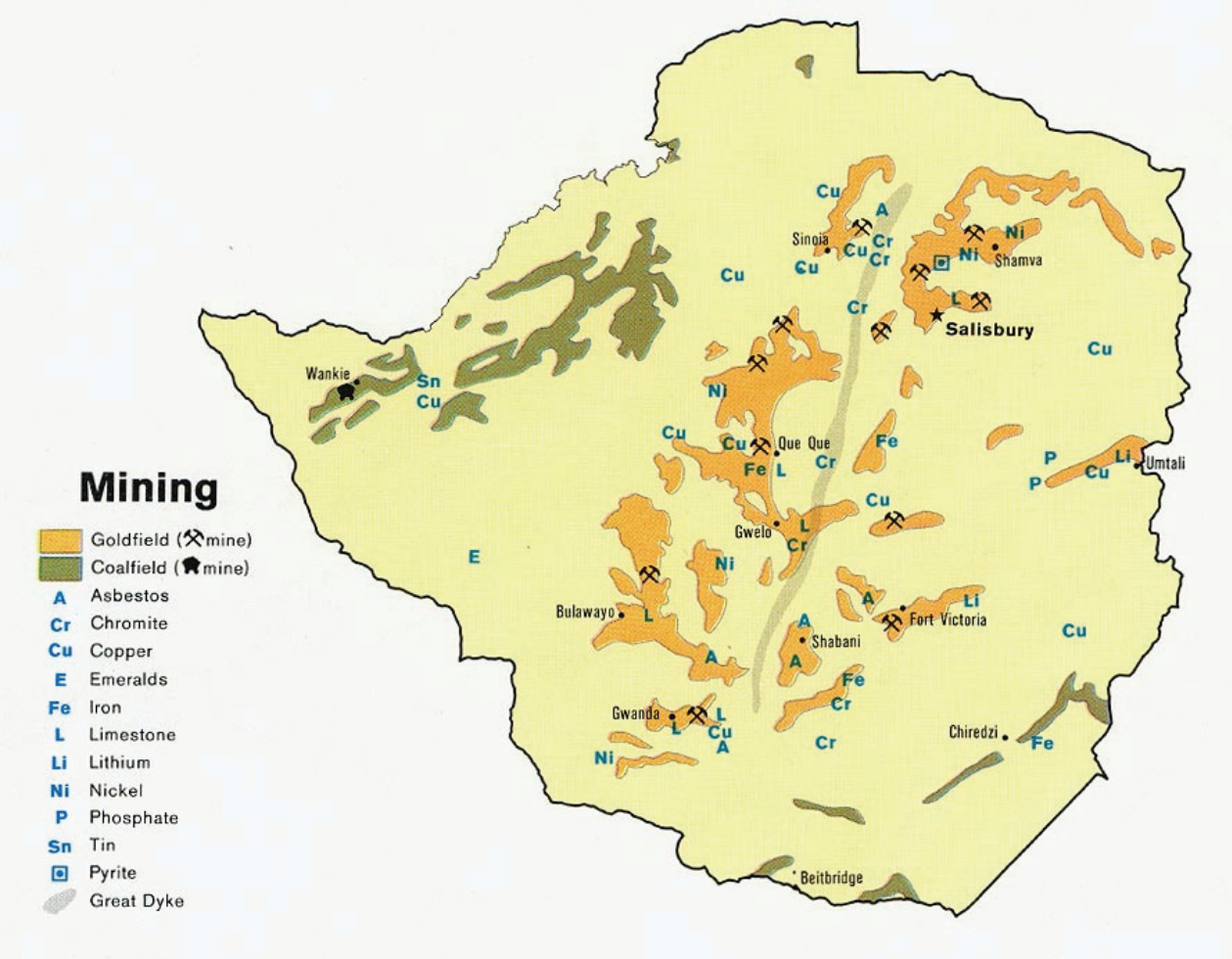

Figure 2-2: The map of Zimbabwe showing its mineral fields [5]

2.2 **Energy situation in Zimbabwe**

The country major energy resources are coal, fuel wood, hydro-electricity and petroleum fuels. According to the national energy balance of 2000 [6], fuel wood provides the bulk (53%) of the total energy supply, followed by coal (20%), liquid fuels (14%) and electricity (13%). Coal bed methane exploitation is still in the planning stages. Energy consumption has grown at an average rate of about 3.5% per annum since 1990. Access to electricity is estimated nationally at nearly 40%, but access to electricity in the rural areas of the country is much lower, at about 19%.

2.2.1 The history of power sector in Zimbabwe

Electricity generation in Zimbabwe in the period before 1993 was dominated by hydro generation with a smaller share covered by thermal from coal. The other sources like oil, gas, combustible renewable and waste and geothermal, solar and wind insignificantly contribute or practically do not contribute to the generation of electricity (as can be seen these have no share in the graph of Figure 2-3) Since the early eighties the Kariba Power Station (the biggest hydro power generation station in the country) has been affected by drought and the flows into the lake have been progressively low, resulting in a critical fall in levels which almost rendered the station in-operable in 1992/93. The drought resulted in change of preference towards thermal plants (as shown by greater area in purple colour on the graph of Figure 2-3 after 1993) which are less affected by poor rains. The graph has been taken from [1] as it is, so other fuels although indicated on the legend of the graph are not used for the purpose of electricity generation in the case of Zinbabwe.

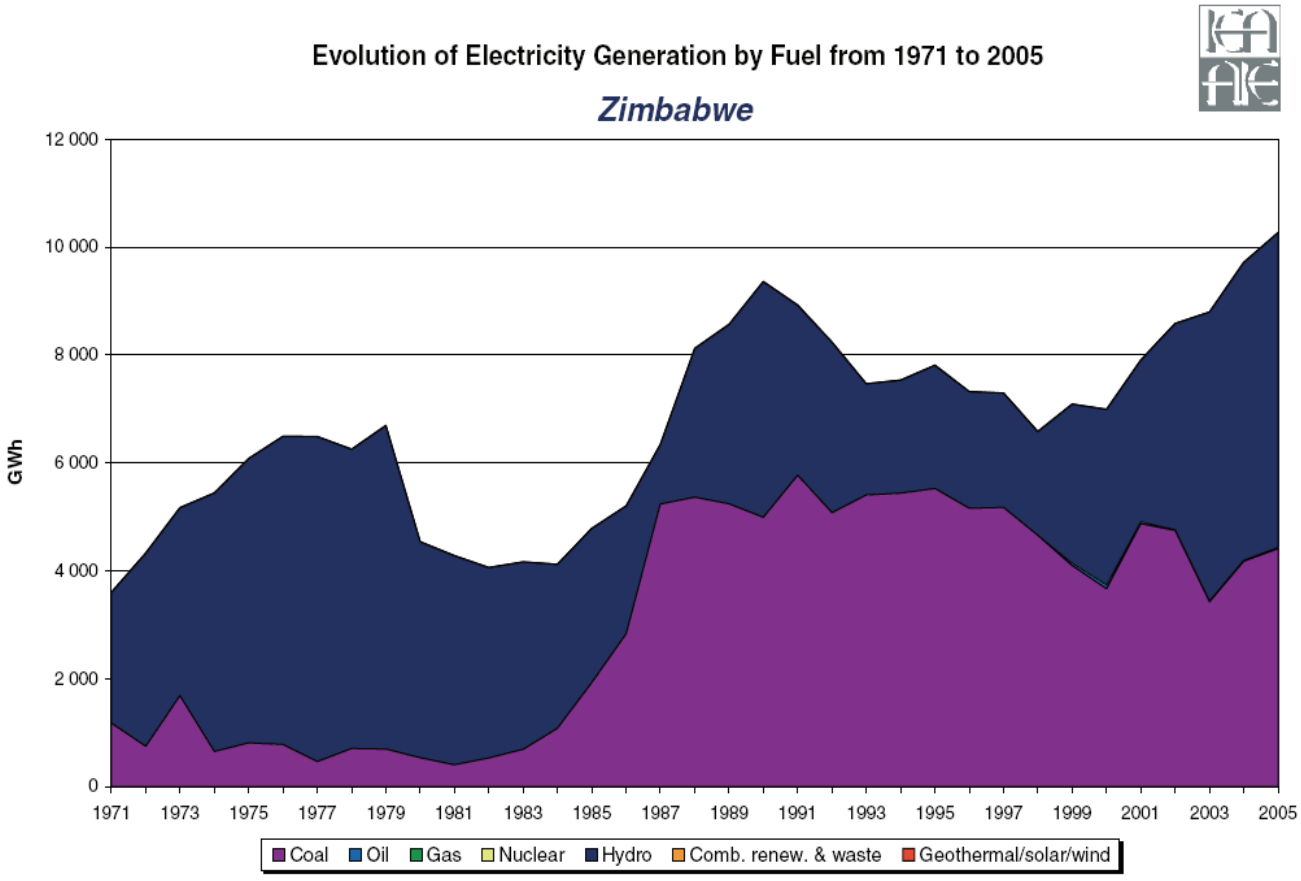

Figure 2-3: Evolution of electricity generation by fuel from 1971 to 2005 in Zimbabwe [Source:NON-OECD/IEA 2007, [1]]

The Zimbabwe Electricity Supply Authority (ZESA) has been responsible for the generation, transmission and distribution of electricity in Zimbabwe. It had five major power stations, with a total capacity of 1,920 MW [7] as shown in Table 2-1. Coal plants contribute a combined total capacity of 1,170 MW while hydro generates only 750 MW. However, Zimbabwe is currently facing a shortage of electrical energy due to generation shortfalls and has to import about 40 % of its electricity requirements from neighbouring countries, including the Democratic Republic of Congo, Mozambique, Zambia and South Africa (of which the shares are shown in Table 2-2). These large power imports constitute a significant foreign currency outflow that is straining on the foreign currency situation in the country.

Station	Kariba	Hwange	Harare	Bulawayo	Munyati	Total
Plant type	Hydro	Coal	Coal	Coal	Coal	
Capacity (MW)	750	920	80	90	80	1,920
Available Capacity(MW)	500	760	55	85	75	1,475
Net energy generated (GWh)	2,998	4,809	22	48	44	7,926
Plant load factor (%)	64.61	47.66	3.44	6.50	5.42	49.18
Efficiency (%)	91.42	27.80	20.18	20.91	18.38	53.77

Table 2-1 Overview of internal electricity supply in Zimbabwe, Sources: [7]

Country	Interconnection Voltage (kV)	Maximum Capacity (MW)	Available Capacity (MW)
Mozambique	400	500	500
South Africa	400	500	150-500
Zambia	330	700	100-200
DR Congo	(to Zambia) 220	250	150

Table 2-2: Zimbabwe's power imports, Source: [7]

2.2.2 Electrification levels

Due to a number of government initiated reforms in the power sector, access to electricity grew from 20 to 39 % between 1991 and 1999 [7] and to 42 % between 1999 and 2001, [8]. The diagram of Figure 2-4 shows electrification access in Zimbabwe for the rural (blue), urban (yellow) and the national (red) sectors. In the period after 2003, ZESA was connecting on average 21,839 new domestic consumers every year [9]. Greater emphasis has been placed on rural electrification, as reflected in the Rural Electrification Charter of 2002 whereby ZB$ 24 billion (US$436,4 / Eur461,6 million at an official rate of Zim$55/US$ and Zim$52/Euro[3] in 2002 using conversion rates from [10] (see footnote), then was to be devoted to rural electrification under a five-year project. By end 2003, about 100 rural centres were being electrified per month by this initiative [9]. This as a result has increased the demand of electricity disproportional to the generation capacity, hence further increasing the dependence on imports.

[3] In 2002 on average 1USD was changed at 1,057856 EUR according to the U.S. / Euro Foreign Exchange Rate Monthly Averages of daily figures Noon buying rates in New York City for cable transfers payable in foreign currencies. Date Range:1999-01-01 to 2008-07-01 from Board of Governors of the Federal Reserve System http://research.stlouisfed.org/fred2/data/EXUSEU.txt

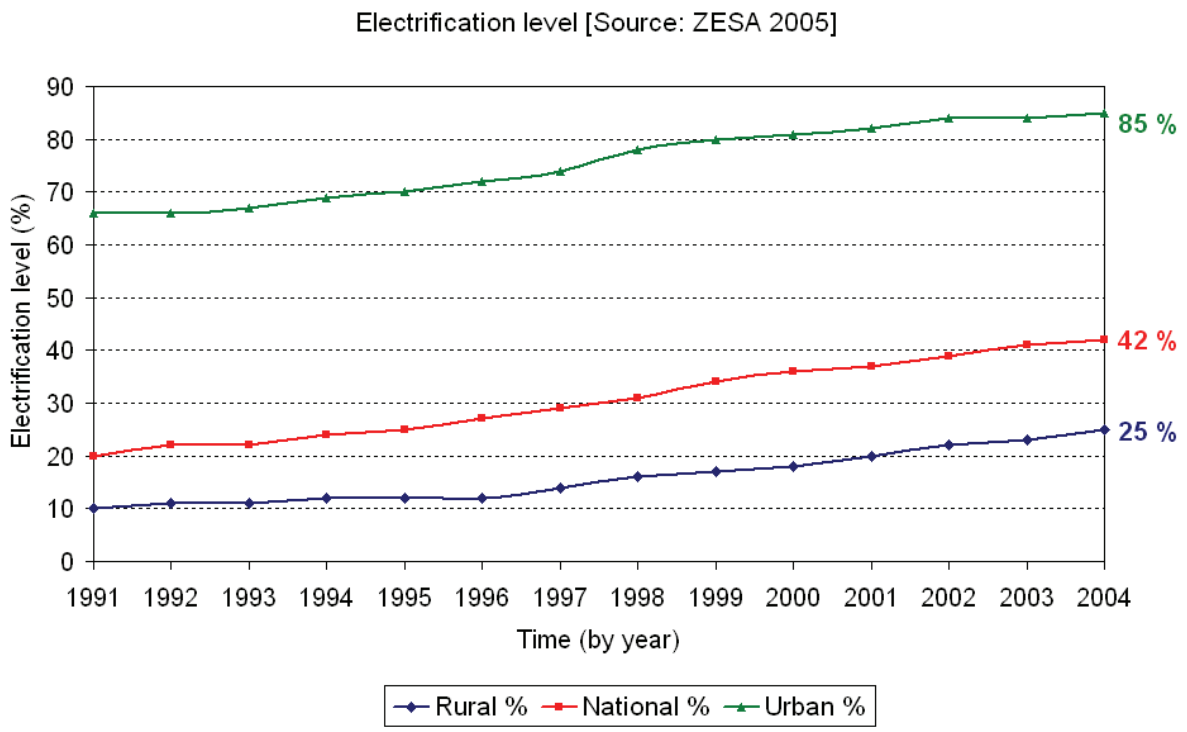

Figure 2-4: Electrification access in Zimbabwe in rural (blue), urban (yellow) and the national (red) sectors, Source: [11]

Now with the difficult economic situation in the country the power utility is presently embarking on heavy load shedding which is seriously affecting many sectors of the economy. However, some of these sectors have the potential to generate their own electricity and easy the pressure on the national grid and even capable of feeding the excess to it. These potential sectors can be even more effective if they can cluster together as interconnected Micro-Grids which in addition to feeding excess energy to the grid share this among themselves even at relatively long distances as demonstrated experimentally in the next chapters of this thesis. So the next section looks at the resource availability in the country.

2.3 Renewable energy resource in Zimbabwe

2.3.1 Solar energy

Like many countries close to the equator Zimbabwe has a relatively high solar potential with an average of 2100 kWh/m^2/year. The country's involvement in the solar Photovoltaic (PV) technology dates back to the early 1980s where a number of pilot projects were implemented. Major PV projects implemented in the 1990s include the German Technical Cooperation (Deutsche Gesellschaft für technische Zusammenarbeit - GTZ) funded solar water pumping for domestic consumption, and Global Environment Facility (GEF)/United Nations Development Programme (UNDP) solar home systems project which saw according to estimates as of 2001 about 85,000 SHSs in the country, making it the country with the largest number of such systems in the continent [12]. The latter attracted a lot of attention from other donors as it coincided with the chairmanship of the President of Zimbabwe R. G. Mugabe, to the World Solar Summit in 1996.

However, as reported in [12] the performance of the installed systems were not pleasing. For example, about 30 % of the GEF project SHSs had failed just two years after installation. In general, it was observed that donor-funded projects were more prone to failure than privately implemented projects. Reasons for these failures are varied but in short the projects proved unsustainable.

2.3.2 Biomass

Biomass is another potential source of electricity in the country although this has not been accorded the deserving merits. According to a report of studies carried out by African Energy Policy Research Network (AFREPREN) [12] more than 200 biogas plants have been installed around Zimbabwe and have been mainly installed by the Department of Energy. The Appropriate Technology Section of Silveira House (a church-based organisation) and Biomass Users Network (BUN) also actively promoted the use of biogas in rural areas, but without subsidies. However, due to the poor performance of the biogas digesters attributed to the poor construction of rural household biogas digesters, especially at the beginning of the programme and poor maintenance by users resulted in

many of the digesters falling into disuse. Mainly the units are located at schools, rural homes and selected industries and mostly for the purpose of heating. Large-scale modern biogas digesters have also been tried briefly. As early as in the 1980's at Kushinga Phikelela Agricultural Training Institute a modern 80 m^3 turnkey biogas plant of the TOTEM concept (TOTal Energy Module) was installed donated by the Italian Government. This was meant to generate electricity for the Institute's dairy project. In the early 1990's a portable pilot biogas plant was installed at a food-processing factory (Cairns Foods) in Harare by a United Nations Industrial Organisation (UNIDO) / Department of Energy and Cairns Foods pilot project. The purpose of this project was to demonstrate the potential of using agro-industrial wastes (potato and coffee) for generation of biogas and stabilising organic waste. However the project is said to have not convinced industry to attempt full scale implementation [12]. The fact that biogas digesters demand considerable management input has led to wholesale abandonment, especially by families. The majority of biogas digesters were *welfare* type installations, with an insignificant minority of owners paying the full price for their installations and most of the installations were *not for income generation* purposes.

The vast livestock population (see Table 2-3) in Zimbabwe offers great potential of using biogas from the animal waste for electricity generation. In addition municipalities in all the major cities in the country lose a lot of methane at their sewage treatment digesters by just venting it to the air.

In the south of the country there are two sugarcane-crushing mills that use more than 1.3 million tonnes of bagasse to generate electricity used by the sugar factories [12]. In addition to the electricity the estate also produces alcohol (about 40 million litres per year), silage as fertilizer and cattle feed.

Wood is still the most important domestic fuel in the country. It is the major source of energy for cooking, lighting and heating for over 70% of population.

Livestock	Communal area	Resettlement area	Small scale Commercial area	Large scale commercial area	Total no. Of animals	Dung amount [kg/(unit livestock-day)	Total dung Per day in tonnes/day
Cattle	302991	165280	185422	1436143	2089836	40	83593,440
Pigs	111970	9056	57444	118474	296944	1,5	445,416
Sheep	319774	8240	2028	83290	413332	0,5	206,666
Goats	2281908	19601	72601	Not available	2374110	0,5	1187,055

Table 2-3 Livestock population in Zimbabwe and dung potential, Source: [13]

2.3.3 **Micro and Mini hydro**

Great micro and mini hydro potential exists in the eastern highlands of the country, for example unconfirmed potential of more than 10 MW exists along the two big rivers, Rusitu and Nyahode. There are also several stand-alone mini-hydro schemes with small capacities around the country (Table 2-4). These schemes have been put up with financial assistance from donor agencies and Non-Governmental Organisations (NGOs) such as the Intermediate Development Technology Group (ITDG) and Environment and Development Activities (ENDA) Zimbabwe. Rusitu power project (750 kW) was the first and only small hydropower plant to be developed as an Independent Power Producer (IPP) and connected to the national grid. The project was commissioned in June 1997 and has been selling power to ZESA.

Name	Capacity(kW)	End Use
Svinurai	20	Electrification of households
Mutsikira	25	Drives a hammer mill, water pump for irrigation, a saw and a grinder
Aberfoyle	25	Electrification of households
Nyafaru	40	Electrification of households
Kwenda	74	Water pump for irrigation
Kwenda	80	Water pump for irrigation, electrification of households
Claremount	250	Electrification of households
Rusitu	750	Electrification of households

Table 2-4: Mini-Hydro Sites in Zimbabwe, Source:[7]

2.3.4 **Wind**

As a landlocked country, Zimbabwe does not have very large wind resources when compared to countries with long coastlands and flat landscapes. In the whole country there has not been any recorded place with an annual mean speed of 5 m/s. Thus it would not be economical attractive to engage in much wind project for the purpose of electricity generation. However there are a few sites on the electricity generation from wind. The best use of this kind of wind speed would be water pumping by windmills.

2.4 **Conclusions**

From the review of the Zimbabwean energy situation it is clear that the country needs to consider a number of energy policy modifications to encourage the exploitation of the abundantly available renewable energy source in the country. The country has great potential not only in such resources as coal which need huge investment to be able to utilize it, but also such that can be exploited at small scale and yet very sustainable like the use of farm waste and hybridize this with PV or wind where possible to make these more reliable and sustainable. Thus the application of the concept of Micro-Grids is very attractive. This concept is reviewed in the next chapter.

Chapter 3 **Micro-Grid concept and the droop control**

3.1 **Introduction**

Over the course of the past century electric power provision has transformed from small independent grids serving just a few customers to complex network served primarily by large generating plants whose power is distributed to customers via a high voltage transmission system and lower voltage distribution systems. With the ever increasing demand of reliability, quality and efficiency of power supply, the conventional unidirectional flow of energy is slowly pointing towards the bi-directional due to the emergence of the so called Independent Power Producer (IPP) or Distributed Energy Resources (DERs) connected to the distribution level of the power system (see Figure 3-1). This renewed interest in distributed energy resources (DERs) has seen the emergence of new and more advanced power systems architectural concepts like “micro-grids”, which can serve a small group of co-located customers [14]. Research has successfully demonstrated the feasibility of Micro-Grids operation through laboratory experiments [15]. This concept is also proving successful from the field reports of projects like the ‘More Micro-Grids’ funded by the European Commission.

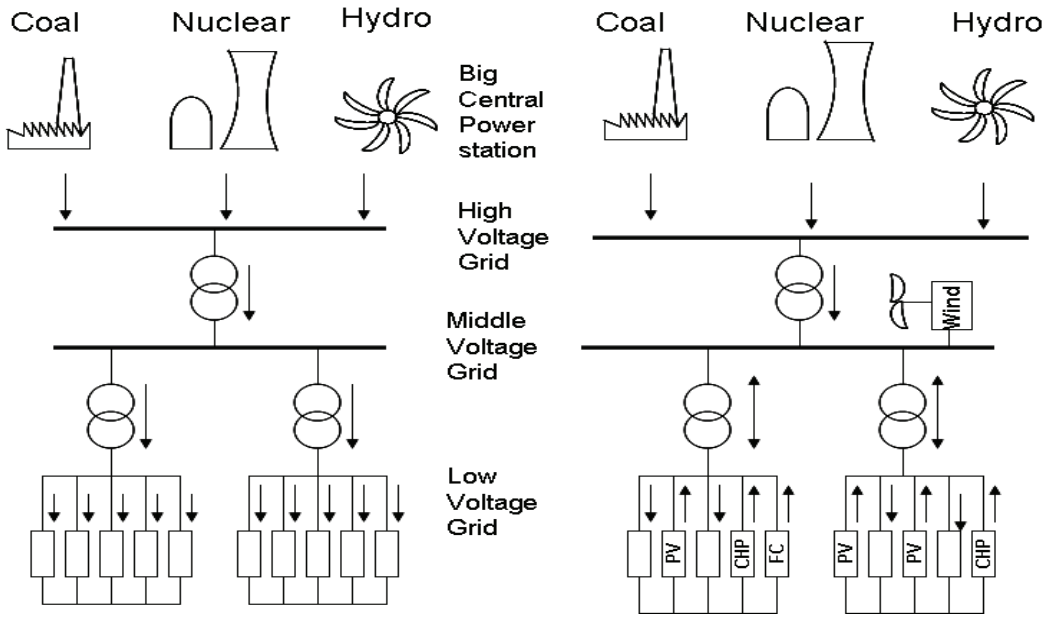

Figure 3-1: Direction of load flow in Electrical energy supply system, left conventional structure without IPP and right structure with IPP, [17]

In this chapter of the thesis a brief outline of the concept of a Micro-Grid is reviewed with emphasis put on the voltage control mechanism. The method of droop control as applied in voltage source inverters (VSI) which form the heart of the Micro-Grid is reviewed, especially when the Micro-Grid operates in island mode.

3.2 Micro-Grid concept review

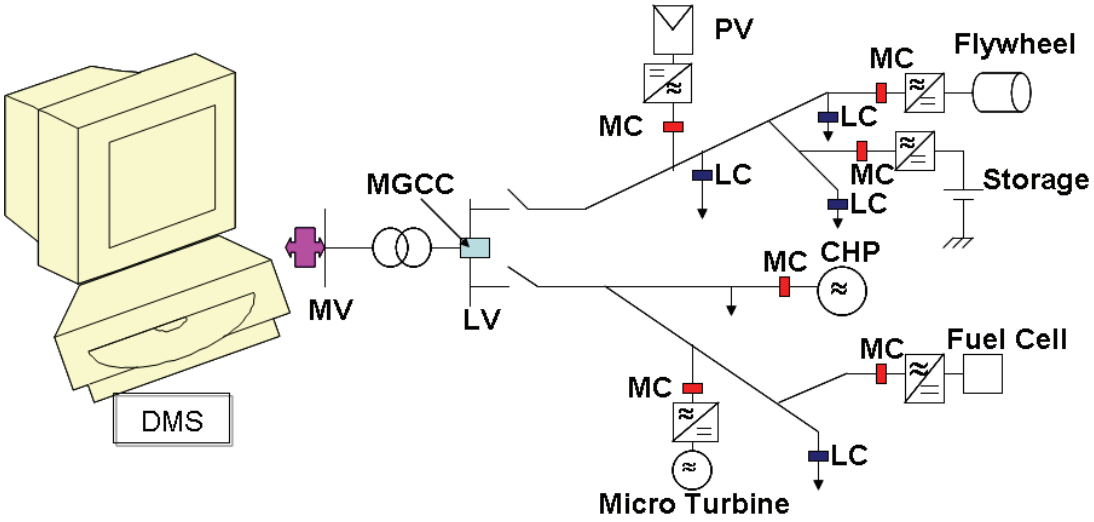

Figure 3-2: Micro-Grid with several microsources with their microsource controllers (MC), loads with their load controllers (LC), showing the Micro-Grid Central Controller (MGCC) connected to the low voltage (LV) side of the transformer and a distribution management system (DMS) on the medium voltage (MV) side [18]

As shown in Figure 3-2, Micro-Grids comprise Low Voltage distribution systems with distributed micro sources (MS) both controllable and uncontrollable, such as micro-turbines, fuel cells, PVs, etc., together with storage devices, i.e. flywheels, energy capacitors and batteries, and loads (some of them interruptible), a hierarchical type management and control scheme supported by a communication system [19]. Such concept has been developed within the framework of the EU R&D Micro-Grids project [19]. In this architecture the Micro-Grid is controlled and managed by a Micro-Grid Central Controller (MGCC) installed at the MV/LV substation. The MGCC possesses several key functions (such as load forecasting, demand side management, economic scheduling of micro generators, security assessment, etc.) and heads the hierarchical control system. In a second hierarchical control level, controllers located at loads or groups of loads – load controllers (LC) and controllers located at the micro sources – micro source controllers (MC) exchange information with the MGCC and control local devices. The whole system operation requires communication and interaction between two sets of devices: LC on one hand, as interfaces to control loads through the application of an interrupt - ability concept, and on the other hand MC controlling micro generation active and reactive power production levels.

Unlike simple low voltage grids with DGs, Micro-Grids have the ability to behave as a coordinated entity in interconnected and islanded operation. However, being dominated by inverter interfaced distributed sources that are inertia-less, Micro-Grids are faced with challenges on issues like management of instantaneous active and reactive power balances, power flow and network voltage profiles. Furthermore the relatively high resistance of the low voltage networks cause more problems of efficient voltage regulation as is explained in the next sections of this chapter. Due to the crucial role of inverters in Micro-Grids a short review of their control models, the PQ and VSI control is first given below.

3.2.1 PQ Inverter Control

A PQ controlled inverter injects into the AC grid the power available at its input terminals. An example of the application of a PQ control is a PV unit, where the DC power produced in the PV array is time-varying and the inverter continuously adapts its output to match the power produced in the PV array. Since the response of the inverter control systems is usually very fast (few milliseconds), the main dynamic behaviour of the primary energy sources has a large influence in the global dynamic behaviour of the Micro-Grid, namely when commands are sent by the MGCC to the primary energy sources of the controllable MS. The reactive power injected by PQ-controlled inverters corresponds to a set point that can be defined locally or centrally in the MGCC.

The PQ control of an inverter can be performed using a current control technique: the inverter current is controlled in amplitude and phase to meet the desired set points of active and reactive powers [20]. In this sense, a PQ controlled inverter is a current source controlled by the variations in the primary energy source to which it is coupled.

3.2.2 Voltage Source Inverter Control

A VSI is controlled in order to feed the load with predefined values for voltage and frequency, according to a specific control strategy – for example the power frequency droop control as described in the next sections. Depending on the load, the VSI real and reactive power output is defined. The control principle of the VSI in this case emulates the behaviour of a synchronous

machine. Thus it is possible to control voltage and frequency on the AC system by means of inverter control. Frequency variation in the Micro-Grid provides an adequate way to define power sharing among several VSIs with different active power/frequency droop parameters since this variation is related with system frequency [21].

3.3 **Active and reactive power flow**

Power flows, both actual and potential, must be carefully controlled for a power system to operate within acceptable voltage limits. Reactive power flows can give rise to substantial voltage changes across the system, which means that it is necessary to maintain reactive power balances between sources of generation and points of demand on a 'zone basis'. Unlike system frequency, which is consistent throughout an interconnected system, voltages experienced at points across the system form a "voltage profile" which is uniquely related to local generation and demand at that instant, and is also affected by the prevailing system network arrangements. Below is a review, as presented in [22] and [23] of the power flow equation leading to the derivation the droop control mechanism applied in the VSIs.

Consider E voltage of a source supplying a load through a line of impedance Z. The power flow into the line at point A, as represented in Figure 3-3, is described as [22] and [23]]:

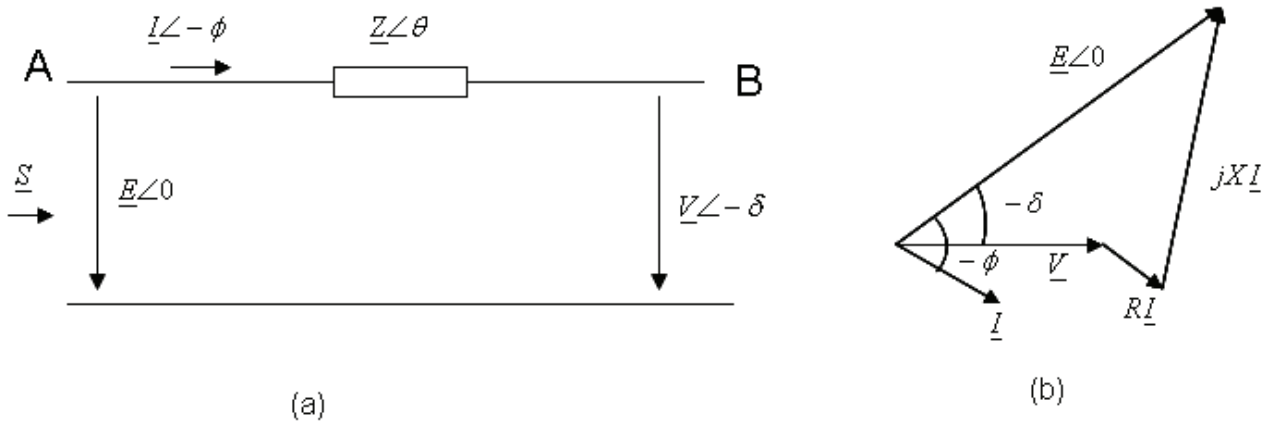

Figure 3-3: (a) Power flow through a line, (b) phasor diagram [22] and [23]

$$P + jQ = \underline{S} = \underline{E}\,\underline{I}^{*} = \underline{E}\left(\frac{\underline{E} - \underline{V}}{\underline{Z}}\right)^{*}$$

$$= \underline{E}\left(\frac{\underline{E} - \underline{V}e^{j\delta}}{\underline{Z}e^{-j\theta}}\right) \qquad [3.1]$$

$$= \frac{E^2}{Z}e^{j\theta} - \frac{EV}{Z}e^{j(\theta+\delta)}$$

S is the apparent power, P and Q the active and reactive powers respectively and ϕ, θ and δ are the corresponding angles of the current phasor $\underline{I}$, complex impedance $\underline{Z}$ and the load voltage phasor $\underline{V}$ taking the source voltage $\underline{E}$ as reference.

That is total apparent power flowing into a line at point A can also be expressed as:

$$S = \frac{E^2}{Z}(\cos\theta + j\sin\theta) - \frac{EV}{Z}[\cos(\theta+\delta) + j\sin(\theta+\delta)]$$

$$S = \frac{E^2}{Z}\cos\theta - \frac{EV}{Z}\cos(\theta+\delta) + j\left[\frac{E^2}{Z}\sin\theta - \frac{EV}{Z}\sin(\theta+\delta)\right]$$

Thus, active and reactive powers flowing into the line are described as:

$$P = \frac{E^2}{Z}\cos\theta - \frac{EV}{Z}\cos(\theta+\delta) \qquad [3.2]$$

$$Q = \frac{E^2}{Z}\sin\theta - \frac{EV}{Z}\sin(\theta+\delta) \qquad [3.3]$$

With $Ze^{j\theta} = R + jX$, thus $Z = \sqrt{R^2 + X^2}$, and $\cos\theta = \frac{R}{Z}$, $\sin\theta = \frac{X}{Z}$ and using the trigonometric identities $\{\cos(\theta+\delta) = \cos\theta\cos\delta - \sin\theta\sin\delta, \sin(\theta+\delta) = \cos\theta\cos\delta + \sin\theta\sin\delta\}$

$$P = \frac{E^2}{Z}\frac{R}{Z} - \frac{EV}{Z}\left[\frac{R}{Z}\cos\delta - \frac{X}{Z}\sin\delta\right]$$

$$P = \frac{E}{R^2 + X^2}[R(E - V\cos\delta) + XV\sin\delta] \qquad [3.4]$$

And

$$Q = \frac{E}{R^2 + X^2}\left[-RV\sin\delta + X\left(E - V\cos\delta\right)\right] \quad [3.5]$$

Equations (3.4) and (3.5) are the general form of the active and reactive power flow for two parallel connected voltage sources in medium voltage grids characterised by both resistive and inductive lines. In the next sections brief explanation of the voltage and frequency control in high and low voltage grids during parallel operation is given.

3.4 Voltage and frequency control in high voltage grids

Voltage and frequency control concept was obtained from the active and reactive power equations. Here the voltage control in high voltage networks, e.g. transmission lines is described. In these networks reactance is much higher than resistance ($X>>R$), the resistance R can be neglected ($R = 0$). The power angle δ in these lines is small and we can assume that cos(δ) = 1 and sin(δ) = δ. Taking into account these simplifications the equations (3.4) and (3.5) can be transformed to the equations (3.6) and (3.7) below.

$$P = \frac{EV}{X}\delta \quad [3.6]$$

$$Q = \frac{E\left(E - V\right)}{X} \quad [3.7]$$

As can be seen from equations (3.6) and (3.7) the power angle is proportional to active power while the voltage difference $E - V$ is proportional to the reactive power. The power angle can be controlled by the generator torque therefore the control of active power P is realized by controlling the frequency setting in the power droop. In the same way, the control of the voltage U is provided by controlling the reactive power Q. Such a way the voltage and frequency can be determined by using the active and reactive power values. This dependence can be expressed in the following linear equations, see equations (3.8) and (3.9). [23]

$$f - f_0 = -k_p\left(P - P_0\right) \quad [3.8]$$

$$U - U_0 = -k_q\left(Q - Q_0\right) \quad [3.9]$$

Where f_0 and U_0 are the nominal frequency and voltage respectively, P_0 and Q_0 the fixed active and reactive powers of the inverter and k_p in Hz/W and k_q in V/VAr are constants of proportionality between active power and frequency change and reactive and voltage change respectively (or frequency droop coefficient and voltage droop coefficient respectively). The above equations constitute the reactive power/voltage and active power/frequency droops for the control of inverters, the so called "Conventional droops", and their graphs are shown in Figure 3-4 [24]

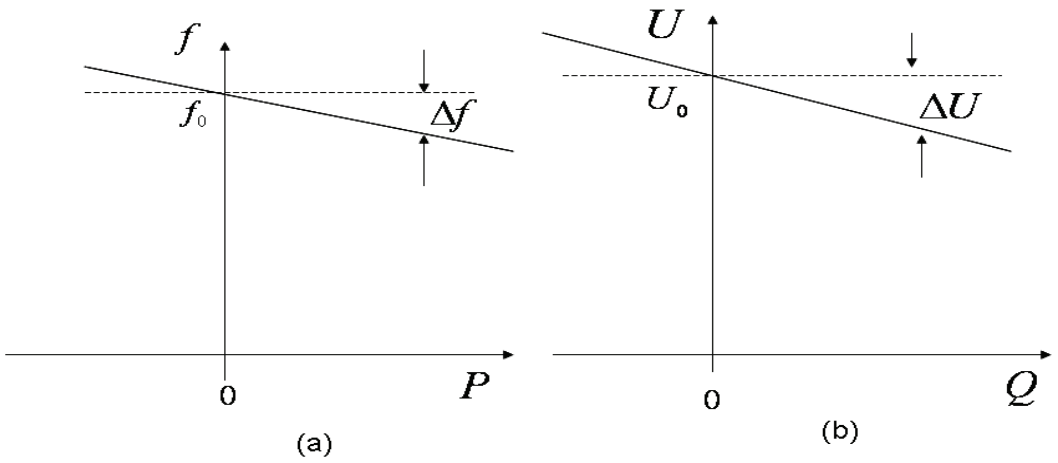

Figure 3-4: Frequency (a) and voltage (b) droop diagrams. Conventional droops. [23]

3.5 **Droop control in conventional power systems**

The droops derived in the previous section are applied in generators with turbines in power plants. These generators work relatively stiff because speed is controlled by a proportional speed governor. Out of a speed deviation it derives a signal for the turbine valve to regulate active power. A reactive power flow affects the grid voltage. Its deviation is the input signal for the proportional excitation controller. By using proportional controllers for these two tasks there are deviations of frequency and voltage which are proportional to the load. Providing active (respectively reactive) power leads to a proportional reduction of frequency (respectively voltage).

The above properties are transferred to inverters, however taking in consideration as stated in [25] that, first the per unit quantity of the output reactance of an inverter is nearly one order smaller, thus a small difference in the output voltage leads to high currents. Second there are no rotating parts with inertia, so frequency and phase angle can change very fast. Third an inverter has not the overload capability of a machine.

A significant difference between a synchronous generator in a power plant and an inverter is that active power can't be controlled by a steam valve or anything similar. For this reason an active power controller is implemented instead of a speed controller and for consistency a reactive power controller instead of an excitation controller. The inverter behaviour is similar to the synchronous machine if the set-point values for the two power controllers are derived from droops [25] like those shown in Figure 3-4.

Based on conventional droops this control concept can be derived from inductively-coupled voltage sources. A voltage source combined with an inductance represents a high voltage line with a stiff grid or a synchronous machine (generator). Here the reactive power is related with the voltage and the active power with the phase shift or respectively with the frequency. The relationship changes with the low voltage line due to its predominantly resistive character, where reactive power is related with the phase shift and active power with the voltage. Nevertheless, the droop concept is still operable due to its "indirect operation" [26].

3.6 Voltage and frequency control in low voltage grids

In low voltage distribution lines the active resistance is much higher than the reactance of the lines ($R >> X$) and therefore the voltage and frequency control principles are different compared to high voltage networks. By analogy with the high voltage networks reactance can be neglected ($X = 0$). The power angle δ is also small and we can assume that $\cos\delta = 1$ and $\sin\delta = \delta$. Taking into account these simplifications the active and reactive power expressed in the equations (3.4) and (3.5) can be written in the forms (3.10) and (3.11).

$$P = \frac{E}{R}(E - V) \qquad [3.10]$$

And

$$Q = \frac{EV}{R}\delta \qquad [3.11]$$

From the equations (3.10) and (3.11) it can be seen that in low voltage lines the voltage difference $E - V$ depends mainly on active power while the power angle δ which represents frequency depends mainly on the reactive power.

The control in low voltage networks is realized by the active power/voltage and reactive power/frequency droops, so-called opposite droops, see Figure 3-5.

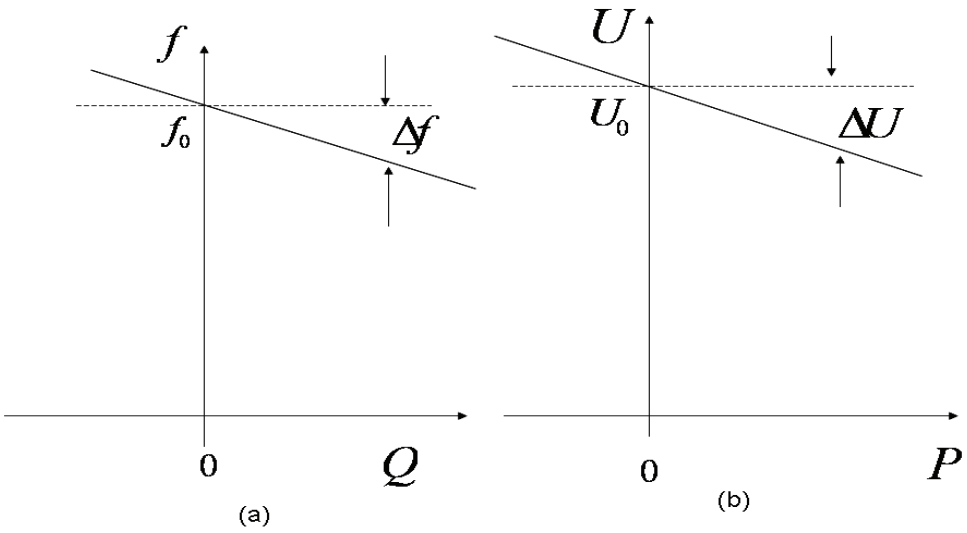

Figure 3-5: Frequency (a) and Voltage (b) droop diagrams. Opposite droops. [26]

From the system's view the major control parameters of the low voltage systems are the voltage control and the active power dispatch. The following table gives a comparison of guaranteeing the major control parameters in conventional and opposite droop controls for the low voltage networks.

	Conventional droop	Opposite droop
Compatible with HV-level	Yes	No
Compatible with generators	Yes	No
Direct voltage control	No	Yes
Active power dispatch	Yes	No

Table 3-1: Comparison of droop concepts for the low voltage level [26]

It was shown in [26] as seen in Table 3-1 that the only advantage of using opposite over conventional droops on the low voltage level is the direct voltage control against three advantages offered by the conventional droop, namely, compatibility with HV-level and generators and active power dispatch. In the low voltage grid the voltage profile is linked with the active power distribution and the reactive power to the phase angle. Thus reactive power is not directly linked to the voltage control. As once indicated earlier, from a system's view the voltage control and the active power dispatch are the major control issues. But if one would control the voltage through active power, no power dispatch would be possible. Each load would be fully supplied by the nearest generator and thus voltage deviations would be present in the grid. However, as has already been indicated using conventional droops results in compatibility with the high voltage level, possibility of power sharing also with rotating generators and a precise power dispatch. Thus as has been shown in [26], in principle the conventional droop method can be applied even in the low voltage grid due to the generator's voltage variability by means of exchanging reactive power. The reactive power of each generator is tuned in a way that the resulting voltage profile satisfies the desired active power distribution. In the same reference [26] operating points of conventional droops in the low voltage grid were derived through the assessment of stability of the simplified power flow equation in the form of equation (3.10) with E, the source voltage substituted by the inverter voltage U_{inv}, the receiving end voltage V by U_{grid} and the power by the inverter power P_{inv}, with R the line resistance.

$$P_{inv} = \frac{U_{inv}^2}{R} - \frac{U_{inv}U_{grid}}{R}$$

Rearranging the above equation for the inverter voltage U_{inv} results in two solutions of the quadratic equation:

$$U_{inv1,2} = \frac{U_{grid}}{2} \pm \sqrt{\frac{U_{grid}^2}{4} + P_{inv} \cdot R} \qquad [3.12]$$

Both solutions have to be taken into account for describing the process. U_{inv1} is a voltage close to the grid voltage and U_{inv2} is a slightly negative voltage. This implies a 180º phase shift. Therefore in Equation (3.13) a factor k is introduced with $k_1=1$ for the first solution and $k_2=-1$ for the negative solution. The factor k takes an approximation of the cos-function.

$$P_{inv} = \frac{U_{inv1,2} - U_{grid}}{R} \cdot U_{inv1,2} \cdot k_{1,2} \qquad [3.13]$$

The inverter power P_{inv} is adjusted by changing the inverter voltage U_{inv} with the reactive power:

$$U_{inv1,2} - U_{grid} = Q_{inv1,2} \cdot q_{droop} \qquad [3.14]$$

This is a function of the angle δ

$$Q_{inv1,2} \approx \delta \cdot \frac{U_{inv1,2} \cdot U_{grid}}{R} \qquad [3.15]$$

δ is got from the integral over time of the generator's frequency difference to the grid as shown in Equation (3.16) below:

$$\delta = \int \Delta f dt \qquad [3.16]$$

And Δf is given by Equation (3.17):

$$\Delta f = (P_{set} - P_{inv}) \cdot p_{droop} \qquad [3.17]$$

The integral character of this process ensures the above-mentioned precise power distribution. Merging Equation (3.13) to (3.17) and solving for P_{inv} results in:

$$P_{inv} = \int P_{set} - P_{inv} dt \cdot \underbrace{\frac{p_{droop} \cdot q_{droop} \cdot k_{1,2} \cdot U_{grid} \cdot U_{inv1,2}^2}{R^2}}_{=C} \qquad [3.18]$$

This describes a first order lag with the solution:

$$P_{inv} = P_{set}(1 - e^{-C \cdot t}) \qquad [3.19]$$

The simplicity of this solution is mainly due to regarding U_{inv} as time-invariant and the neglect of the power acquisition's dynamic. Equation (3.19) only becomes stable if the constant C is positive, which requires

$$p_{droop} \cdot q_{droop} \cdot k_{1,2} > 0 \quad , \qquad [3.20]$$

with p_{droop} and q_{droop} as the respective droop-factors. The four stable operating points can be derived from Equation (3.20) and are summarised in Table 3-2 below.

case	*description*	p_{droop}	q_{droop}	*K*	*comment*
1	inverse conventional	positive	positive	1	allowed
2	Conventional	negative	negative	1	allowed
3		positive	negative	-1	not allowed
4		negative	positive	-1	not allowed

Table 3-2 Stable Operating Points of Conventional Droops in the Low Voltage Grid [26]

Case 1 and 2 (the inverse conventional and the conventional droop) are characterised by the same sign of both droop factors. This requires k to be 1, which results in an inverter voltage which is near the grid voltage (see Equation (3.12)). Only little reactive power is needed to tune the voltage, whereas in case 3 and 4 huge reactive power is needed. Even worse, the inverter power and a huge amount of grid power are dissipated in the line. Therefore, case 3 and 4 is not allowed. Thus, for the convectional droop to be applied in this case the droop parameters have to be consistent, that is, have to be of the same sign.

3.7 **Implementation of conventional droops in micro source control**

The previously described conventional droops were implemented in the Sunny Island battery inverter [21] micro source control. However, due to the relative easiness of measuring instantaneous active

power value to frequency in real micro systems, frequency is used as a function of active power i.e. the voltage source inverter's (VSI) output power is used to adjust its output frequency. This control method was called "selfsync" and was successfully implemented for the first time in the "Sunny Island" inverter by SMA Technologie AG [21].

The major advantages of using this control method are additional micro-sources can be connected at any point of the system without hindrances and these do not require information from the loads or other parts of the system for their operations. Each micro-source has a controller which responds to the system changes and the scheme of operation of which is explained in detail in [27].

3.7.1 Power/frequency droop control

As presented in [27], when a Micro-Grid operates in the grid-connected mode loads may be supplied by the micro-sources of the Micro-Grid and by the main grid. If the main grid suddenly cuts off the power supply, Micro-Grid needs to transfer autonomously to the island mode of operation.

When regulating the output power, each source has a constant negative slope droop on the P , ω plain as shown in Figure 3-6. The figure shows that of the slope is chosen by allowing the frequency to drop by a given amount, $\Delta\omega$, as the power spans from zero to $P_{\max}$, dashed line and P_{01} and P_{02} are power setpoints for two units. This is the amount of power injected by each source when connected to the grid, at system frequency.

If the system transfers to island when importing from the grid, then the generation needs to increase power to balance power in the island. The new operating point will be at a frequency that is lower than the nominal value. In this case both sources have increased their power output with unit 2 reaching its maximum power point. If the system transfers to island when exporting power to the grid, then the new frequency will be higher, corresponding to a lower power output from the sources with unit 1 at its zero power point.

The characteristics shown on Figure 3-6 are steady state characteristics. They have a fixed slope in the region where the unit is operating within its power range. The slope becomes vertical as soon as any limit is reached. The droop is the locus where the steady state points are constrained to come to

rest, but during dynamics the trajectory will deviate from the characteristic. A further analysis of Micro-Grid operational control can be seen in [27].

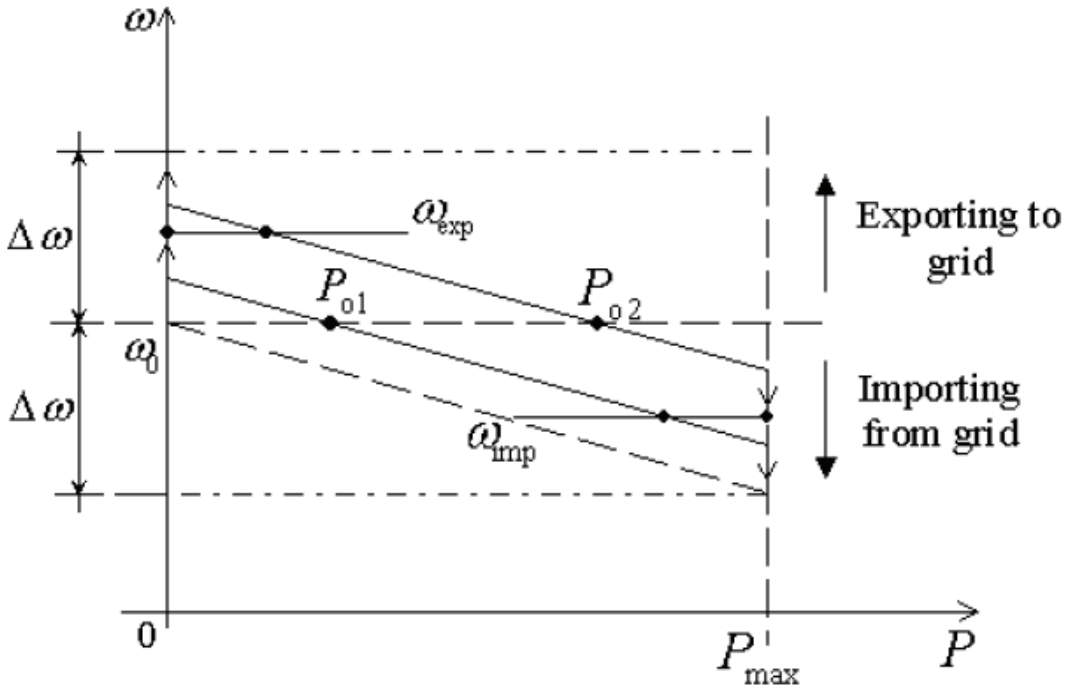

Figure 3-6: Active power vs. Frequency droop. [27]

3.7.2 Voltage versus Reactive power (Q) Droop Control

In Micro-Grid systems, the presence of large number of microsources and loads makes the co-ordination and integration of these not attainable with basic PQ power controls. Hence, voltage regulation is essential for local reliability and stability. Without local voltage control, the system could experience voltage and/or reactive power oscillations. Voltage control also ensures that there are no large circulating reactive currents between sources. In a conventional power grid, impedance between generators is usually large and circulating current can be reduced. However, impedance in Micro-Grid is small and problem of circulating current between microsources can be significant. This situation requires a voltage vs. reactive power droop control as shown in Figure 3-7. When the reactive power generated by the microsource becomes more capacitive, the local voltage set point is reduced. Conversely, as reactive power becomes more inductive, the voltage set point is increased [29] [30] [31].

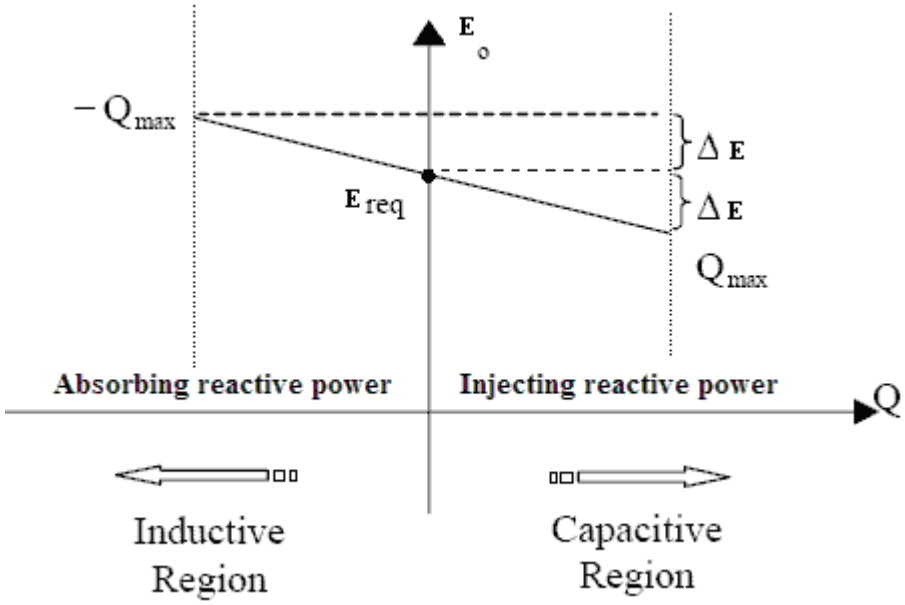

Figure 3-7: Example of a Reactive power (Q) vs. Load Voltage (E) droop characteristic [29] [30]

There is limit on the amount of reactive power ($Q_{\max}$) that the system is possible to inject and it is determined by the rating of the inverter. To define the system rating, it is possible to decide how much the voltage ΔE is allowed to increase or decrease corresponding to that amount of maximum reactive power. From the plot, the equation of the line is,

$$E_0 = E_{req} - m_Q Q \qquad [3.21]$$

And thus,

$$m_Q = \frac{\Delta E}{Q_{\max}} \qquad [3.22]$$

From equation [3.21] above, E_0 will be equal to E_{req} only when the reactive power (Q) is zero and the gradient m_Q is the coefficient of the droop curve and is defined by equation [3.22], [29] [30].

Q-voltage droop function block is shown below. The calculated Q and the required voltage (E_{req}) at regulated bus is input to the block, the output is the new voltage set-point (E_0).

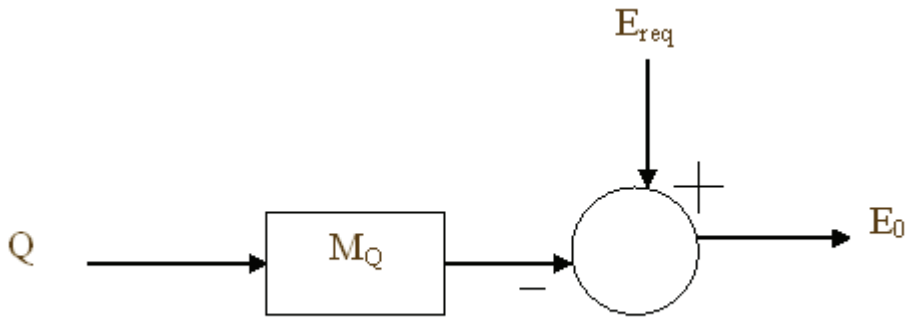

Figure 3-8: Q -Voltage droop function block. [29] [30]

E_0 is the input to the voltage control block and a new set-point is obtained from previous block. $E_{measured}$ is obtained from the voltage/phase calculation block. The error in voltage (E_{error}) will pass through a P-I controller. The output from the P-I controller will then sum with the required voltage (E_{req}) to generate a desired voltage magnitude at the inverter. The block is shown below.

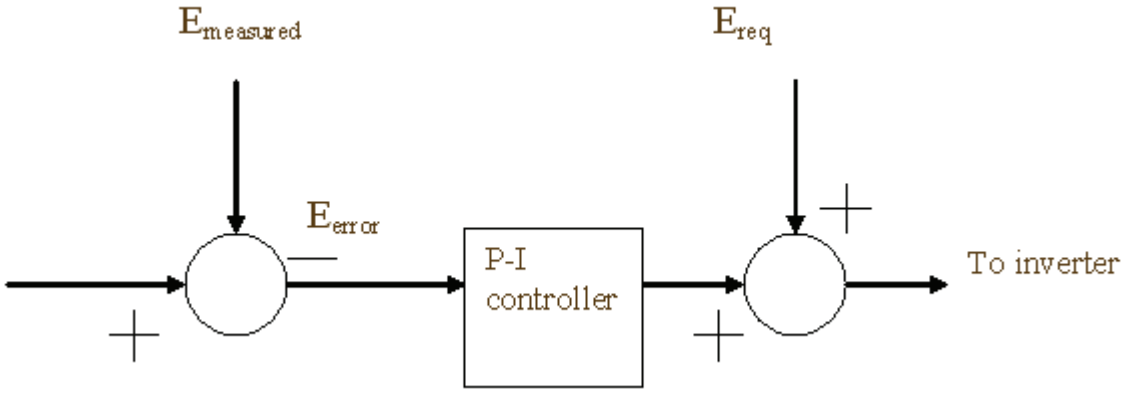

Figure 3-9: Voltage control function block. [29] [30]

The total function of both blocks is summarized,

- When the inverter produces positive Q, the Q will be multiplied by the droop gradient (m_Q) and summed with the E_{req} to obtain the new set-point (E_0).
- From the droop gradient, the corresponding new bus voltage set-point (E_0) is a smaller value.

- E_0 is subtracted from $E_{measured}$ to obtain a different E_{error}, and feed it to the P-I controller.
- The P-I controller produces a correction signal ΔE and add up with the E_{req} to give a desired voltage magnitude to the inverter. In this case the voltage magnitude would be larger to reduce the Q power.

3.8 Control strategies for Micro-Grids in island mode of operation

If there are no synchronous machines to balance demand and supply in a Micro-Grid, inverters should be responsible for controlling frequency during islanded operation. A voltage regulation strategy is also required; otherwise the Micro-Grid could experience voltage and/or reactive power oscillations [32].

In the presence of the main power supply all inverters of the micro sources within the Micro-Grid can be operated in the PQ mode, because a voltage and frequency reference is provided by the main grid. However if the main grid network is lost all the inverters will shut down because there will not be a voltage reference within the Micro-Grid and it will not be possible to obtain an exact power balance between load and generation. This means that a general frequency control strategy should be followed in order to operate the Micro-Grid in islanded mode. Two possible operation strategies employed are the Single Master Operation (SMO) and Multi Master Operation (MMO) as described below.

In each case a VSI unit has to be present in order to provide a voltage and frequency reference in case a disturbance occurs in the main grid. A VSI has the ability to react to power system disturbances (for example, load-following or wind fluctuations) based only on information that is available locally at the inverter – voltage and current measurements [33]. Such a VSI should be coupled with a storage device with enough capacity in order to be able to compensate natural load and production variations.

3.8.1 Single Master Operation

In a SMO mode, most of the MS are connected to the network through inverters with a PQ control type and only one VSI (Inverter 1) associated with an energy storage device – the master – provides the frequency reference, see Figure 3-10. As explained in [18] such VSI should be responsible for fast load-tracking. This inverter operates in the conventional droop mode under the control of its own control block, see Figure 3-10.

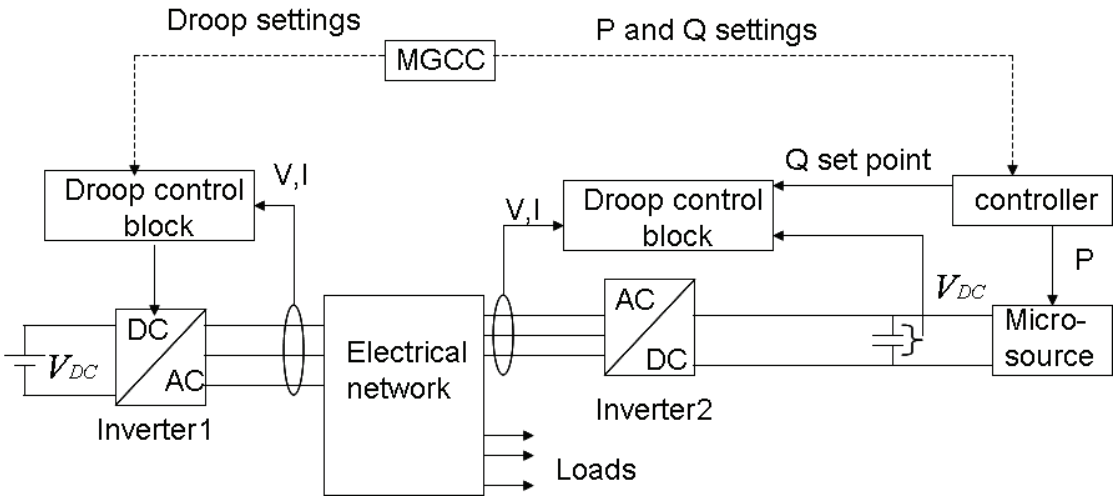

Figure 3-10: Single Master Operation [34]

If necessary its droop settings can be changed from the MGCC according to the operating conditions and in order to avoid large frequency variations. In this case, PQ controlled micro source (Inverter 2 in Figure 3-10) can receive from the MGCC set points through its controller or can adopt a local PI (proportional integrator) frequency control, defining target values for active output powers of its primary energy sources. Assuring a zero frequency deviation during any islanded operating condition should be considered as a key issue for any control strategy. As a matter of fact such procedure is needed to avoid storage units to inject (or absorb) active power whenever the Micro-Grid frequency deviation is different from zero [18].

3.8.2 **Multi Master Operation**

In a multi master approach, there are several inverters operating as VSI (i.e. as masters, inverter 1 and 3 as shown in Figure 3-11) with a pre-defined frequency/active power and voltage/reactive power droop. Other PQ controlled inverters may also coexist in the Micro-Grid, (inverter 2) see Figure 3-11. Each of the master inverters operates in conventional droop mode under the control of each one's own control blocks like in the single master case. In this operation mode the VSI can be connected to storage devices or to the micro sources.

Generation profiles of the Micro-Grid in this case are also determined by the MGCC. They can be modified by changing the frequency of the master inverters or by controlling the output power of the micro sources. An overview of this control strategy is shown in Figure 3-11 [34]. This operation is a more advance strategy than the SMO in that the parallel operation of VSI is possible and hence the possibility of connecting more and even distant Micro-Grids or microsources.

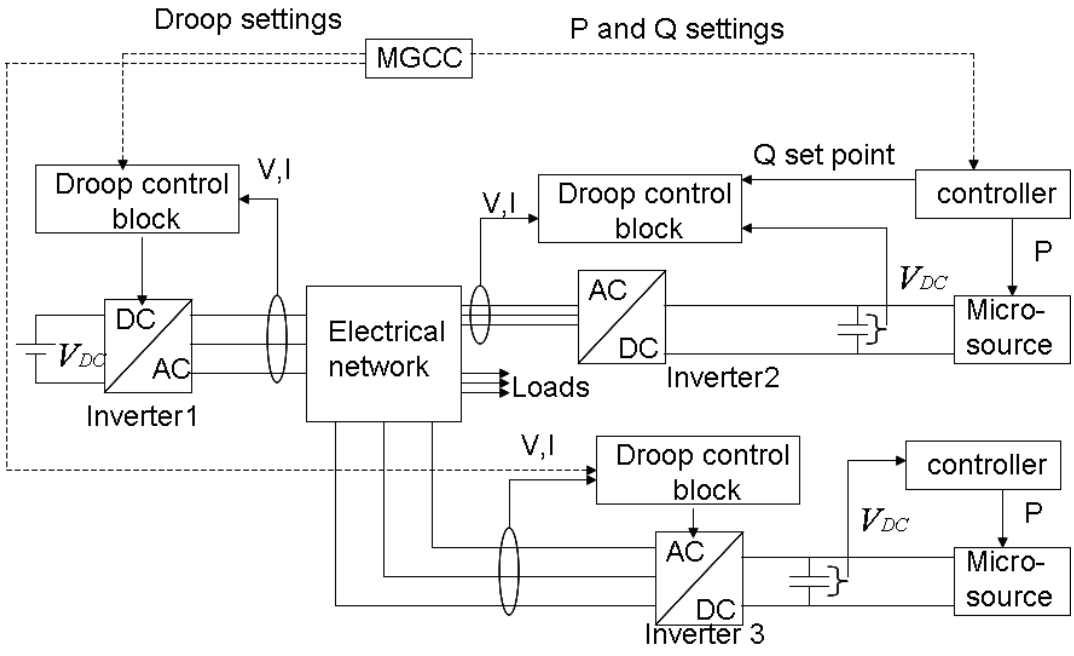

Figure 3-11: Control scheme for Multi Master Operation [34]

3.9 **Conclusions**

So in this chapter the background to the importance of the concept of Micro-Grids, the understanding of their operations and control strategies were reviewed.

Chapter 4 **Micro-Grids load sharing via medium voltage (MV) system**

4.1 **Introduction**

This chapter looks at the interaction of distant multi-Micro-Grids connected through medium voltage lines. The questions of interest are load sharing among the Micro-Grids and possible voltage support in the medium voltage level. These aspects are experimentally studied. The experiments were prepared and executed in the Design Centre for Modular Supply Technology (DeMoTec) of ISET as part of a task in the European Commission Project, “More Micro-Grids” (Contract No: SES6-019864). The task is centered at investigating how low voltage Micro-Grids or micro sources in the low voltage grids share active power during transients and how they exchange reactive power via the medium voltage system which connects them. These aspects are not yet sufficiently studied given the fact that in the old power systems power was unidirectional, that is, from high voltage transmission to the low voltage distribution where the consumers were conceived passive. Nowadays these distribution systems are active, that is, they are also generating and feeding energy to the transmission system. These scenarios thus complicate the control of the system, since the medium voltage level manifests mixed characteristic of resistive/inductive nature while the low voltage is predominately resistive. Thus the investigation also looks at the effectiveness of the micro source controls (the droop parameter setting effects on this power sharing). The following sections give a detailed description of the experimental setup, the equipment used and presentation of the results.

.

4.2 Experimental setup description

The circuit of the experimental power system is shown in Figure 4-1. Three Micro-Grids, MG1, MG2 and MG3 connected by three 100 kVA transformers via medium voltage transmission lines, $L_{1,5}$, $L_{2,5}$ and $L_{3,5}$ (as depicted in Figure 4-1) were built up in the Design Centre for Modular Supply Technology (DeMoTec) of Institut für Solare Energieversorgungstechnik (ISET) e. V., Kassel. Micro-Grids, MG1 and MG3 have each a three-phase micro source (MS1 and MS3 respectively) built from three single phase battery inverters – the Sunny Island 4500 from the company SMA Technology AG, connected together to form a three-phase cluster, with total rated power of 10.8 kW and the third (MG2) acts as a load. The three Micro-Grids were disconnected from the external grid by the Grid switch as marked on the diagram of Figure 4-1. Also it is possible to separate the Micro-Grids from the medium voltage by opening the Micro-Grids switches marked MG1 Switch, Load Switch and MG3 Switch. The setup provides nine measurement points for voltage and current three of which are on the low voltage side marked Haag Device, (logged by power analysers from the company Haag GmbH) and the remaining six measurement cells marked Metering Cell 1.2, 2.2 and 3.2 and 1.4 2.4 and 3.4 as adopted from the hardware system of the medium voltage system simulator hardware pictured in Figure 4-2 (left). In principle the experiment simulates two case scenarios of the test power system which are:

Case1: Micro-Grids MG1 and MG3 in Figure 4-1 generate more power than their local load demand and the MG2 produces less or has no generation at all and thus needs to import power from the other two. In this case the main schema is used, that is, the three major switches MG1 Switch, Load Switch and MG3 Switch are closed. The Micro-Grids MG1 and MG3 export power through the MV system to supply the excess load in MG2. The active power sharing and reactive power exchange between these three distant Micro-Grids is assessed.

Case 2: Either Micro-Grid MG1 or MG3 generates more or less power than their local demand, and thus need to export or import power as the case may apply. The case is analysed experimentally by first connecting the load to either MG1 bus-bar or MG3 bus-bar using switches MG1-Load Switch or MG3-Load Switch respectively. In both cases the switch marked Load Switch in Figure 4-1 remains open. Then to allow either Micro-Grid MG1 or Micro-Grid MG3 to import/export power to/from the

other the switches MG1 Switch and MG3 Switch are closed, thus the power import/export is via the MV system.

For these two cases above the active power sharing was investigated through the ohmic load operation while the reactive power exchange could be assessed during inductive load operation. The no load operation was aimed at evaluating the energizing power requirements for the medium voltage system, that is, mainly the transformer reactive power requirement and active power losses. In the next section brief description of the equipment used is given.

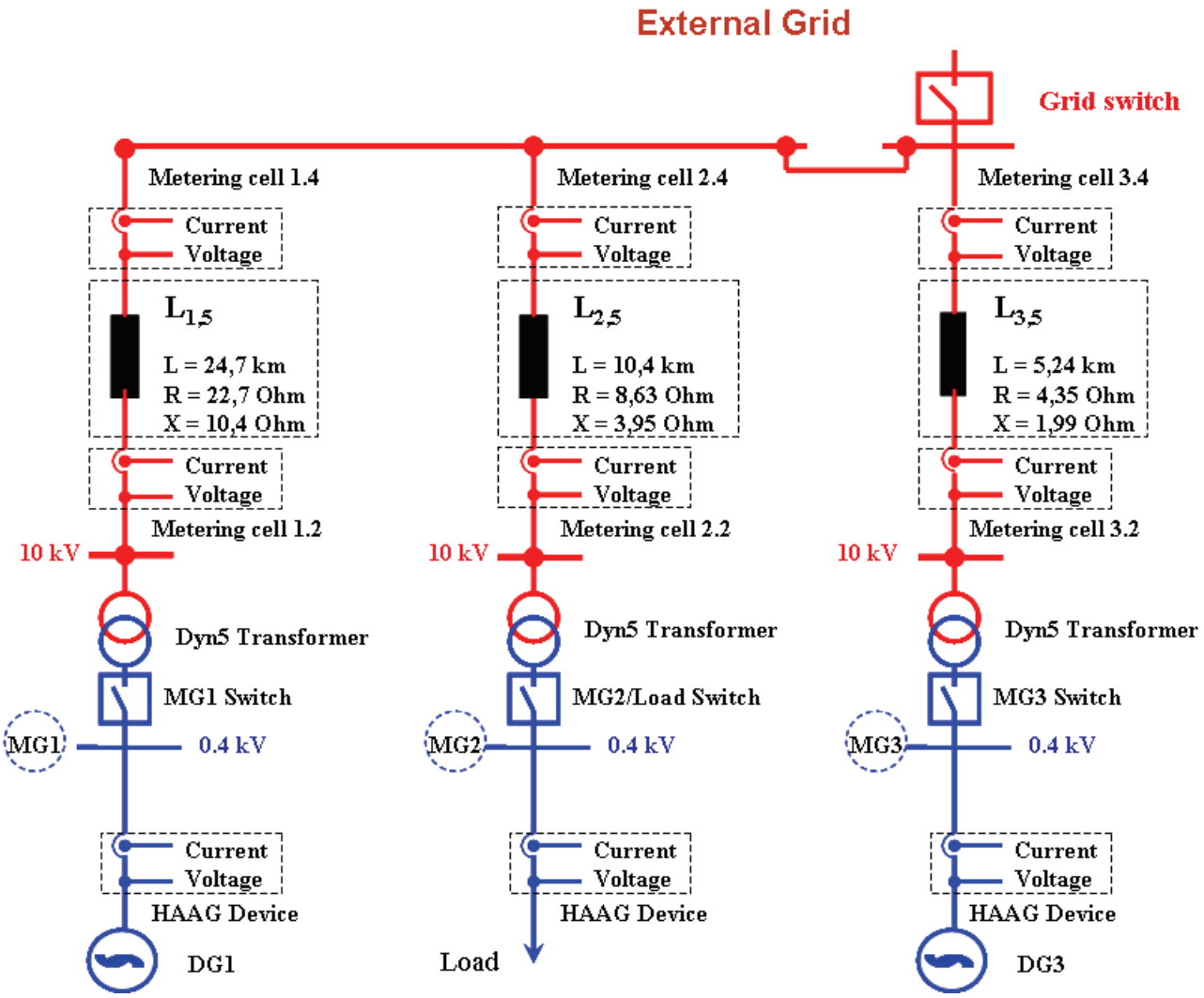

Figure 4-1: Principle schema of the 10 kV line impedance simulation network

4.3 Equipment description

In this section each of the main equipment used in these experiments is briefly described. Here the description is limited to the general aspects, leaving the details of their function to the respective manuals of the equipment in question.

4.3.1 The Line Impedance Simulation Network (LISN) description

The Line Impedance Simulation Network (LISN) is able to provide a configurable MV-grid. It consists of three coupled transmission circuits $L_{1,5}$, $L_{2,5}$ and $L_{3,5}$ as shown in Figure 4-1. These interlinked transmission circuits can simulate either overhead lines or cables. Through the variation of the resistance and the reactance of each transmission circuit different line lengths can be simulated. Figure 4-2 shows the general view of Hardware Network Simulator (left), one of the transformers in security cage (middle) and a view of transmission line consisting of configurable resistors, inductors and capacitors to simulate the line impedances.

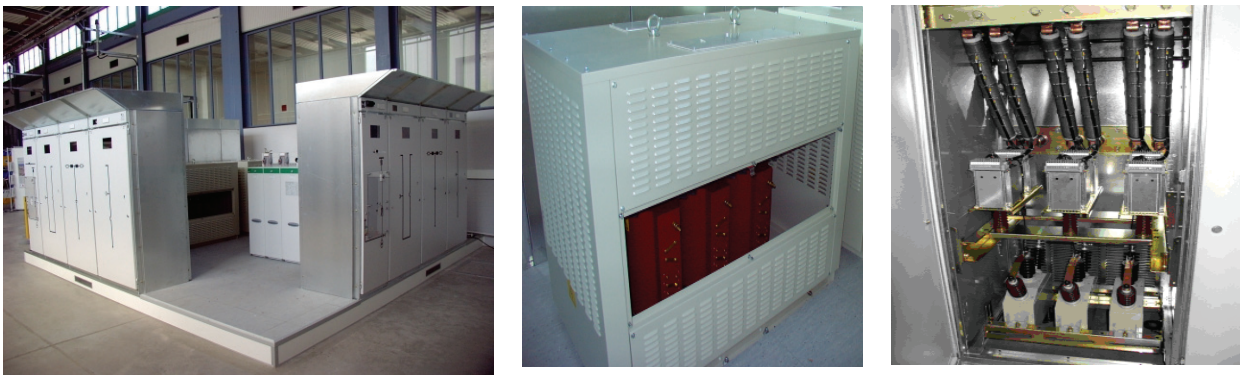

Figure 4-2: General view of Hardware Network Simulator(left), one of the transformers in security cage (middle) and a view of transmission line (consisting of configurable R,L,C elements) [35]

For measurement on the medium voltage side a so called Multifunctional Intelligent Digital Relay (MIDR), belonging to the LISN equipment, was used. This MIDR contains a voltage and current measurement units at the beginning and the end of the interlinked transmission lines. In Figure 4-3

the main elements of the MIDR are shown. The medium voltage system is connected to the low voltage level, that is, to the three marked Micro-Grids in Figure 4-1 by three 10 kV/0.4 kV transformer with a nominal apparent power of 100 kVA.

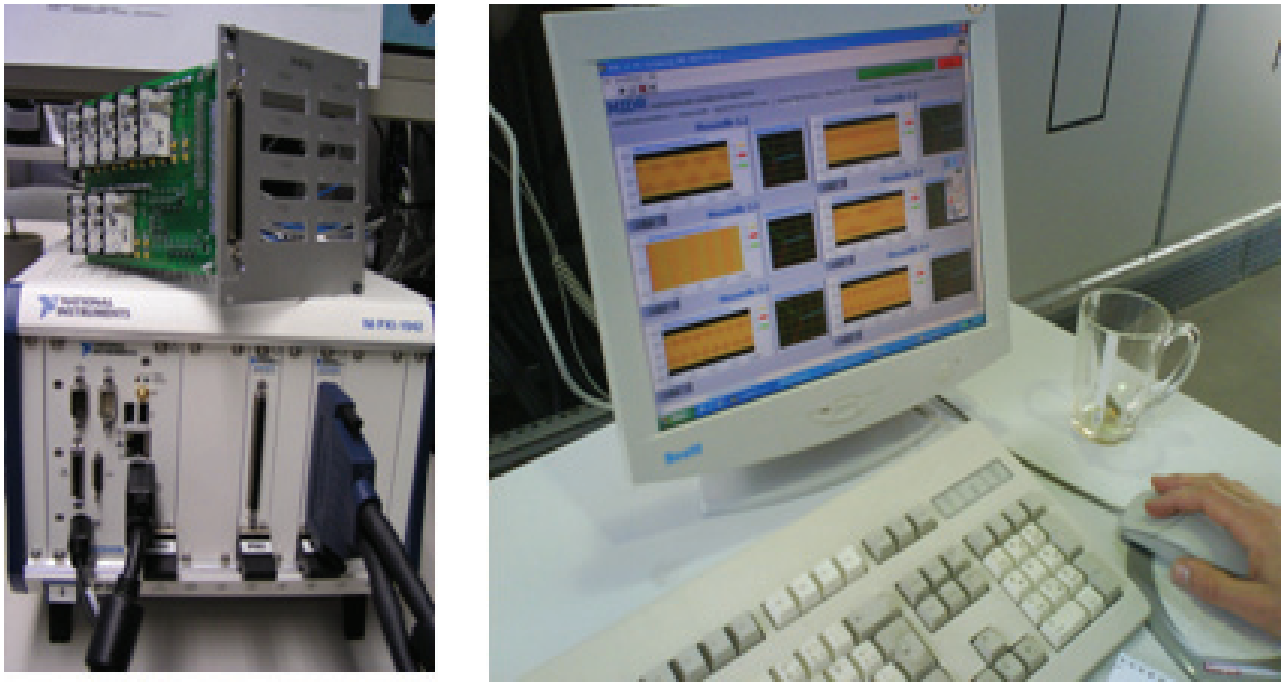

Figure 4-3: Some elements of the Multifunctional Intelligent Digital Relay (MIDR), A/D-conversion of measurement values on the left side and control of the MIDR with LabView on the right side

4.3.2 The battery inverter Sunny Island 4500

Single phase Sunny Island 4500 (SI 4500) Inverters with control approach based on the *selfsync*™ method [21] and using active power/frequency and reactive power/voltage droop control mechanisms were used to form 3-phase clusters. One of the clusters is shown in Figure 4-4 with the connected HAAG measurement device. The cluster has total nominal apparent power output of 10.8 kVA.

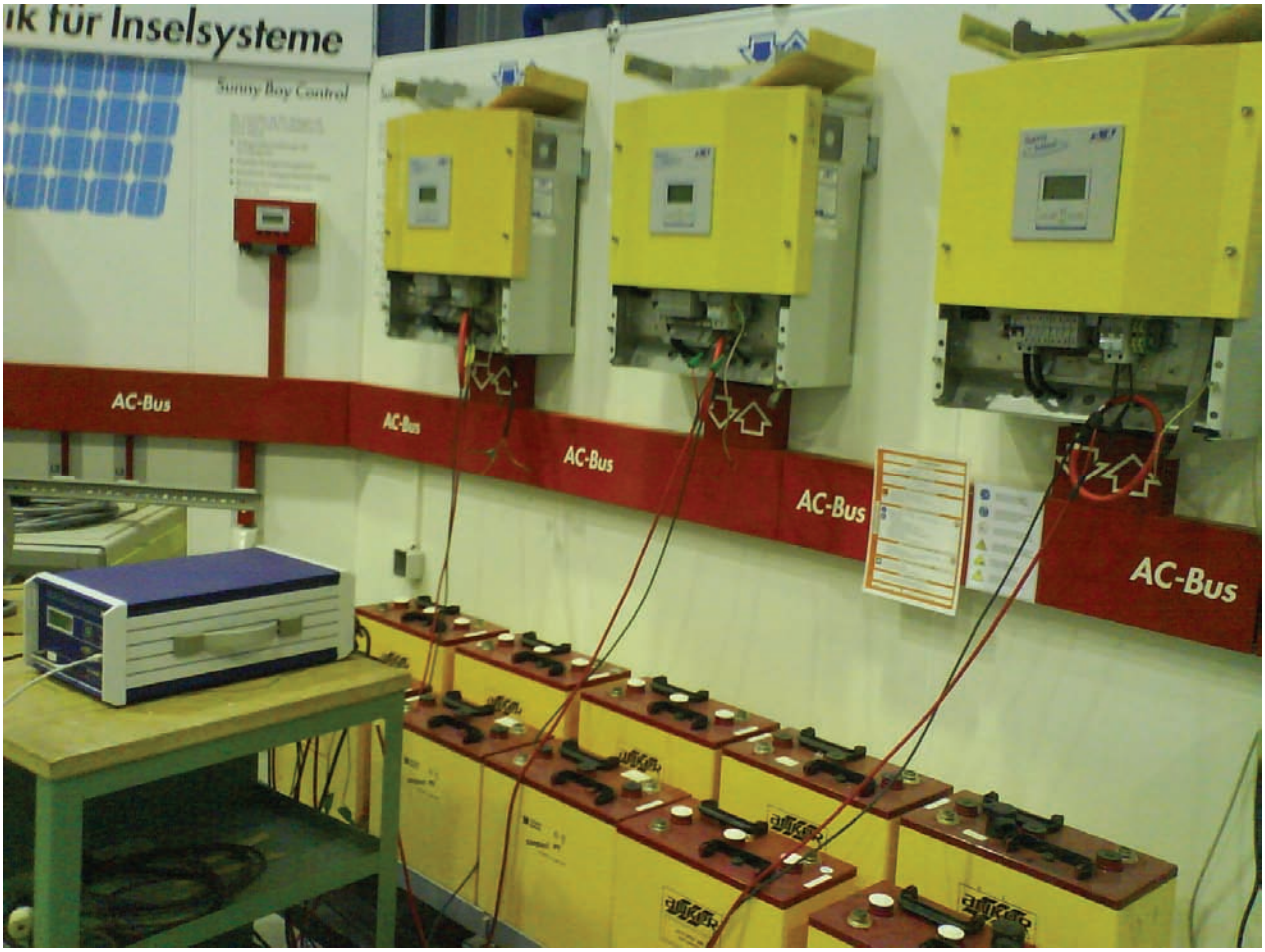

Figure 4-4: Three phase Sunny Island 4500 battery inverter cluster with connected Haag measurement devices [Photo by author]

4.3.3 **Loads**

Figure 4-5 shows an ohmic load bank (left) with selectable load values between 0.1 kW and 4 kW per phase and to the right is the asynchronous motor from the company VEM (G21R 160 M 4 HW) with 11 kW rated power. By doing a start up and shutdown of the motor without load, dynamic studies within this experiment could be done. In Table 4-1 the technical data of the motor is given.

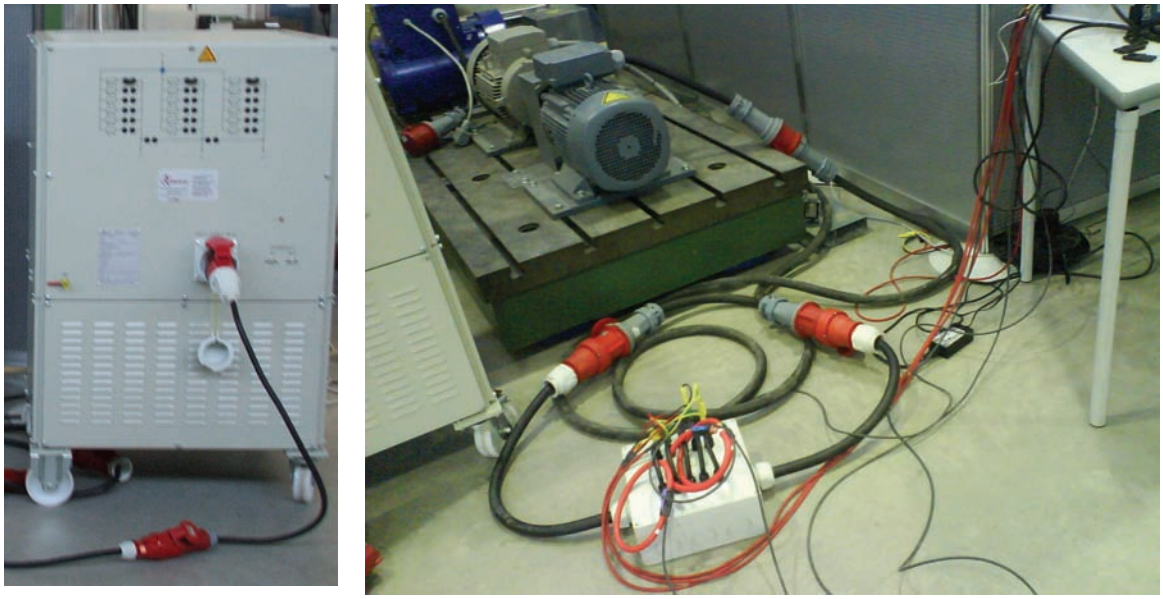

Figure 4-5: Ohmic load bank with a three phase power of 12 kW (left) and the VEM asynchronous motor with 11 kW rated power (right) [35]

Manufacturer	VEM Motors GmbH
Number of pole pairs	2
Connection	Y
Rated electrical active power Pe,r	11 kW
Rated electrical apparent power Sr	13.2 kVA
Rated mechanical active power Pm,r	12.6 kW
Rated power factor cosφ	0.83
Rated electrical frequency fr	50 Hz
Rated mechanical speed nr	1545 r.p.m.
Rated voltage Ur	400 V

Table 4-1: Technical data of the VEM asynchronous motor [35]

4.4 Experimental scenarios

4.4.1 No load case setup

The setup for the no load scenario is shown in Figure 4-6. In this case the two Micro-Grids are connected to the medium voltage system through their respective switches while the load switch is left open. The whole system is allowed to run for some time and all the nine measurement points logging the current and voltage. This scenario enabled the initial incite in the power sharing among the Micro-Grids in question. Basically this scenario serves to show the losses associated with the transformers and the medium voltage lines.

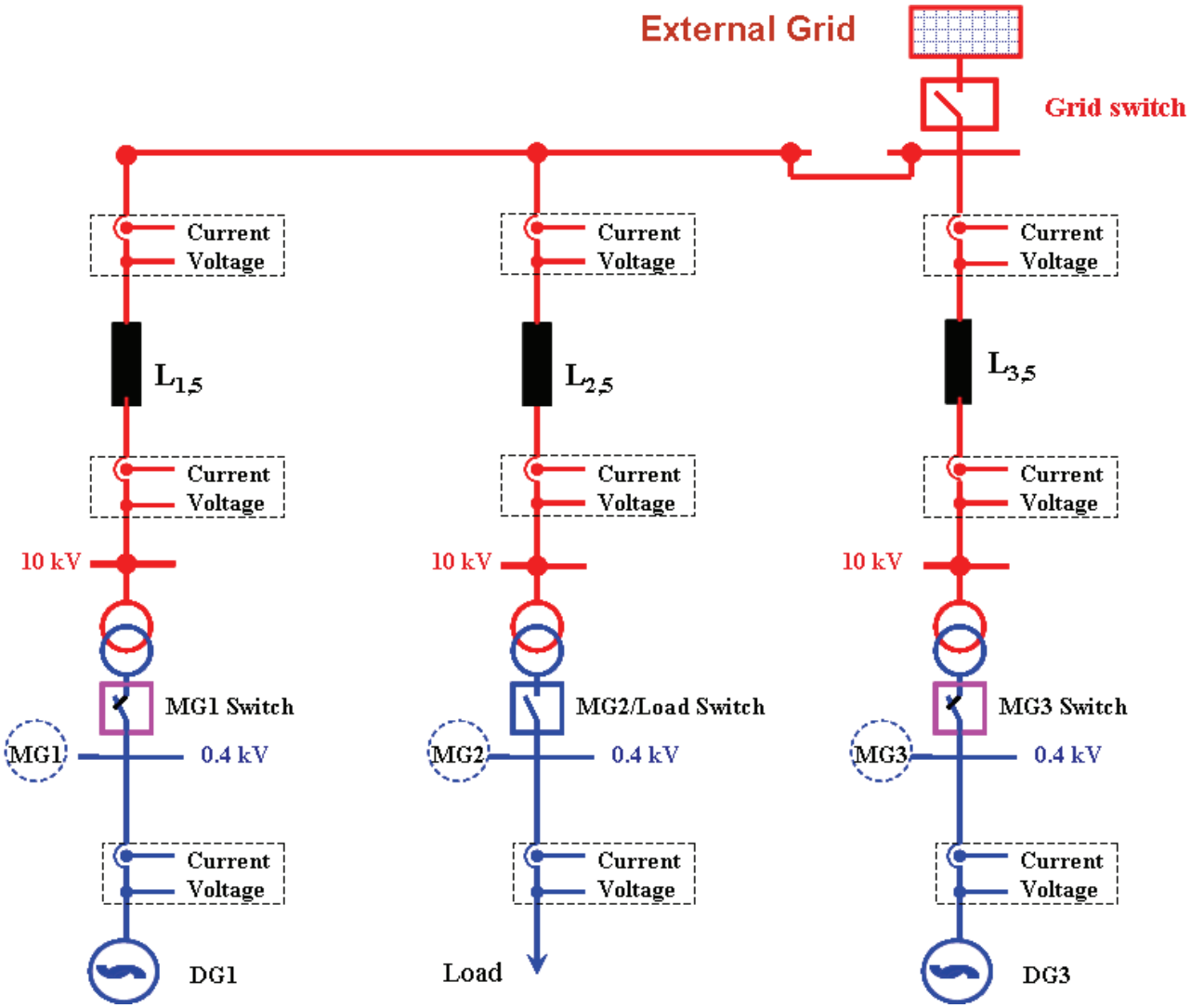

Figure 4-6: No load test experimental diagram

4.4.2 No load operation results and discussion

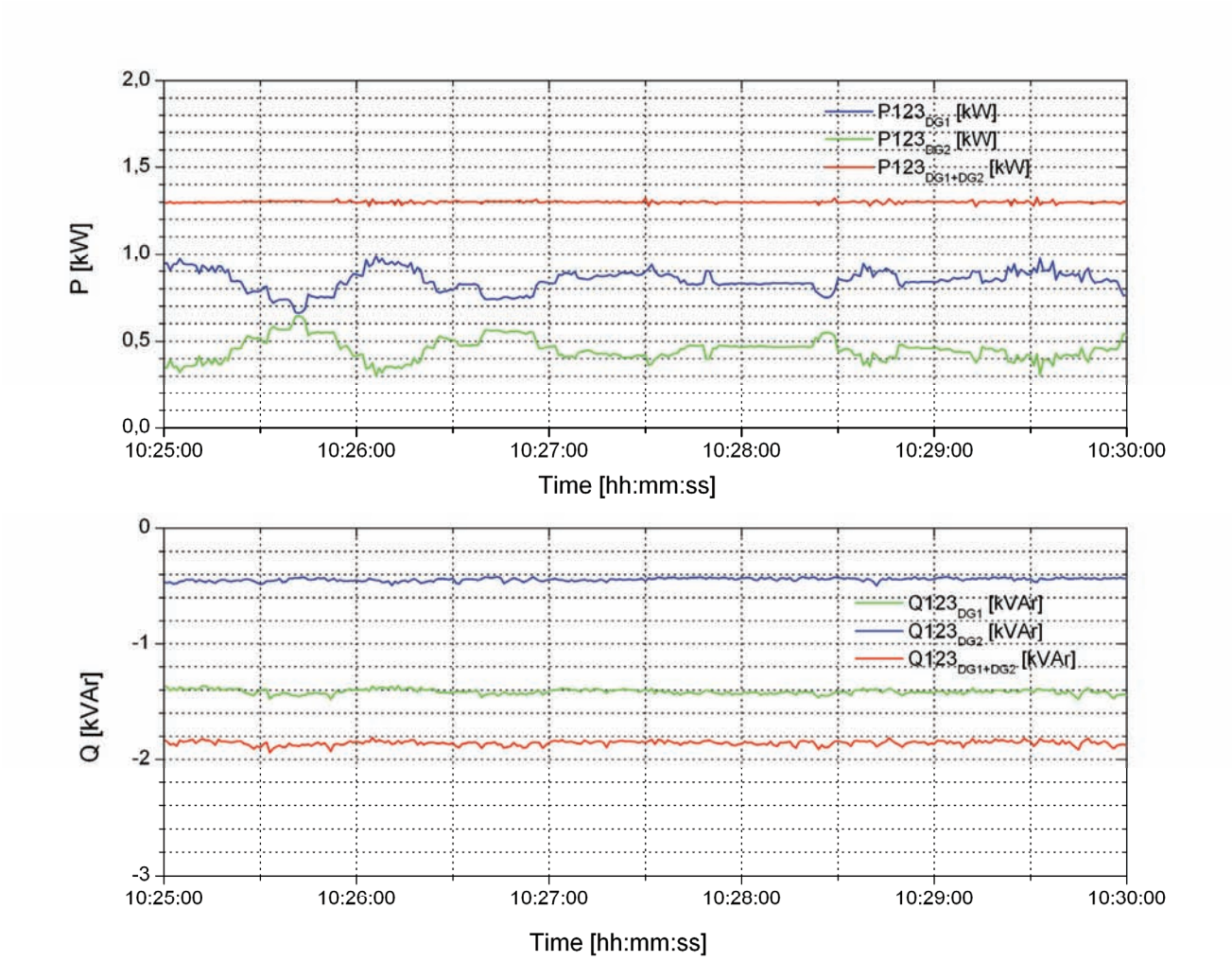

Figure 4-7: Active and reactive power demanded by the medium voltage system (transformers and lines) at no load operation per source (DG1 in blue, DG2 in green) and totalised (red)

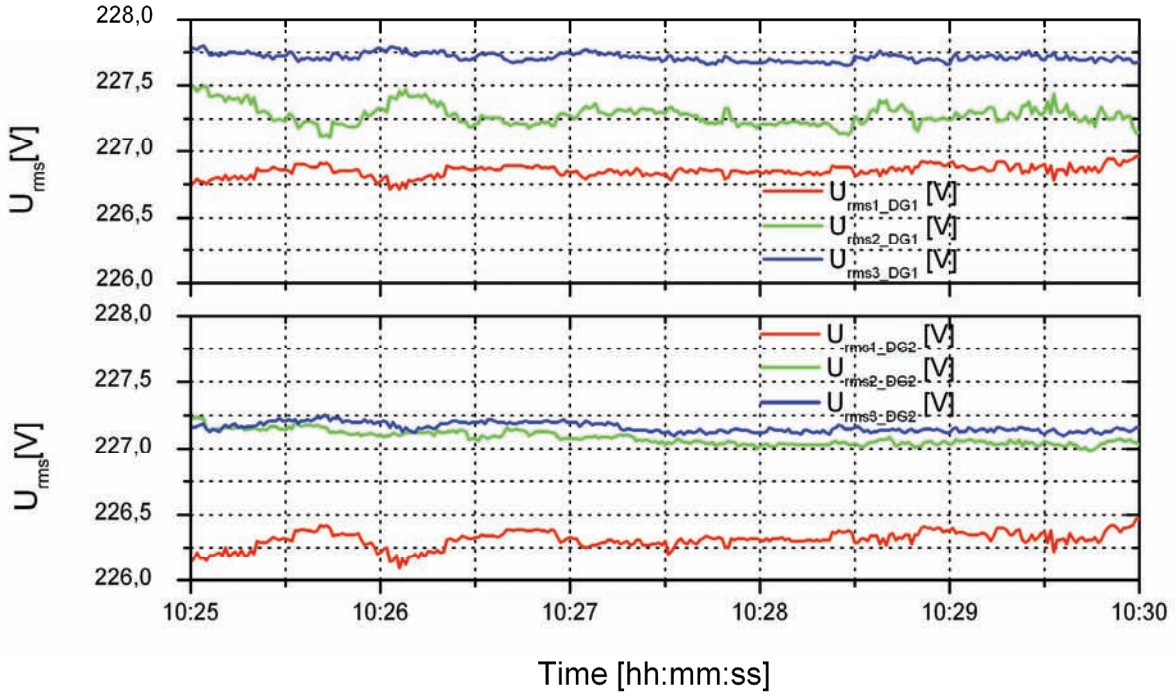

Figure 4-8: Comparison of phase rms voltages of the sources during no load operation, (phase 1 red, phase 2 blue and phase 3 green)

In Figure 4-7 the network losses are shown as the power supplied from the two sources without any load connected to the system. The three phase sums of active and reactive power from DG1 ($P123_{DG1}$, $Q123_{DG1}$ in blue), DG2 ($P123_{DG2}$, $Q123_{DG2}$ in green) and the total powers supplied by the two DGs, ($P123_{DG1+DG2}$, $Q123_{DG1+DG2}$ in red) are shown. The time duration considered for these observations is five minutes. The sum of the active power $P123_{DG1+DG2}$ is about 1.3 kW, that is, the power needed to energize the transformers and losses in the transmission wires. From the graphs of Figure 4-7, it can be noted that the two sources DG1 and DG2 do not share equally the power, DG1 takes the greater share of this power demand, and the other thing seen again in the figure is the active fluctuation of the individual powers.

The total reactive power required to energize the transformers and the lines losses without load is about -1800 VAr. The minus sign indicates that inductive reactive power is delivered to the MV-system. Compared to the active power sharing, the amount of reactive power provided by the inverter clusters is more stable. It is seen again that most of the reactive power is made available by

DG1 (note that comparison is based on the magnitude of reactive power and not sign). Although the system was expected to be symmetric with all phases with no load, in practice this proves not so. The phases voltages are not the same with maximum difference of about 1 V for both the sources. The above unsymmetrical problems on the phases of the system may be attributed to the reason that the three phase DG (inverter cluster) is built from connecting three single phase inverters in parallel and the inherent internal parameters may not be the same. In addition the simulator for the MV line may be also not exactly symmetric in terms of line impedances.

So the results of the no load test have shown that the transmission (MV) system consumes a considerable amount of power, (in the case of this experiment with six battery inverters with a total nominal power of 21.6 kW the MV system will thus consume about 6 % of the total capacity) just for energizing mainly the transformers and of course a little portion taken by the MV lines. About 1.3 kW of active power and 1.8 KVAr of reactive power are required in this case. So it sounds uneconomic to try to connect distant and small power systems. The power sharing among the generators is dependent on among other aspects, the physical structure of the network, and also the generator settings.

4.4.3 **Experimental setup for active power sharing with ohmic load**

The experimental setup shown in the diagram of Figure 4-9 allows the investigation of the active power sharing and reactive power exchange in the case when the two Micro-Grids supply the load via a medium voltage system. In this case for the active power sharing investigation resistive load was connected at the Micro-Grid bus-bar by closing switch marked “Load Switch” in the circuit diagrams. The reactive power exchange aspect was also studied using the same circuit but connecting an asynchronous motor in place of the resistive load.

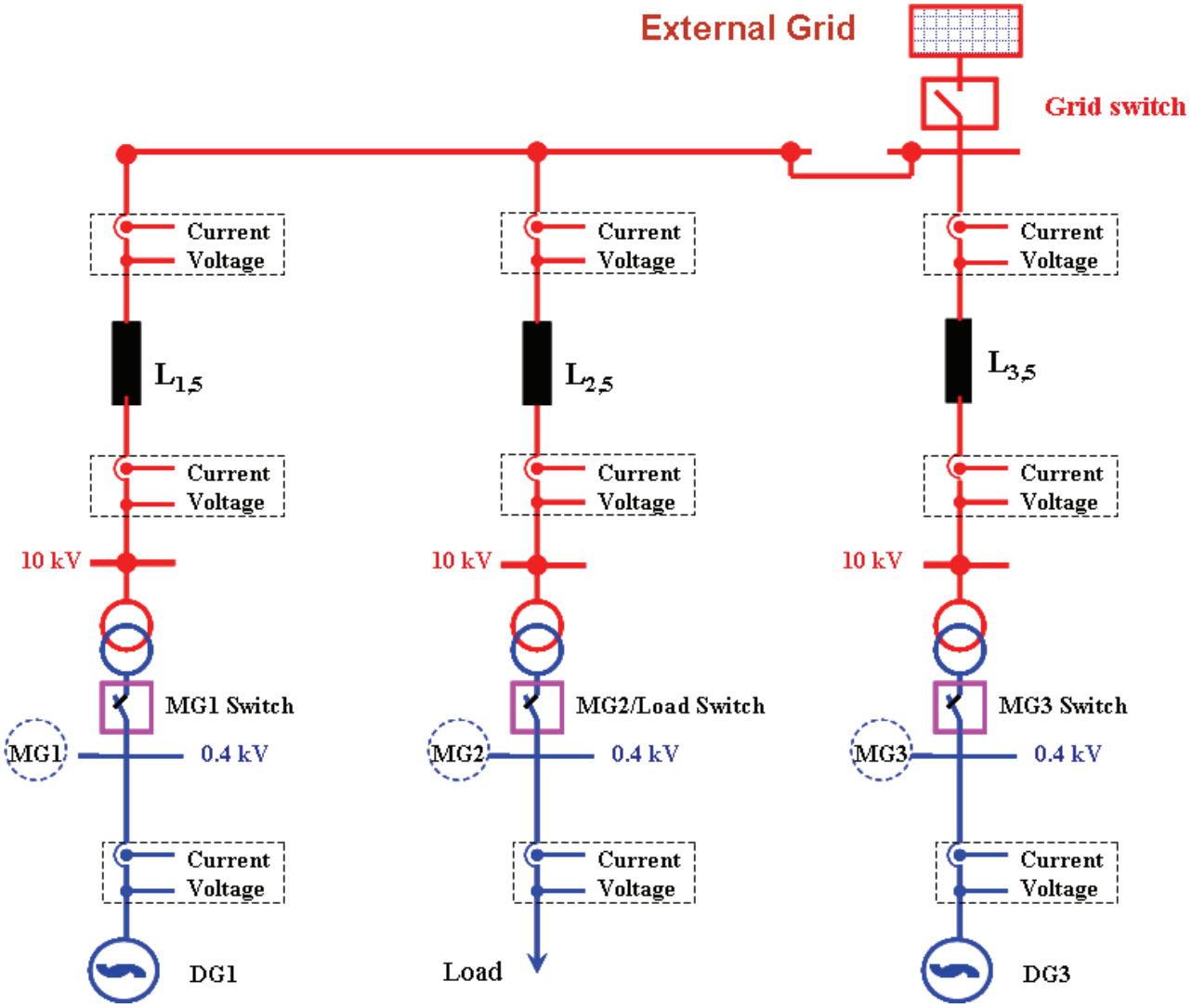

Figure 4-9: The two Micro-Grids supplying power a distant load via the MV system

4.4.4 Results of the active power sharing with ohmic load

The diagrams from Figure 4-10 to Figure 4-13 show the analysis of the results of the experiment with ohmic load supplied through the MV system as shown in the circuit diagram of Figure 4-9. The load is changed in steps up to 4.3 kW as can be seen in Figure 4-10. It can be seen that the load flow is associated with an additional reactive power exchange. The change of active load of 4.3 kW has a corresponding reactive power change of about 0.65 kVAr (as can be read from the grid graph of Figure 4-10. The explanation to this is in two. On one hand as expected the active power flow causes an additional reactive power demand in a power system that can be calculated as ($q = x * i(t)^2$), where q is the reactive power flowing due to the flow of i(t) current through a line of reactance x.

However, this value should not be very big especially in this setup where the reactive component (the transformer and medium voltage lines) have very small current flowing in them and squaring this makes it even smaller given the size of active power flowing (in this case less than 5 kW for the two inverter clusters and thus in the MV the current is so small - in the range of a fraction of an ampere). But in the case of Micro-Grids with droop controlled inverters active power flow could cause an additional reactive power exchange since this active power flow will cause a voltage drop sensed at the inverter output and thus due to the droop control mechanism of the inverter, as a response the inverter will change its set voltage to a higher value and thus supply more reactive power according to the droop parameter set to the inverter (as in Figure 3-4).

In Figure 4-11 the three phase active and reactive power for DG1, DG2 and the sum of all inverters are shown. The total load levels were set at 0 kW, 1.5 kW and 4.5 kW on the low voltage resistive load bank simulator for three phase power. It has to be mentioned that $P123_{DG1+DG2}$ (the total supply of power from the two DGs) in Figure 4-11 includes the power demanded by transformers and lines in addition to the load applied. The splitting of the active power distribution between DG1 and DG2 can also be assessed in Figure 4-11 whereupon DG2 now bears the bigger part. This is intuitionally expected that the source closer to the load has to supply more power to it. However, in this experiment other reasons could not be ruled out like the battery management mechanism of the Sunny Island inverters (i.e., the influence of the state of charge (SOC) of the battery is always taken into account). If the SOC is too low, the inverter is going to charge the battery from the MV-grid. Furthermore it could again be noted that the contribution of each inverter cluster to the delivered active power is not constant.

On the reactive power, as expected, the variation of each inverter cluster's contribution with change of load is not big as the load is resistive. With this zoomed view of the total three phase reactive power $Q123_{DG1+DG2}$ some statements about the reactive power-exchange can be made. If there is a step in the active power at the load the inverter response in the supply of reactive power is not immediate. This is associated with the droops and internal control system of the inverter and respectively the additional need of reactive power through the higher current of the lines and transformers on the MV-side.

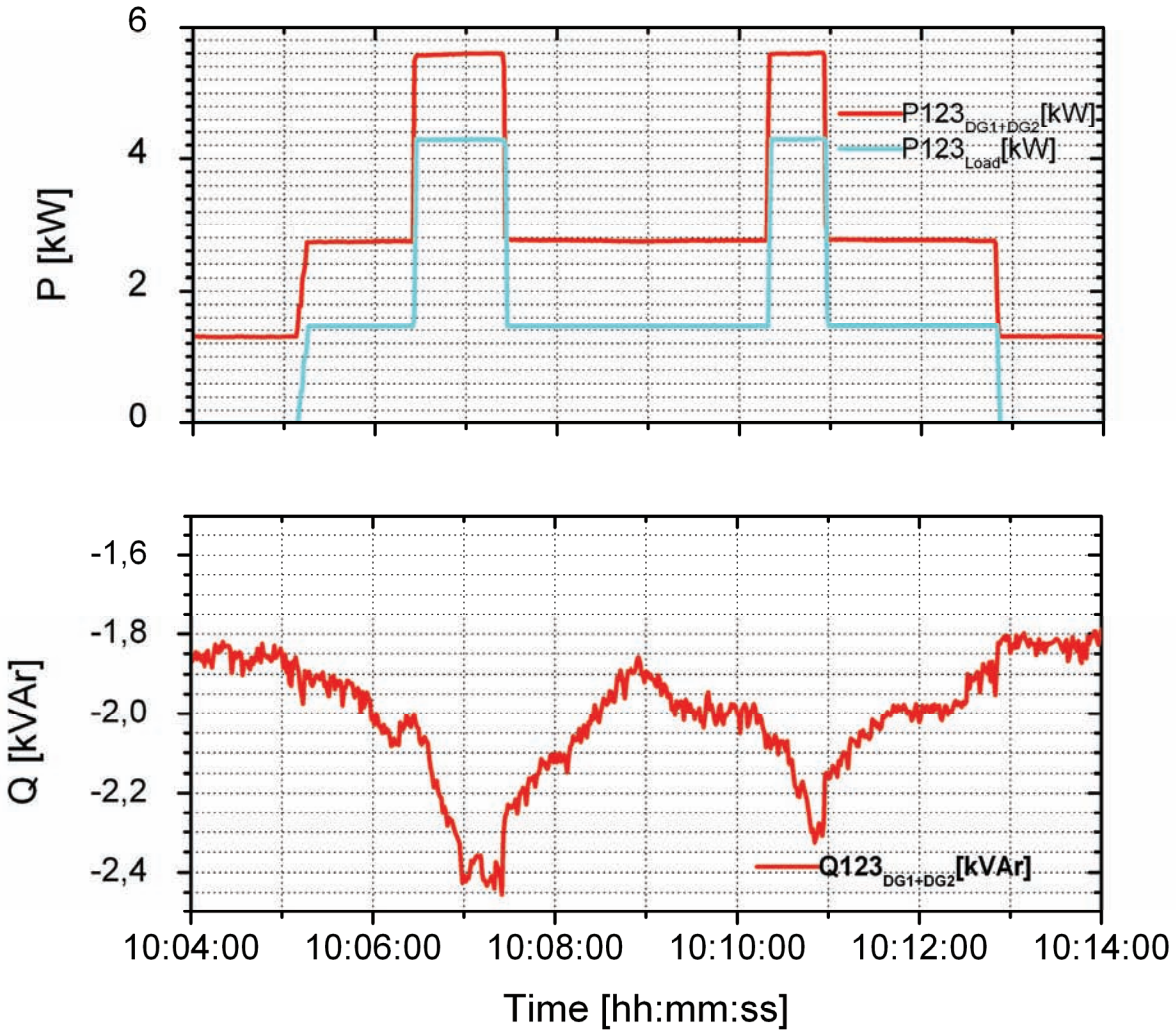

Figure 4-10: Active power of the load and total active and reactive power from the inverters

In Figure 4-12 the active and reactive power separated by phase for DG1 and DG2 are presented. The inverter cluster DG1 has an unsymmetrical active and reactive power injection, especially phase 1 is differing from phase 2 and phase 3 for the reactive power. The active power of phase 2 of DG1 (Figure 4-12 upper left in green) also has negative values which indicate an active power reception from the MV-grid. DG2's active and reactive power splitting is nearly symmetrical.

In Figure 4-12 the three quantities, active and reactive powers and voltages are plotted in their respective phases. In this the response of each parameter to the load changes is evident. It is seen that the three phases do not respond the same way, especially in terms of reactive power injection when

load changes. Phase 1 of DG1 contributes more and reacts faster. It is also important to mention that the inverter connected to the later phase was the master of the cluster. Here also the dependence of reactive power with the voltage can be seen. The drop in voltage is accompanied by an injection of reactive power. The voltage profile at the load node shows an additional voltage drop in comparison to the voltage profiles of DG1 and DG2. This results from voltage drops across the transformers and lines and this depends on the power transfer in the grid. Through the injection of additional reactive power voltage profile could be corrected.

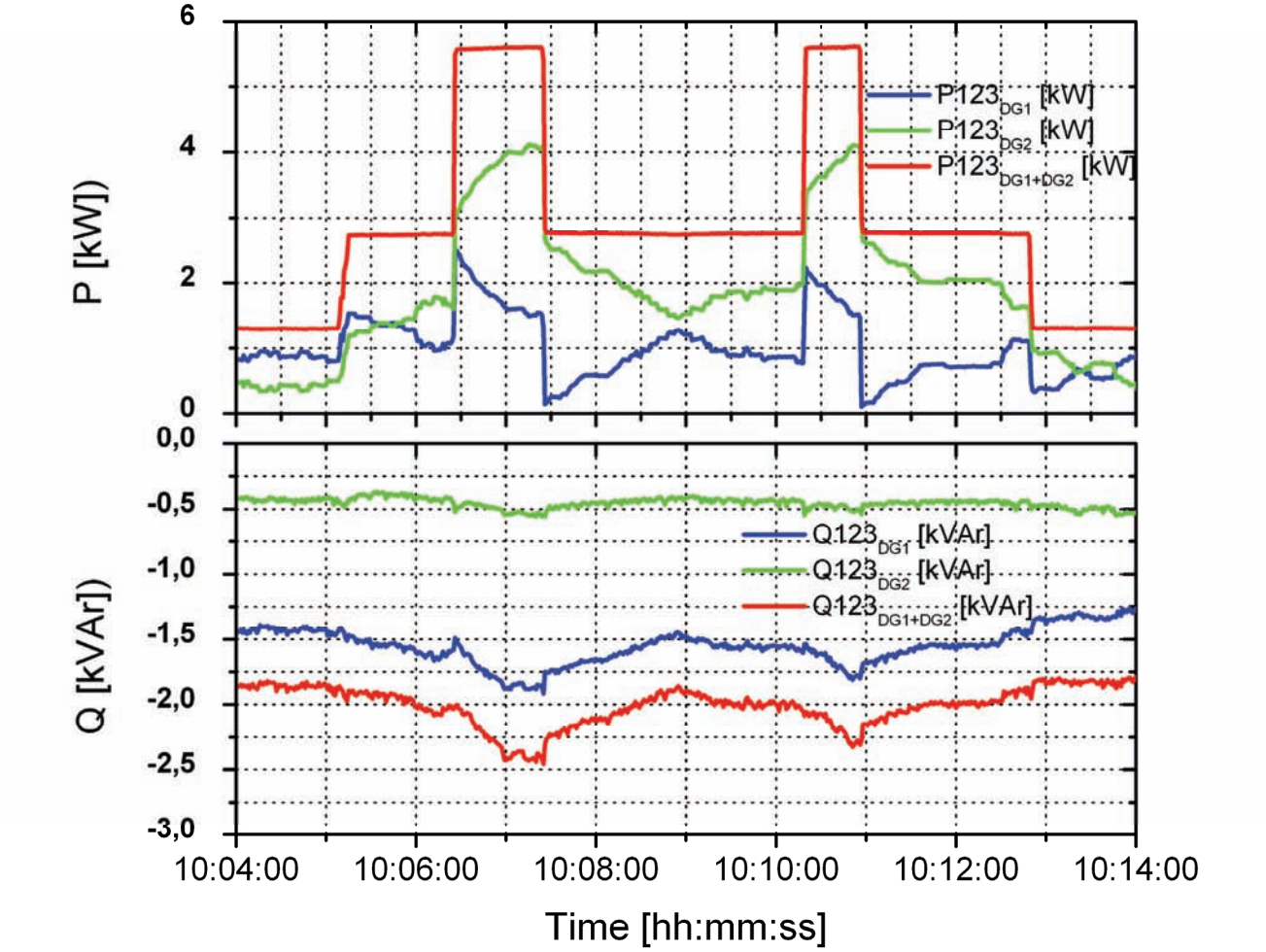

Figure 4-11: Three phase active and reactive power per inverter cluster (DG1 in blue, DG2 in green) and totalised (red)

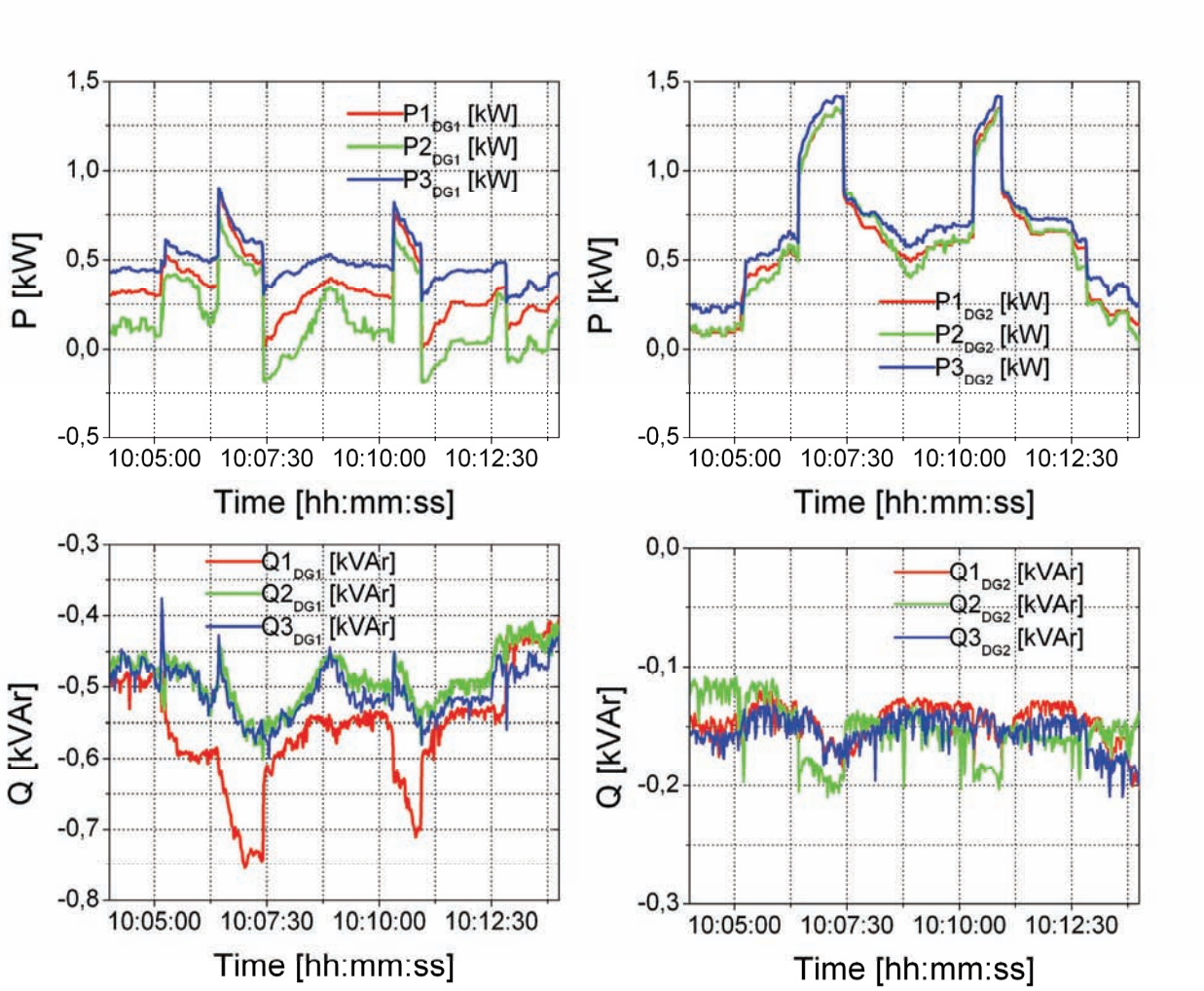

Figure 4-12: Active and reactive power separated by phases (phase 1 is red, phase 2 is green and phase 3 is blue) and clusters for different ohmic loads

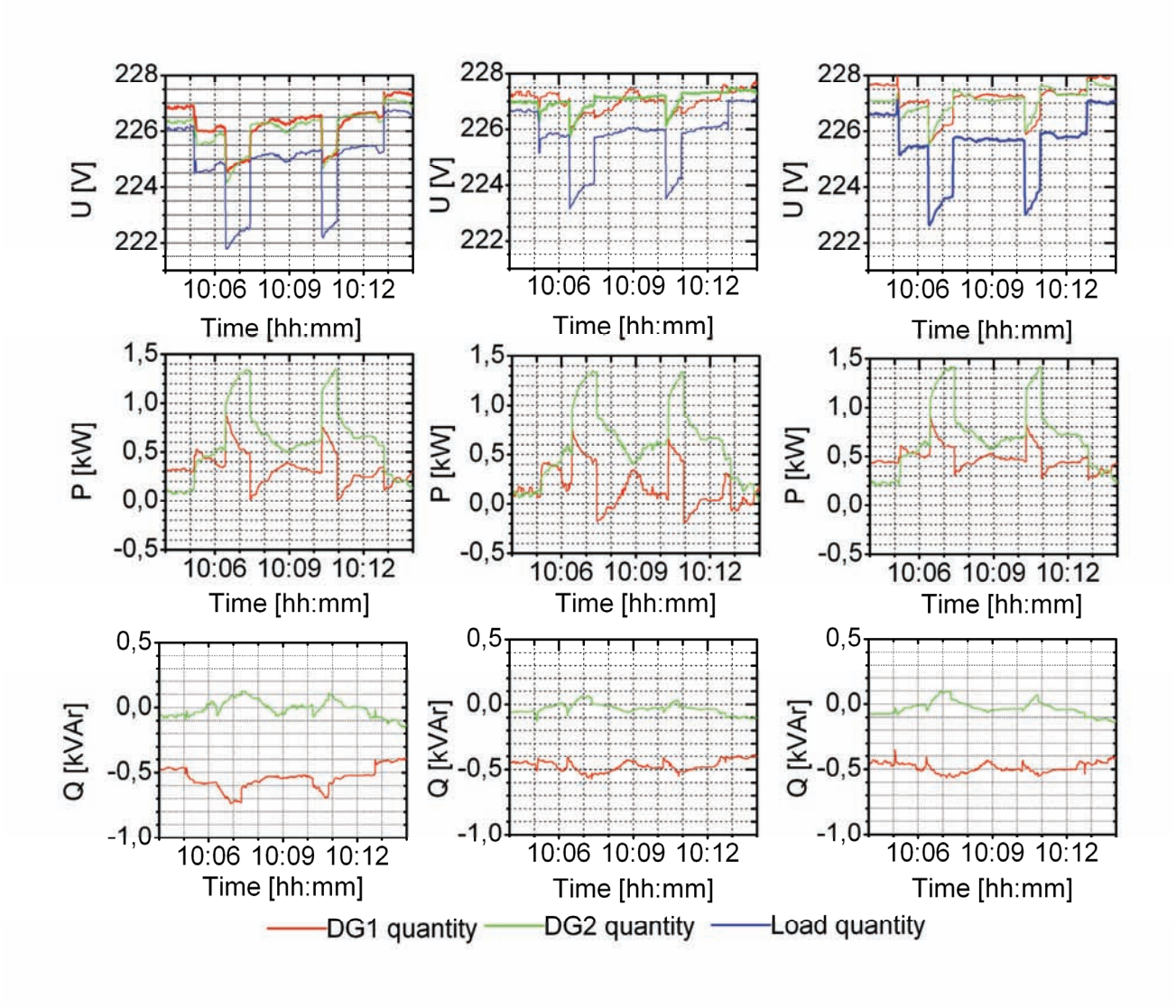

Figure 4-13: Per phase load voltage (in blue on the top row) and the corresponding voltage profile at the DG and load nodes and the per phase active and reactive power (all phase 1 quantities are on the first column from left, phase 2 on the middle column and phase 3 on the extreme right column) with DG1 quantities in red colour while of DG2 in green and the load in blue

In Figure 4-13 shows the profiles of phase powers and voltages of the DGs and the load voltage. From the upper column from the graph of the above figure it can be seen that the load and DG voltages differences reached more than 2 V and the lowest voltage at the load was around 222 V which is about 3,5 % lower than the nominal of 230 V.

The above results confirm the parallel operability of Micro-Grids and their ability to share the load and exchange reactive power even via relatively long transmission lines. However, this kind of operation needs one to look out for overall system inefficiency since a lot of power is used just to

energize the system components. In the present case connecting small Micro-Grids (of this power range – 10 kW or so) via such a big MV system (3 x 100 kVA transformers and lines some 20 km or so may end up uneconomic since more than 6 % of the exported energy will be lost in the system.

4.4.5 Reactive power exchange with inductive load result and discussion

In this subsection the results of the experiment for the inductive load operation are presented. As earlier on described an asynchronous motor was run with no load. Two cases are presented. The first case is that the two DGs supply the inductive load via the MV system and the other where one of the DGs is directly connected to the load as represented in Figure 4-6 and Figure 4-14 respectively.

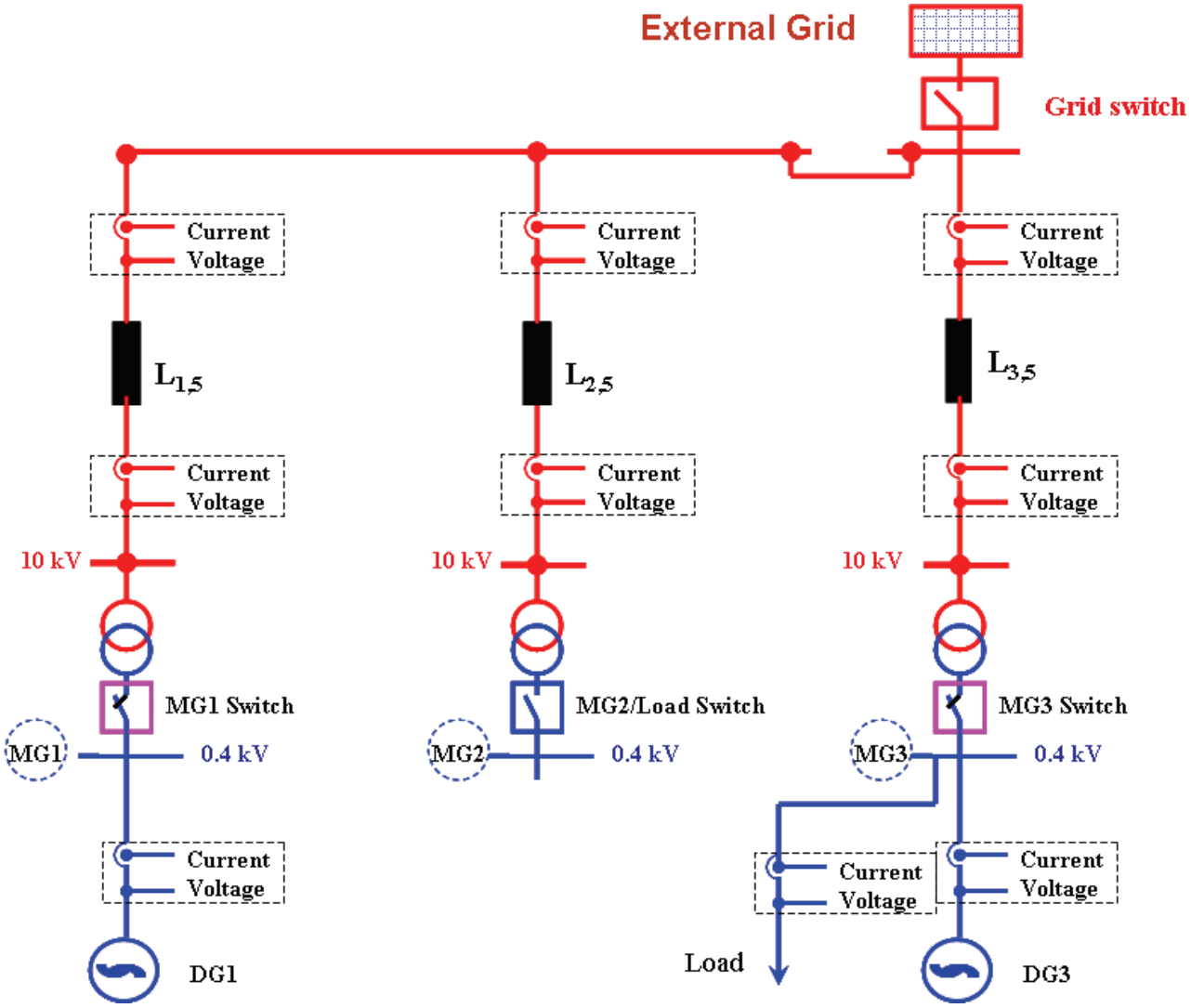

Figure 4-14: Power support among Micro-Grids through the MV system

In Figure 4-15 the three phase active and reactive power exchange between the two DGs is shown. As can be seen from the graph, at start-up of the motor sharp spikes in both active and reactive power are seen and the voltages at the DG nodes experience a sharp decrease resulting in the inverters of DG2 tripping off and only to reconnect about half a minute later. During this time all needed active and reactive power was delivered by DG1. This resulted in a degradation of the phase voltages in this case lower than 200 V (see graph in Figure 4-16 during the time interval 11:13:24 to 11:14:24). It is notable that after the reconnection of DG2 and some transient phenomena both DG units started sharing the needed reactive power for a short time leading to an improvement of the voltage. These high spikes are a result of the high inrush current for asynchronous motor start-up. Figure 4-17 shows an overview of the phase quantities (active and reactive power and voltage) per inverter cluster (all DG1 quantities are marked in red, while DG2 in green and on the load in blue).

At 11:14:20 DG1 was intentionally disconnected from the load and as can be seen from Figure 4-15, Figure 4-16 and Figure 4-17 and DG2 took over the whole power demanded by the system. A detailed view of each phase for active and reactive power is shown in Figure 4-18.

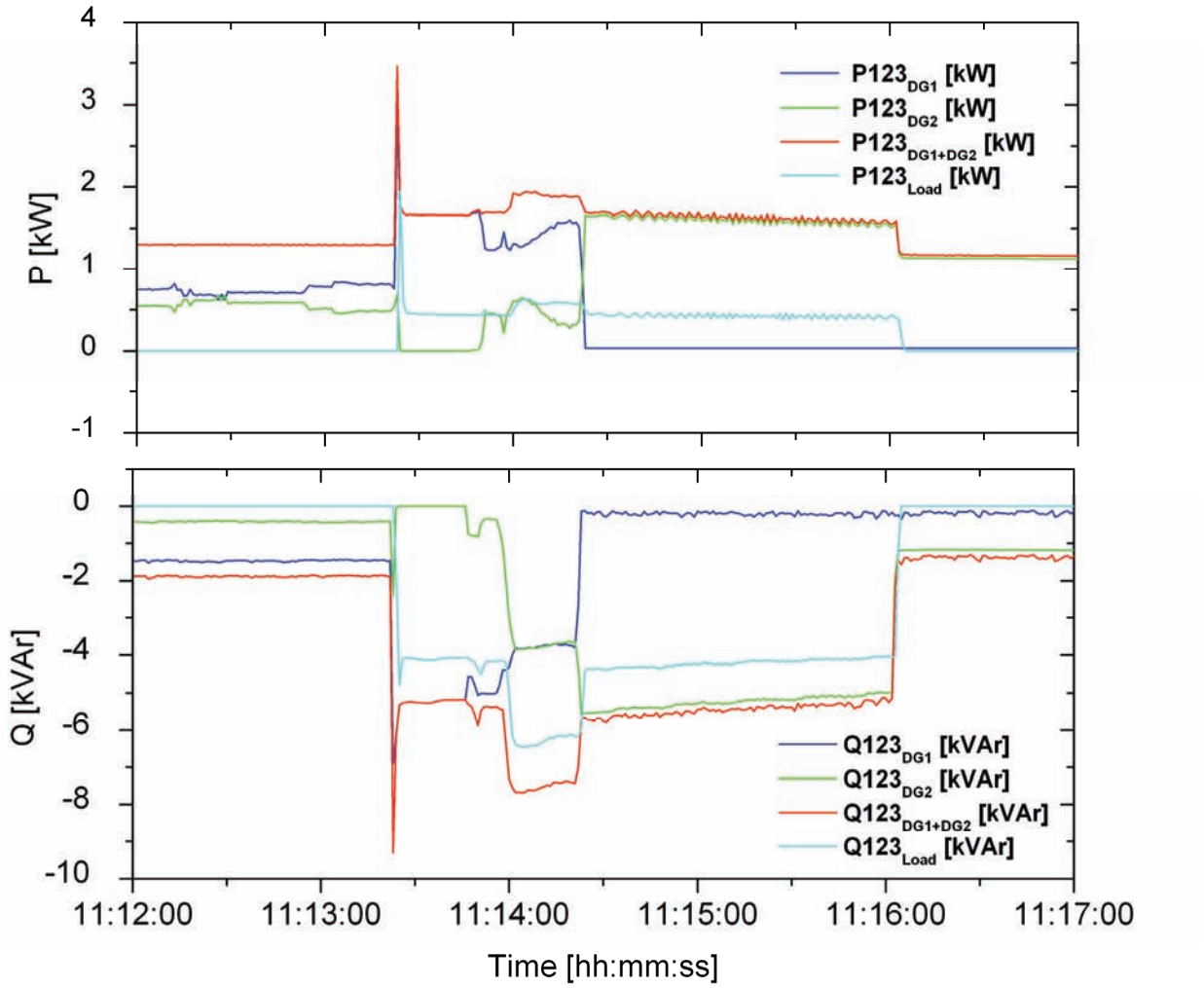

Figure 4-15: Three phase active power and reactive power exchange between the two DGs showing the totals of the phase powers for each DG (with DG1 quantities in blue, DG2 in green), the sum of these totals in red. Included also in this diagram are the three phase totals of the active and reactive power measured at the load node (light blue).

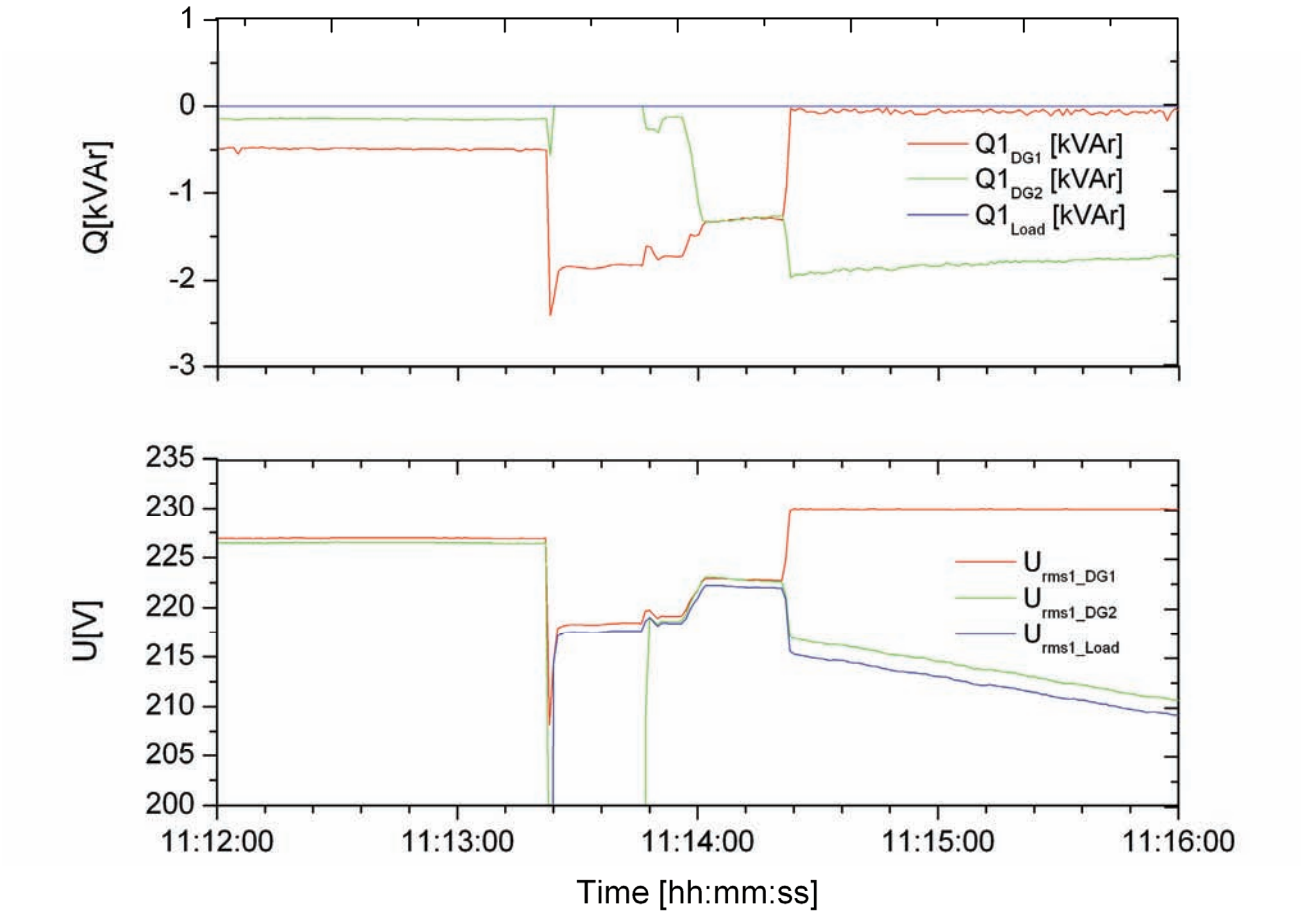

Figure 4-16: Phase 1 voltage and reactive power of the two DGs at inductive load operation (the two DGs supply the power through the MV system)

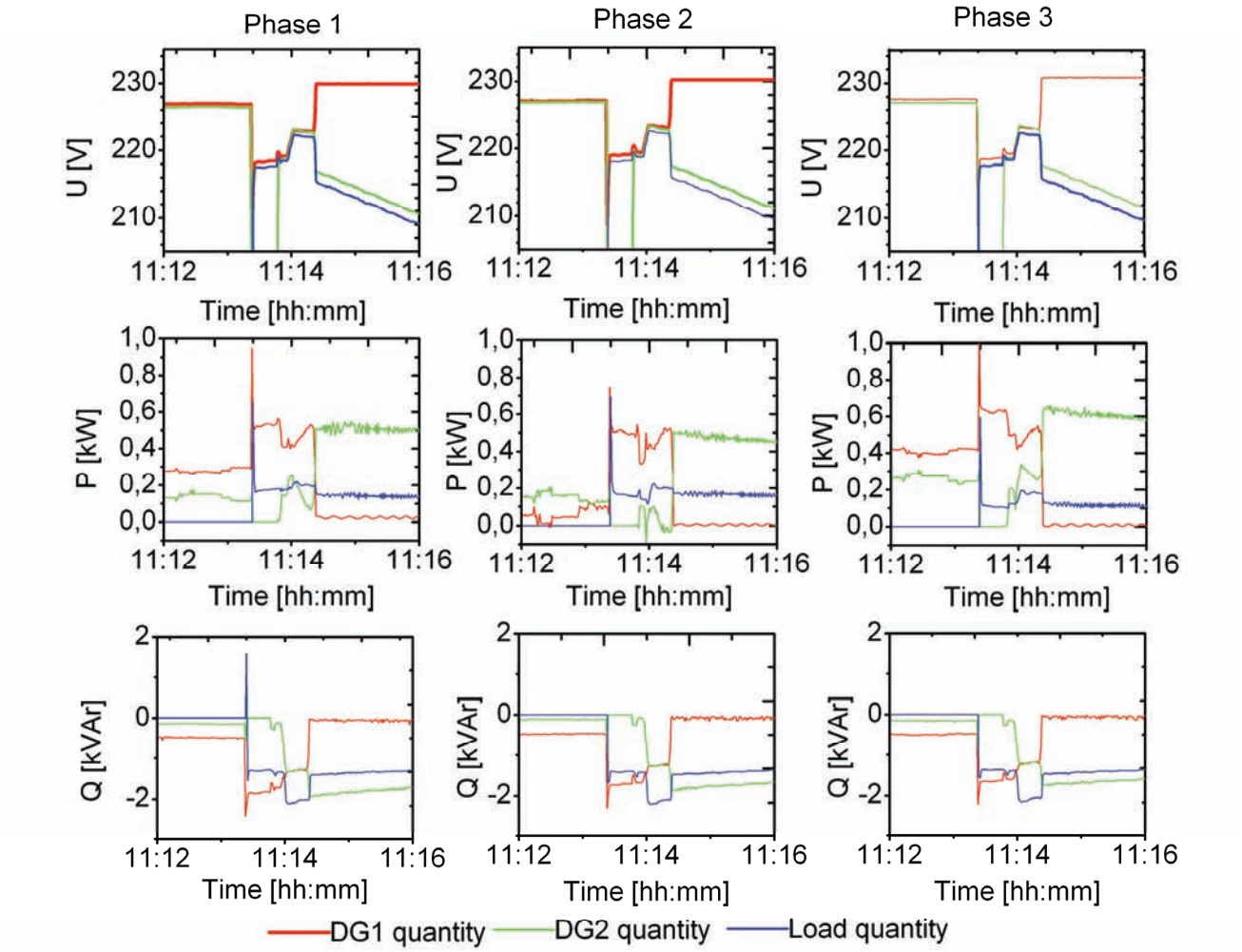

Figure 4-17: The per phase quantities (active and reactive power and voltage) per inverter cluster (DG1 in red, DG2 in green) and on the load (blue), with the columns marked with the corresponding phase

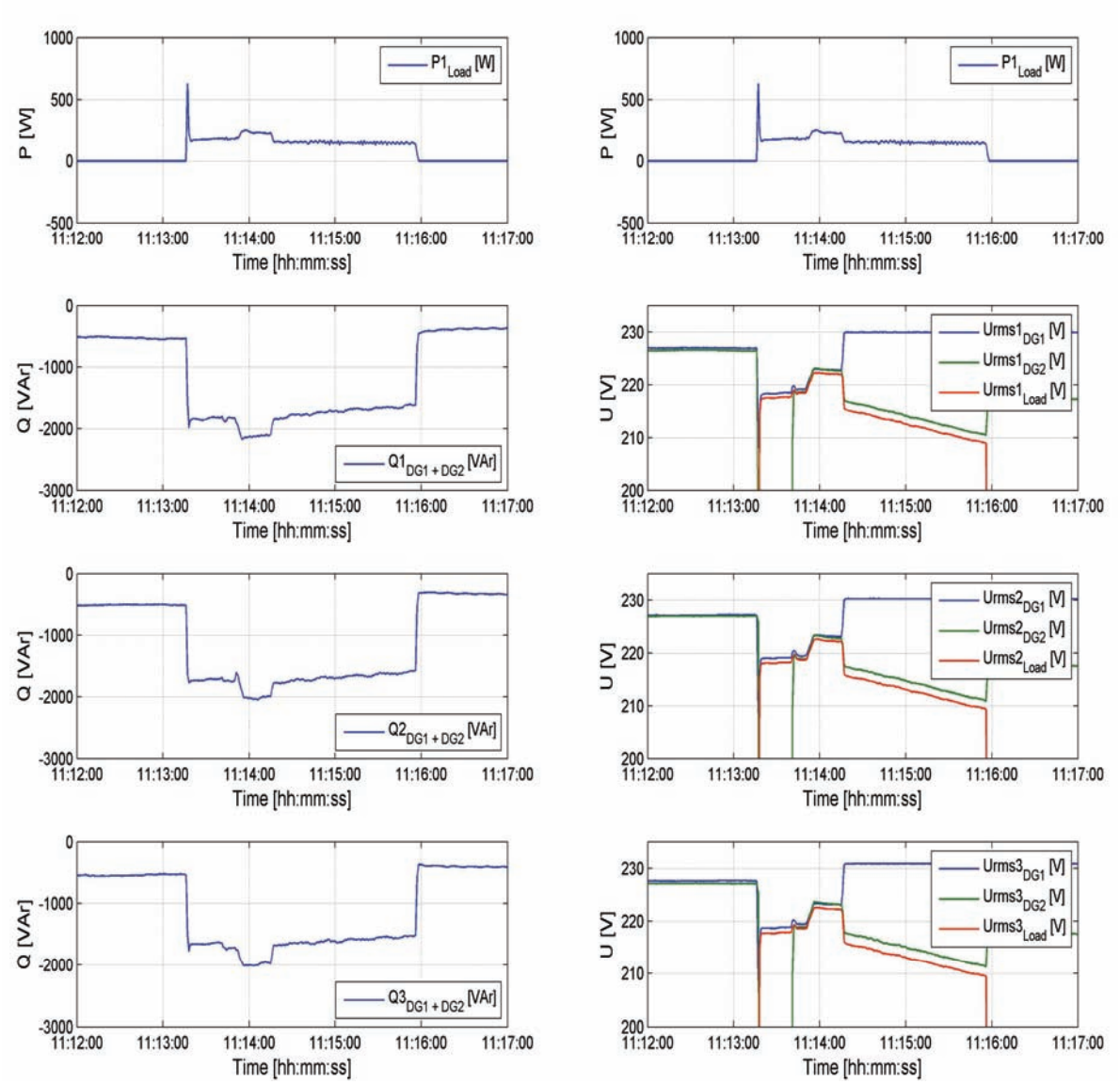

Figure 4-18: Per phase total reactive power and corresponding phase voltages, on the top row the same graph showing load power and the total per phase reactive power and corresponding voltage from second row through to third row (on voltage red is for load, green for DG2 and blue for DG1.

While Figure 4-17 shows the per phase quantities, in Figure 4-18 the total reactive power per phase (sum of the reactive power from DG1 and DG2 on each phase) and the corresponding voltages are shown. The voltage behaviour in the three phases is similar and influenced by the inductive load – the motor. However, the effective voltage drop is not as big as in the case of resistive load, thus the slope for the droop of the inverter must not be set too high for this case since even a small amount of reactive power (loads) could decrease the voltage enormously. Also the additional reactive power for the MV-system has to be considered for an optimal choice of the slope.

In Figure 4-19 the results of the test for the active power sharing and reactive power exchange by Micro-Grids in a case where the Micro-Grids are connected via medium voltage system are shown. This scenario represent a situation when more power demand than generation is experienced in one of the Micro-Grids and thus the others support by exporting the power to the deficient and is represented by Figure 4-14. In this scenario both resistive and inductive loads are applied.

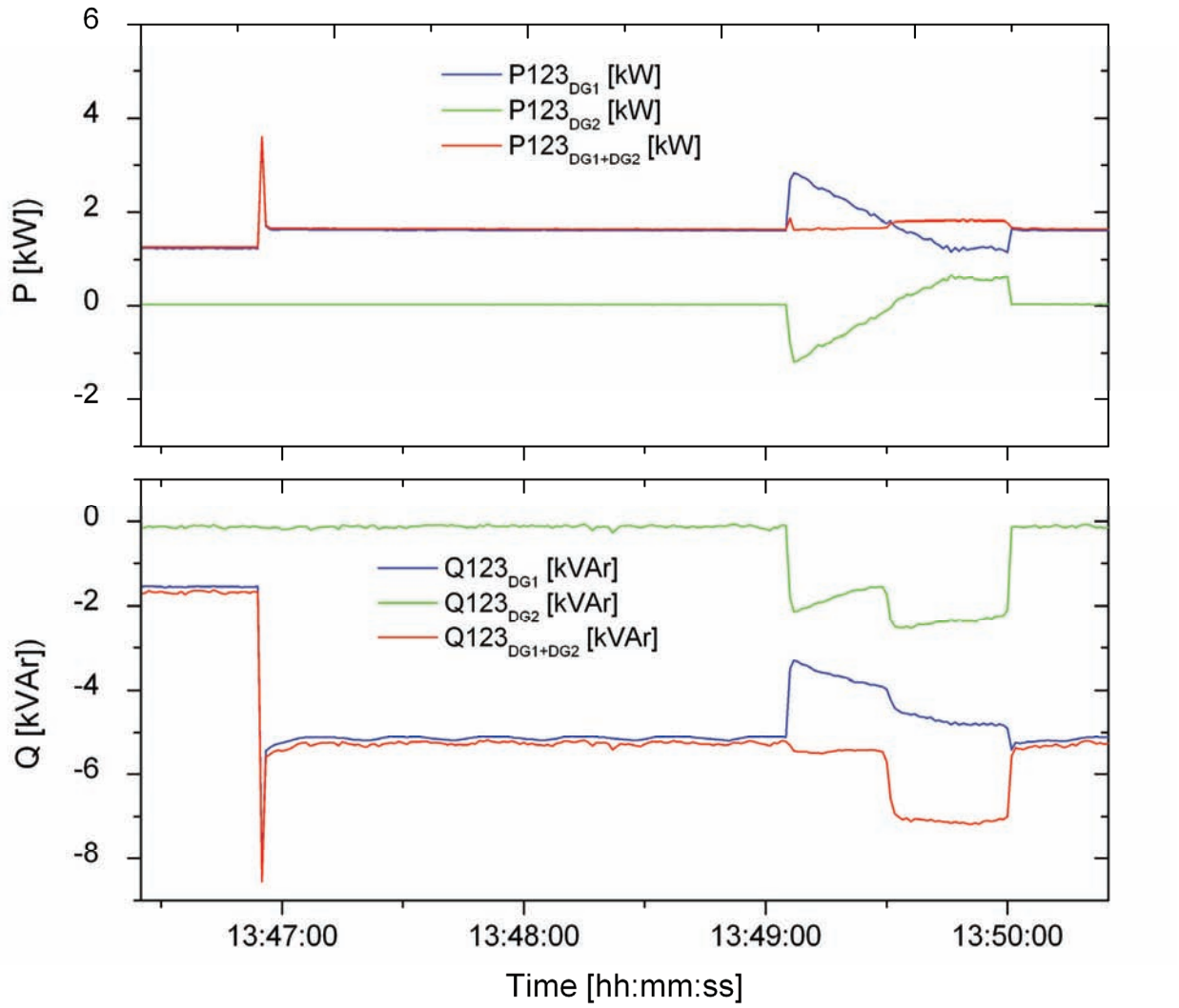

Figure 4-19: Support among connected DGs through the MV

As can be seen from the above graph even the more distant DG is seen assuming the load in the case when the local production is not sufficient or not available at all.

4.5 **Conclusions**

This chapter of the thesis has experimentally demonstrated the reactive power exchange and the transient active power sharing of Micro-Grids via the MV-system. Inverters controlled with the ‘droop concepts’ (f-P and V-Q static control characteristics) were used as the DGs in the experiments. The concept of parallel operation without any dedicated communication of Micro-Grids powered by droop controlled inverters is possible, even if coupled via a MV network was thus proved. It was also shown that active power sharing is done according to the relations of the inverse impedance values of the connecting network elements and according to the inverter internal parameter settings. The sharing of reactive loads by the inverters was seen to be basically according to the (controllable) voltages at the inverters, while the line parameters are of secondary importance. The measurements also show that the controls implemented in the used inverters do not quickly lead to a stationary operation point of the system. Furthermore it may happen that one inverter is delivering active power, while at the same time the other inverter is consuming the active power. An improvement of the implemented controls seems required. It has been noted also that changes of active power demands may lead to changes in voltage and due to the voltage / reactive power droop to changes in the reactive power. In the investigated configuration these interrelations are small; however in other configurations the dependency may become stronger. It can also be noted from this chapter that especially for reactive type loads the droop parameters must be selected carefully in order to guarantee that the voltage stays within certain limits. In contrast to coupling of the inverters in low voltage network works, coupling of the inverters via medium voltage network requires the stronger consideration of network impendence determined by lines and transformers.

Chapter 5 **Experimental simulations of mesh topology of Micro-Grids**

5.1 **Introduction**

In this chapter additional technical aspects of interconnected Micro-Grids in the low voltage level are investigated. The central idea of the chapter is to explore additional ways of voltage regulation especially utilising the micro sources themselves in such power systems with varied topologies. The method of reactive power injection as a way to regulate voltage in meshed low voltage power system is studied by simulation and experimentally validated.

With the ever increasing use of Micro-Grids in power systems more aspects on their operation still need further studies. This chapter is dedicated to the experimental investigation of yet another technical aspect concerning voltage regulation in interconnected Micro-Grids in the low voltage level. The central idea of the chapter is to explore additional ways of voltage regulation especially utilising the micro sources themselves in such power systems with varied topologies. The method of reactive power injection as a way to regulate voltage in meshed low voltage power system is demonstrated both experimentally and by simulation in ATP – EMTP (Alternate Transient Program – Electromagnetic Transient Program) numerical simulation software.

Thus here the test results of a method of voltage control in island low voltage meshed networks are presented. The P-Q coupling of the low voltage grids due to the line characteristics is experimentally assessed with regard to efficient voltage control. A three generator / inverter (with droop control) system connected in a closed loop resembling the simplest possible topology with a meshed network, will be used as a test system. Voltage control is done by injecting reactive power to the nodes where this is required to regulate the local voltage. Below a short background to the problem of voltage control issues is given.

5.2 **Reactive power injection – voltage control mechanism**

As presented in chapter 3 of this thesis, the voltage drop in any RL (resistive-inductive) circuit can be approximated by PR+QX with P and Q being the active and reactive power flow, R and X the resistance and reactance of the circuit. In overhead HV or MV lines, R is much lower than X, so that the injection of reactive power critically affects voltage drops. Active and reactive power effects are reasonably decoupled and this is the basis of system control. On the other hand, in underground low voltage networks, R is much higher than X. This results in strong coupling of active and reactive power. This coupling affects the voltage drop control and may lead to stability problems in Micro-Grids.

Several methods have been presented to solve these problems. In [36] a decoupling method based on a new P and Q variable has been proposed. In [37], an additional power term is added to the angle to improve the stability. In [23], the fictitious impedance method is presented. In this method the inductive response of the source is simulated to make the coupling among the inverters inductive. In [16] a method of inductive decoupling in the low voltage lines was presented. In this an inductor of the correct inductance (i.e., the size of the inductance is such that the reactive and active power in the low voltage grid are decoupled, thus the voltage difference and active power flow could be controlled separately).

In this case here, for meshed low voltage grids voltage regulation was achieved by injecting reactive power of the correct magnitude and sign to the generator node. This has the effect of varying the terminal voltage of the generator thanks to the additional degree of freedom possessed by voltage source inverters with droop control mode. In these inverters the power factor is generally not set to a fixed value (often 1.0) but regarded as an additional degree of freedom of connection which is set in every individual case in order to meet the local requirements. The application of the droop method especially in these low voltage network is possible due to the inductive impedance at the output of inverter (from the harmonic filter mostly LCL type at the AC side of the voltage source inverters and such grid connected inverters).

5.3 Experimental description and objective outlining

Since in transmission grids the lines are generally inductive and thus the voltage is regulated through control of reactive power, the reactive power sources and sinks and other reactive power compensation equipments are strategically positioned along the long transmission systems. Although in the low voltage grids reactive power transfer is not directly linked to the voltage regulation, if the grid is formed by generators/inverters with droop control mechanism, the voltage could still be controlled through the adjustment of the reactive power. Thus this section describes the experiment carried out in the DeMoTec meant to assess voltage regulation in meshed low voltage grids. This experiment aims at practically demonstrating capabilities of voltage regulation by the method of reactive power injection using the DGs themselves – in this case the SMA battery inverter SI5048 (SI_{50}) and SI4500 (SI_{45}) were used. Reactive power of the correct sign and magnitude is intentionally injected to the 'generator' nodes to influence the terminal voltage of these and thereby correct the voltage profile of the grid system. The whole system works due to the droop mode of the inverters. Any voltage change in the grid is sensed by the inverter and the inverter's voltage/reactive power droop controller changes the local set voltage when the reactive power generated by the micro-source exceeds the highest level [27]

The droop control mechanism in the microsources is used in the voltage control in the experimental investigation presented here. Three battery inverter clusters with Q-V droop control function are connected in a closed loop topology as seen in the picture of Figure 5-1 and the simplified line diagram of Figure 5-2. The third inverter cluster was meant only to inject the needed reactive power for the regulation of the voltage of the system. So the two inverter clusters marked $SI_{45-INV1}$ and $SI_{45-INV2}$ were made not to compensate for reactive power that means they only absorb that which is supplied by the third inverter marked $SI_{50-INV3}$. So when the inverter absorb reactive power Q from the inverter injecting this, the Q is multiplied by the droop gradient (k_q) and summed with the required voltage E_{req} to obtain a new set-point (E_0) as explained in previous chapters(see equation (3.21) with (k_q) taking the place of (m_Q)). Important to note here is that the reactive power used for the voltage regulation is supplied from a remote point and thus the voltage controlled from this point.

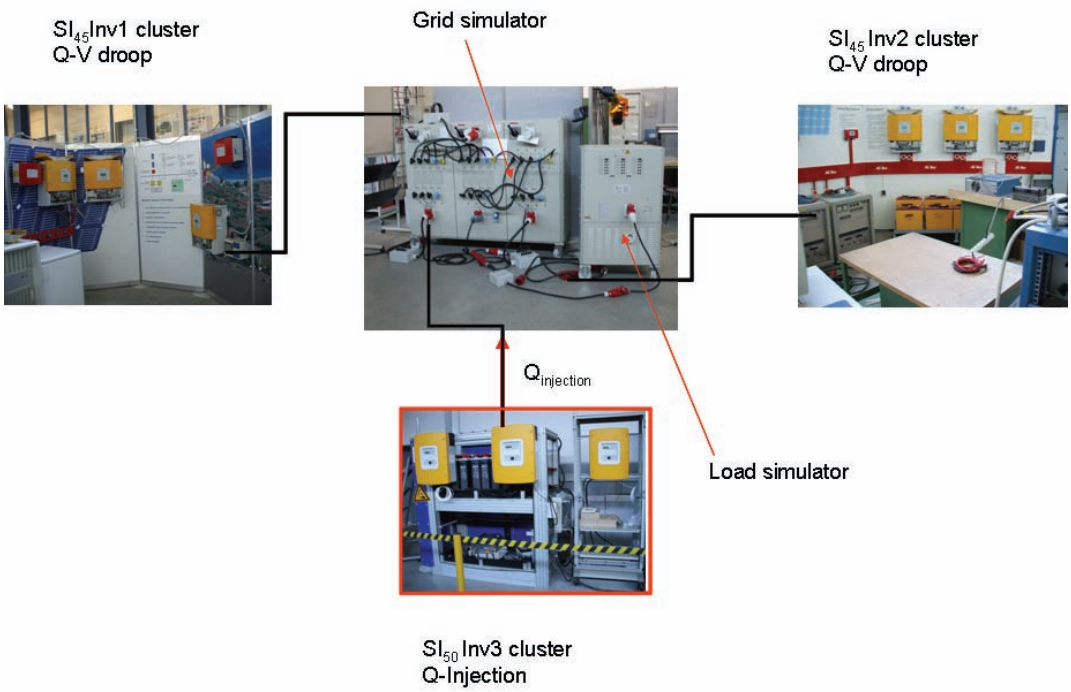

Figure 5-1: Mesh grid experimental diagram in the DeMoTec with component pictures

A balanced three phase mesh grid was built up as shown in the diagrams of Figure 5-1 and Figure 5-2 show the experimental setup of the mesh grid built up in the DeMoTec. The two clusters were built up from SI_{45} and the third from the SI_{50} inverters. The SI_{50} inverter was used to supply the required reactive power without active power support, and the others in droop mode.

In Figure 5-2 the one line diagram of the mesh grid is shown with the corresponding line resistances. The line lengths could be varied by changing the line resistance that selectable from the line simulator. The simulated lengths are shown in Table 5-1 as calculated from the typical line parameters information for low voltage lines given in Table 5-2. The resistive load could also be varied connecting the corresponding load slots on the load simulator. For the analysis of the results only one phase was considered and the others assumed similar since the three phase system was balanced. So the measurement devices were connected on the four points on the circuit on the same phase (see Figure 5-2 points with the HAAG measurement device symbol). The device measured voltage and current and derive the rest of the quantities like powers.

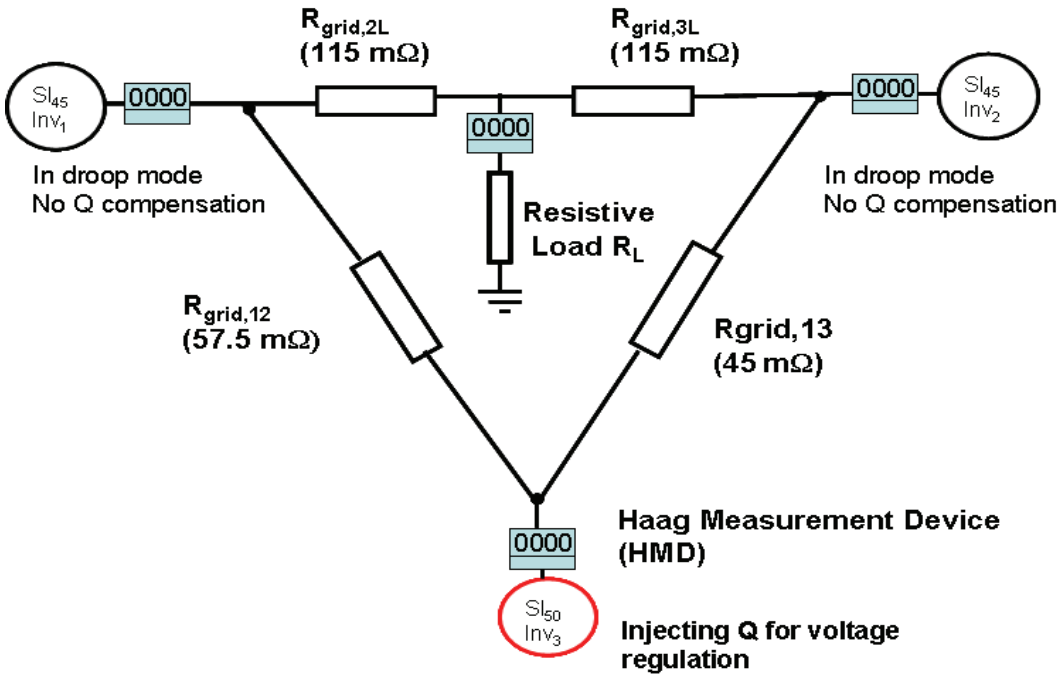

Figure 5-2: One line diagram of the mesh grid

Type of line	R' Ω/km	X' Ω/km	I_N A	$\frac{R'}{X'}$
low voltage line	0.642	0.083	142	7.7
medium voltage line	0.161	0.190	396	0.85
High voltage line	0.06	0.191	580	0.31

Table 5-1: Typical Line Parameters [46]

Line	Line resistance in ohm	Line length in m
R_{12}	0.0575	90
R_{13}	0.045	70
R_{2L}	0.115	179
R_{3L}	0.115	179

Table 5-2: Line resistances used in the experiment and the corresponding calculated lengths according typical parameters give in Table 5-1

5.4 **Experimental procedure**

One cluster was first switched on to form the grid and the others had to synchronise to this formed grid. Different resistive loads were connected in steps and the voltage profile always monitored on the data acquisition device – the Haag power analyser device. Each time voltage profile would be seen to vary significantly reactive power would be injected from the Sunny Island 5048 thanks to this capability the device has. However, unfortunately the parameter for this capability is not at customer level but an SMA level. That means, to have this function one requires the manufacturer key. In particular, in this test, active and reactive power sharing by the inverters (sources) within the mesh could be assessed. Voltage could be controlled at a node by injecting into the node a Q of the correct sign and magnitude. The test was done as follows:

1. With constant reactive power injection, the load was varied and observed how the voltage at the node varied, then maintain the load constant and start injecting reactive power
2. After a the voltage is corrected, the reactive power is maintained constant and start to reduce the load, thus allowing voltage to increase
3. Finally reactive of a opposite sign is injected (in other words the inverter absorbs back the reactive power and that way restore the voltage)

Each time the reactive power injecting inverter was meant not to contribute any active power to the load, that is, its sole purpose was to act as a reactive power compensating device. The results of these experiments are presented below.

5.5 **Presentation of experimental and simulation results**

The objective of the experiment to use the inverter to supply the required reactive power was achieved. Experimental results and some samples of simulation in ATP –EMTP are presented below. The results are presented in the following two major scenarios:

Scenario 1: Constant reactive power injection with varying load

In this scenario the load was varied in steps from 1300 W, 800 W to 300 W while reactive power injected was maintained at a constant value of about -800 VAr as can be seen in Figure 5-3. From the results it can be seen that the inverter's response to load change is not 'instant', although this could also be attributed to human reaction time on manually changing the load by pulling out or inserting the load selection connectors. This is shown in the Figure 5-3 by the peaks at each change of load on each of the parameters plotted that would decay to a constant value after some few seconds. Since the inverters SI_{45} were not set to supply reactive power, voltage (mid diagram) at all nodes would continue to rise (to about 232 V when the load was at 300 W) as the load decreased as shown in Figure 5-3. This part serves to show the effect of reactive power injection. One thing to note here is the share of the load by the two inverters. Inverter 1 in light blue in the diagrams takes the bigger share in both load and reactive power exchange, correspondingly a slightly higher voltage. This can be attributed by the smaller resistance between this inverter and the one injecting reactive power (45 mOhm compared with 57.5 mOhm of the other see Figure 5-2). In this case more reactive current flows through a smaller resistance (short line) and the effect is greater reactive power absorbed at this point and hence higher voltage at the node. With higher voltage more power flows from this node.

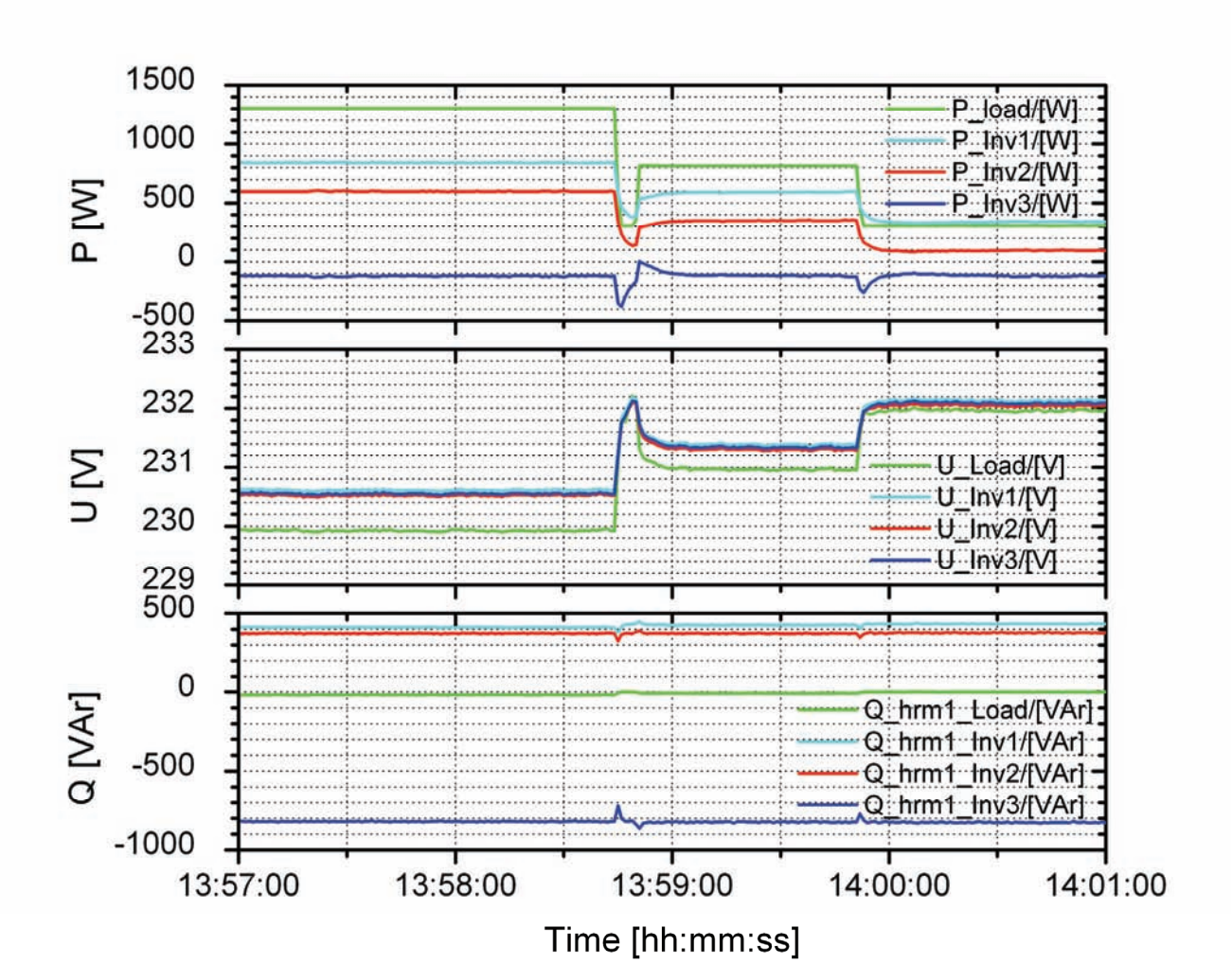

Figure 5-3: Effect of load variation on voltage with a fixed reactive power injection (experimental)

The experimental results are reproduced by simulation shown in Figure 5-5. The simulation circuit is shown in Figure 5-4. The diagram shows the components used in the simulation. Here the voltage source inverter is represented by an ideal AC voltage source with a series connected inductor to represent the inductive output impedance in the real voltage source inverters.

With the above assumption the simulation results approximate acceptably well to the experimental results. However the voltage change at the nodes from one load level to another is more pronounced in the experimental than the simulation, for example, in the experimental results the load voltage changes from 230 V to 231 V and then 232 V when load power changes from 1300 W to 800 W and then to 300 W with a fixed reactive power injection of -800 VAr, while in simulation about 230 V to

230.3 V and then 230. 6 V. This could be the assumptions used in the simulation, for example the voltage source inverter was assumed to be an ideal voltage source with an output inductance in series.

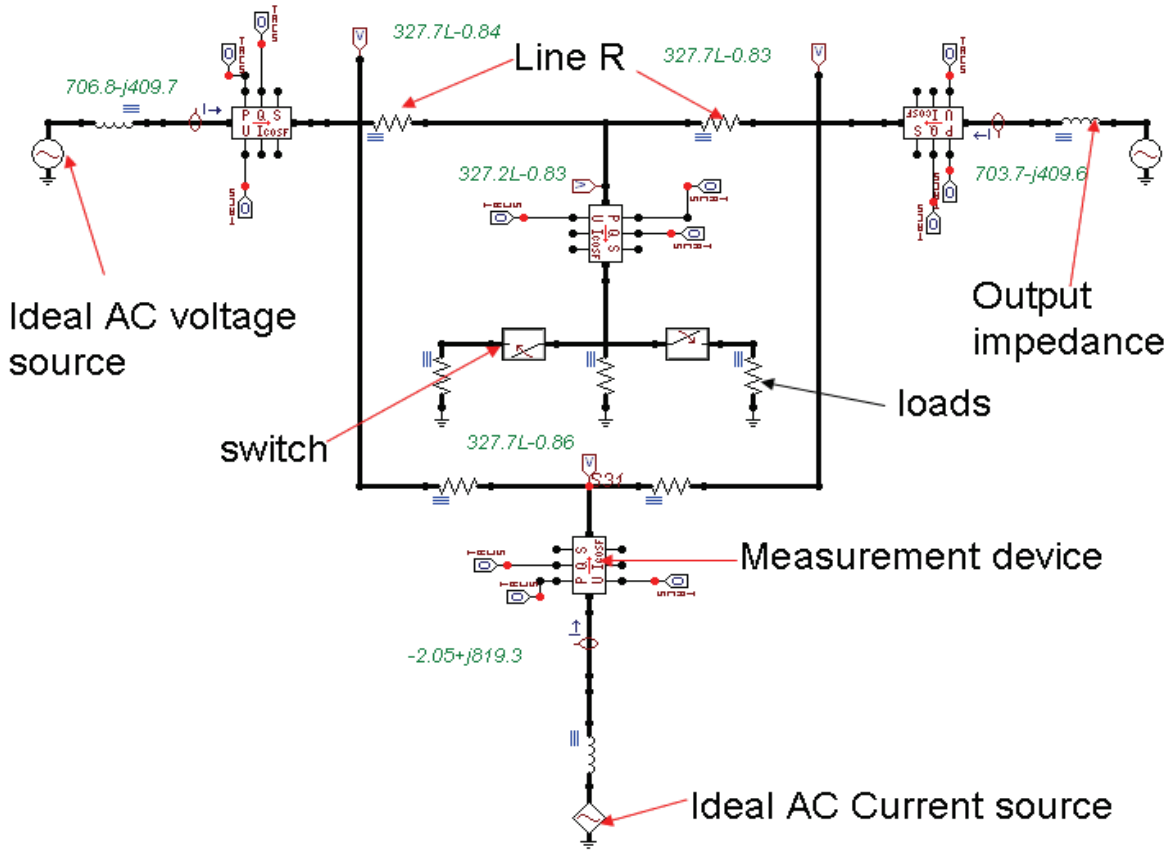

Figure 5-4: Simulation circuit diagram for constant Q injection with varying load

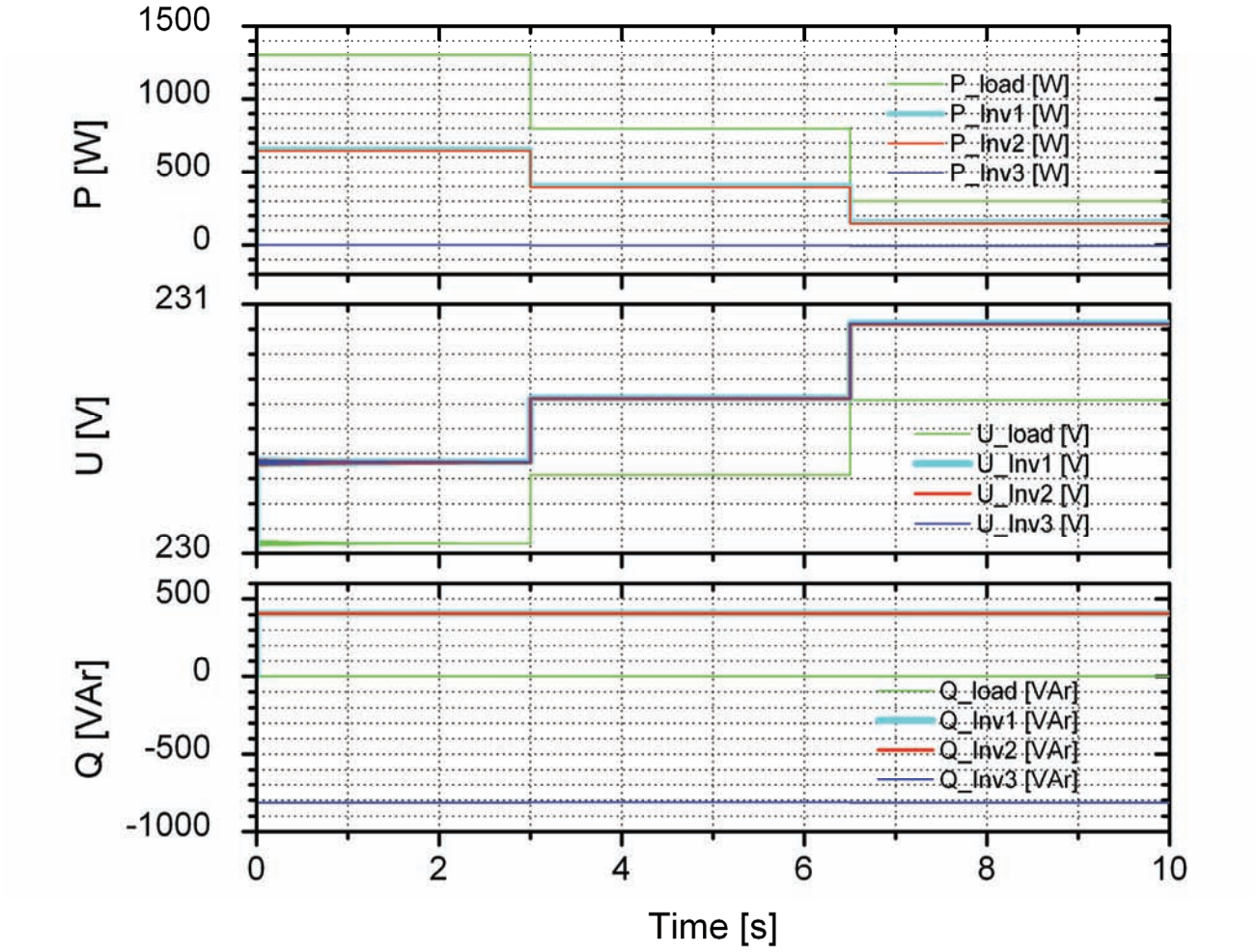

Figure 5-5: Effect of load variation on voltage with a fixed reactive power injection (simulation)

Scenario2: Voltage variation with varying reactive power injection with constant load

The graph of Figure 5-6 shows the scenario where the load is maintained almost constant but with already a high voltage and this is to be regulated to the required nominal of 230 V. The load is at 300 W and the voltages are close to 234.5 V with reactive power from the injecting inverter of close to 1500 VAr. Then reactive power is injected in the opposite direction, that is, becoming less negative and the effect is seen in the voltages dropping to 231.5 and 230.7 V corresponding to the reactive power change from -750 to -500 VAr.

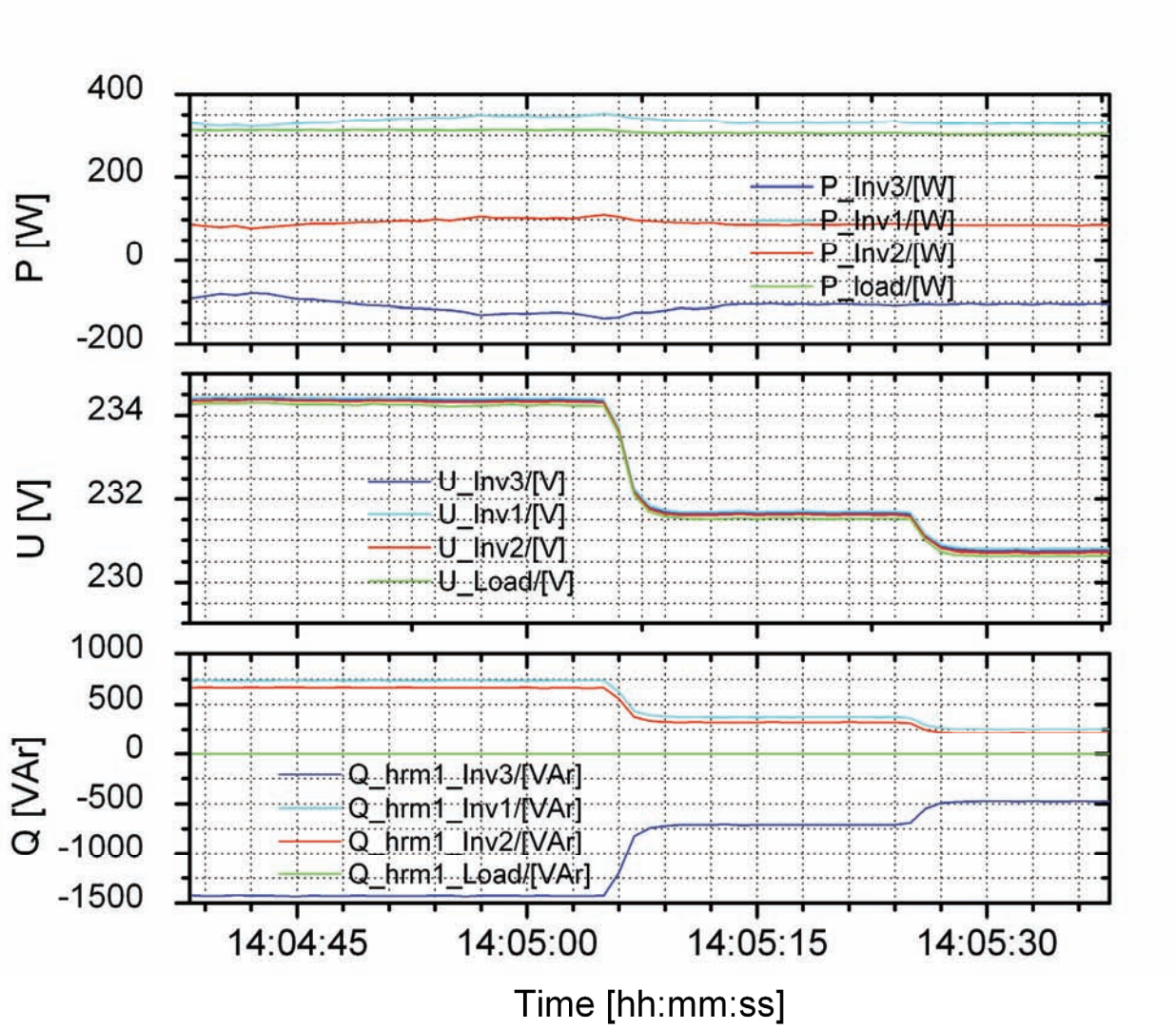

Figure 5-6: Dependence of the node voltages on the injected reactive power with constant load (experimental)

Figure 5-7 shows the simulation results of the dependence of the node voltages on the injected reactive power with constant load. The results show an acceptably good representation of the experimental results. However as in the previous situation, the amount of voltage variation is more pronounced in the experimental results. But, like in the experimental results the simulation voltages are also packed together for the four nodes, thus their difference is difficult to see.

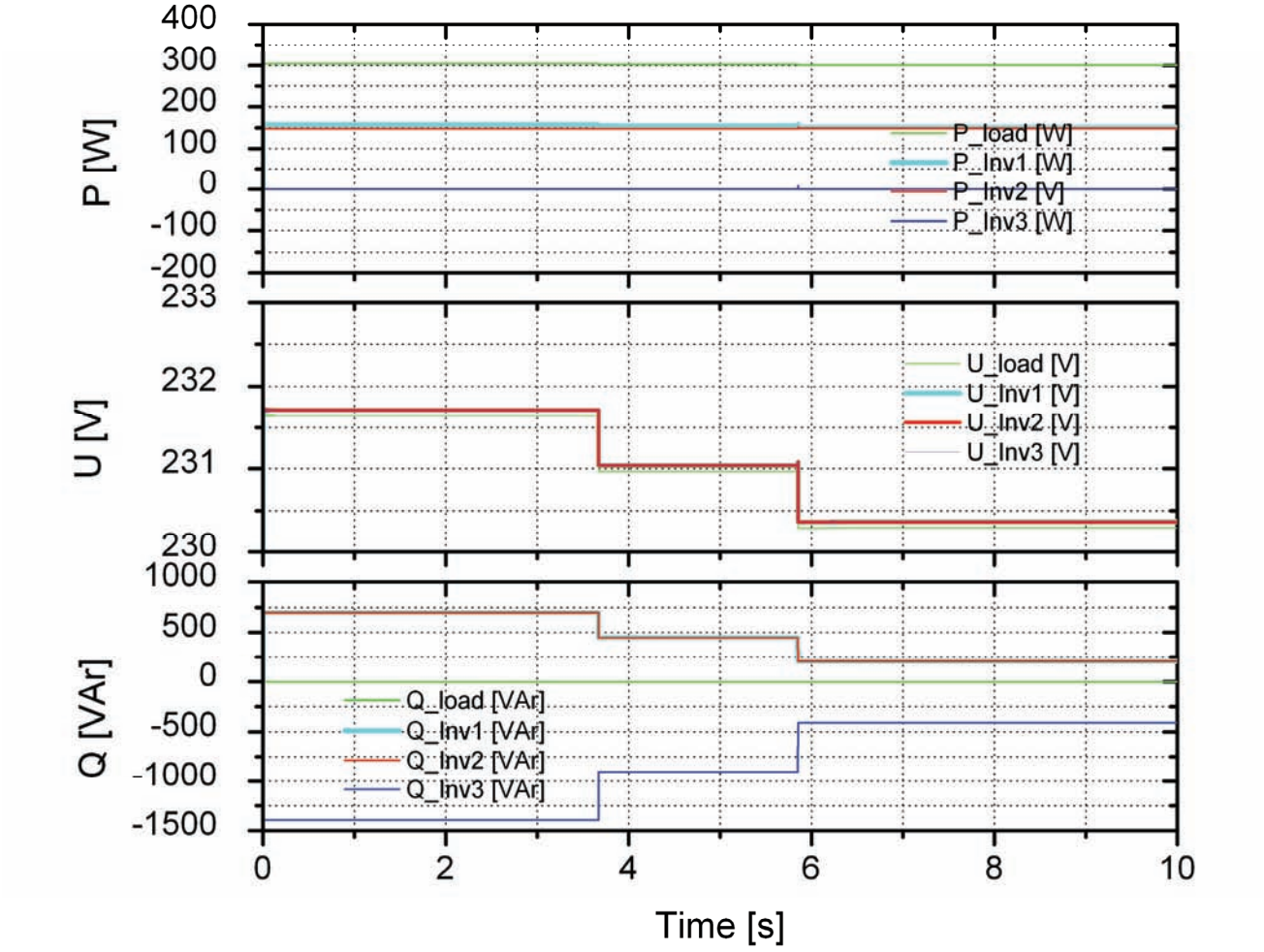

Figure 5-7: Dependence of the node voltages on the injected reactive power with constant load (simulation)

In the diagram of Figure 5-8, with a constant load of 1300 W and thus voltage at the different nodes as low as 225.5 (at the load node), reactive power is injected starting from positive about 450 VAr, then to -100 VAr in steps to -800 VAr and the node voltage follow suite, increasing in corresponding jumps to 230 V for the load node and slightly higher (230.5 V) on the inverter output nodes.

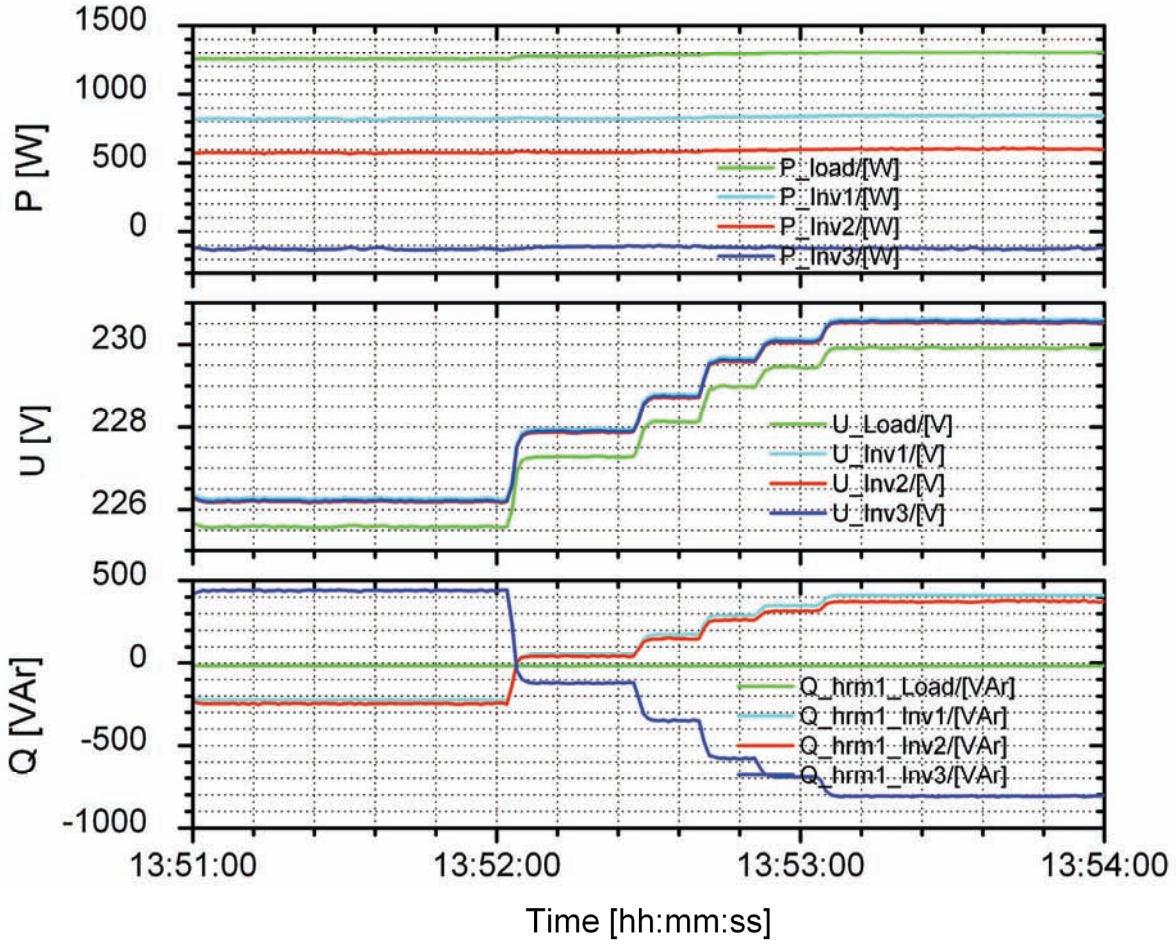

Figure 5-8: Voltage correction by reactive power injection (from positive $Q_{injected}$ to negative $Q_{injected}$) (experimental)

5.6 **Summary and conclusions**

As can be seen from the results of the experiment the voltage profile in the mesh low voltage grid can be effectively corrected by a deliberate injection of the right magnitude and type of reactive power to the generator node. The experimental results are reproduced by simulation in ATP-EMTP. The voltage variations from the simulation are slightly smaller than those obtained from the experiment but however these compare well the experimental results. Thus with reactive power maintained constant, a decrease of load corresponds to an increase of node voltages unless reactive power of the correct magnitude and type is injected. In all these cases we see the distribution of the

active power within the mesh grid. The inverter injecting reactive power has no contribution to the load. This was intentionally set like this. The active power sharing among the other two inverters is according to the reactive power flow share and corresponding nodal voltage profiles.

As can be seen the voltage control capability of the method of reactive power injection is evident. So as conclusion, it has been experimentally demonstrated that voltage at the load could be controlled by injecting reactive power at the nearest generator nodes to the load in the low voltage meshed grid. Thus the benefit of using inverters to inject reactive power in the mesh low voltage networks is that the reactive power can be injected in a continuous way hence control the voltage in the same way unlike the discrete way in most voltage regulation devices in use presently. There will be therefore no need for additional components for the sole purpose of regulating voltage, hence may even reduce the cost of the system.

Chapter 6 **Feasibility study of a village power system for a dairy farm in rural Zimbabwe: Case study**

6.1 **Introduction**

Although most of the commercial farms in Zimbabwe are grid connected, in most cases it is only the farmhouse and strictly the farm activity centres that have access to electricity. The workers' residents and the villages around are in most cases without electricity. The extension of the connection to these villages could be relatively cheap since they are close to the farms. However, with the nationwide grid unreliability due to insufficient generation and foreign currency procurement problems this new demand would always remain poorly covered. To worsen the situation the whole region is facing a power shortage due to higher demand growth rate without corresponding growth in generation. Presently Zimbabwe is generating less than 50 % of its demand. The utility is now resorting to heavy load shedding and this is adversely affecting the farming activities of these farms. However, most of such farms have the potential to generate more than enough electricity for their local use and even have excess for sell to the grid using locally available resources. This study is thus meant to demonstrate the viability and feasibility of local generation of electricity using farm waste and other renewable energy resources locally available. In particular the renewable energy technologies assessed are the biogas and photovoltaic.

6.1.1 **Approach and methodology**

The option of PV/bio-gas hybrid power systems may suit many farming areas around the country. These hybrid power systems especially with the biogas taking the biggest share are not yet popular in the country and region, worse of at the intended scales. So, during my five months period of field work in Zimbabwe I collected energy resource and demand data for three farms which practise crop growing and animal rearing. One of these farms is a dairy farm, and is the case study area and the other two keep beef cattle and grow crops and these are briefly presented in Appendix 1 and Appendix 2. The aim here is to show the resource availability in these farms.

In all the three cases I targeted to interview the managers of the farms to get detailed information regarding the range and size of farming activities carried out at the farm, the energy requirement of the farm and the future plans. In each case I also interviewed some workers from their varied 'income classes' to get a clue of their energy demand. The information collected from the workers would range from family size (number of males and females and their ages), members' occupations, energy consuming gadgets (e.g. radios, refrigerators, television sets, cooking stoves, lighting lambs and others) and the times these are normally used and for how long. Since most of the lower class of the farm workers have no such items their energy demand in case they have electricity would be estimated as will be shown later in this chapter.

To get the views, conceptions and misconceptions of different stakeholders I interviewed and discussed with a number of stakeholders that include farm owners and workers, surrounding villagers and officials from Zimbabwe Electricity Regulatory Commission (ZERC), Zimbabwe Electricity Transmission Company (ZETCO), Zimbabwe Electricity Distributed Company (ZEDC), Rural Electrification Agency (REA), Department of Energy (DoE), and the Ministry of Science and Technology. As a way of raising the necessary awareness I organised and held an all-stakeholders seminar at Bindura University of Science Education – Zimbabwe where presentations on the different aspects of the clean use of local renewable energy resources and policy issues regarding these systems in the country were given. Some local farmers gave presentations on their activities, energy problems, and how they manage their farm and manure wastes. The deliberations left it clear that these farms can benefit a lot by converting their waste into useful and cheap energy and by avoiding some costs in the farm expenditures like avoiding of chemical fertilisers by using the digested slurry.

Out of the three visited farm one was chosen be the study case. The main objective in this regard is to calculate the cost and benefits of running a power system using locally available renewable energy resources – sun and dairy farm wastes. A power system design is presented, however not so detailed but enough to demonstrate the viability and feasibility of such systems.

6.2 **Rosenwald - Lyondalel Dairy Farm**

Rosenwald - Lyondalel Dairy Farm is owned by Dairiboard Zimbabwe Limited located some 20 km from the eastern border town of Chipinge along the Chipinge-Chimanimani road. The farm has a total of 627 dairy cows and has plans to expand the herd size. This area falls under the country's Natural Region I with annual rainfall >1000 mm per year, relatively low temperatures and thus suitable for dairy farming, forestry, tea, coffee, fruit, beef and maize production) see map of Figure 6-1.

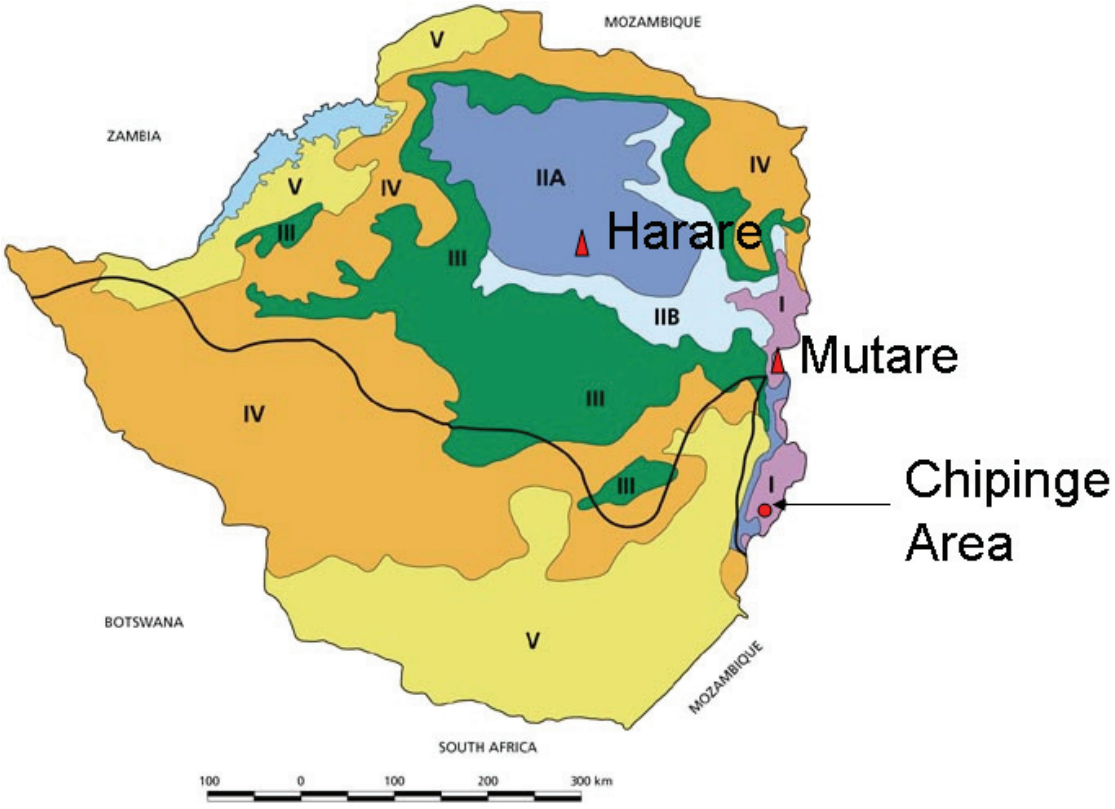

Figure 6-1: Zimbabwe natural regions [38]

Besides dairy farming, Rosenwald - Lyondalel Dairy Farm also tills 40 to 60 hectares for silage maize and 100 hectares for corn maize for cattle feed and also for sell to the Grain Marketing Board (GMB). Thus assuming an average of 550 kg/hectare (i.e. 300 kg/hectare per year of compound D or

compound Z and 250 kg/hectare per year of Ammonium Nitrate fertilisers)[4] [38] per year of chemical fertilisers applied for maize plant, the farm requires about 88 tonnes/year of chemical fertiliser for the total tilled land of 160 hectares and spends over US$10,945.00 per year.

For the electric load points on the farm, the milking parlour, farm workshop and cow spraying area are located within a radius of 100 m and the farmhouse about 500 m from the milking parlour. The workers' settlement compound is some 1.5 km away (see the satellite picture of the area on Figure 6-2).

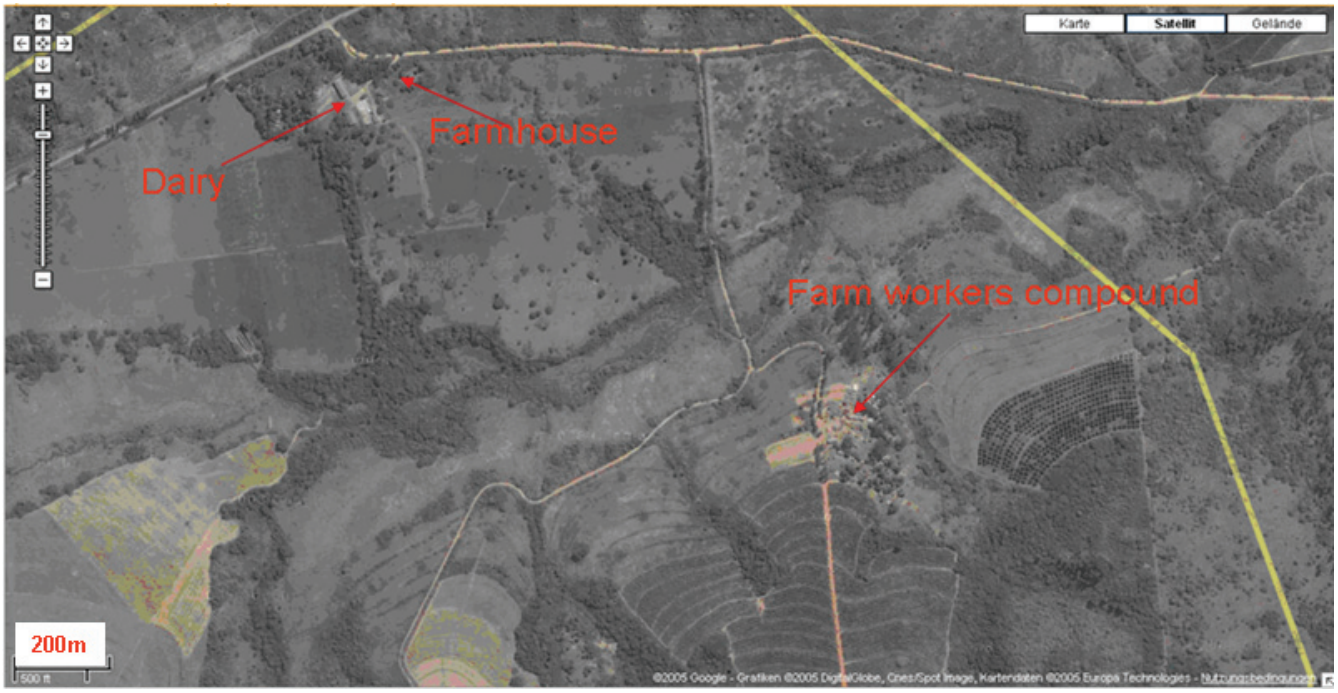

Figure 6-2: Google satellite photo of Rosenwald - Lyondalel Dairy Farm showing the relative positions of the dairy, farmhouse and workers' settlement compound

The farm is surrounded by yet other farms of similar sizes some as close as less than 1 km away. These farms are constant milk suppliers to the Chipinge Dairiboard factory (the biggest sterilised milk production factory in the country - see Figure 6-3) some 20 km from Rosenwald farm.

[4] Compound D fertiliser has 16% Nitrogen, 8% Phosphorous and 34 % Potassium and compound Z has 11% Nitrogen, 21.8 % Phosphorous, 4 % Sulphur and 1 % soluble Zinc

Figure 6-3: Chipinge Steri-Dairy Board Factory (This is the biggest sterilised milk production and packing in the country about 20 km from the farm)

(a) (b) (c)

Figure 6-4: (a) Dairy cows grazing in the paddocks at Rosenwald Dairy Farm, (b) Cow feed in the warehouse at Rosenwald Dairy Farm, (c) Milking equipment at Rosenwald Dairy Farm

6.2.1 Demand analysis

This farm has a relatively high electricity need for its mechanised milking, chilling of milk before collection to the milk processing factory. The electric milking machines use vacuum pumps (see Figure 6-4 (c)). In addition to milking machines, the farm has hammer millers for cow feeds, compressors for refrigerators, and an electric motor for cow spraying[5] to control ticks. The farm is supplied by an AC 3 phase 4-wire, 11 / 0.380 kV, from an 11 kV feeder branching from a main radial feeder from the substation about 20 km away.

The houses in the worker settlement compounds (a kind of concentrated settlement for the farm general workers) consist of a standard 4 - roomed standard brick house and a separate normally grass thatched kitchen hut where open fire cooking is done. These houses are generally about 5 to 10 m apart. Family sizes range from single to seven or more members.

6.2.2 Load estimation and description

The farm village has 26 households in total living within a distance of 10 m from each other. Since most of the household presently have no electricity, to estimate the load demand I interviewed a number of both already electrified and not yet electrified villagers using energy need assessment questionnaires and some informed estimations. The discussions and interviews were done in a way to arouse interest and concern of the villagers to look for possible solutions to their energy problems. The facts and ideas that came out of these discussion-cum-interviews were varying depending on the social and economic class the subjects belonged. So from all interviewees energy demand data including sizes of households (number, sex, and ages), number of houses and rooms which need lighting, duration of stay in the night, other gadgets that use electricity and for how long these are used per day and their power ratings were collected. Also noted from these interviews are the present energy sources in use, for example, cooking would be totally from firewood and lighting is by candles and kerosene lamps. Lighting is needed during the night more in those families with school going children and those with a better income to afford entertainment like television sets. The “new”

[5] Spraying is used in place of dipping to control ticks.

ideas of converting the farm waste like cow dung and crop residues to cleaner energy form like heat and electricity from biogas was received with different reactions. Generation of electricity from biogas from animal waste sounded strange to many of the villagers.

With somehow standard houses of 4 rooms generally found in the workers compounds, the number of wall sockets and lights could be easily estimated. Variations could only be seen from appliances like radio, television sets, stoves, etc., which mostly depend on the household disposable income. The theoretical load diagrams for the site are obtained using methodology presented in [39]. In this case households are grouped according to defined domestic services (S1, S2… S6) as shown in Table 6-1. As can be seen domestic service S1 consists of only 4 lights, while domestic service S2 consisting 4 lights and one radio set, on and on like that, and S6, consisting of 16 lights, 1 radio set, 1 TV set, 1 fridge 150 litres and household appliances like cooking stoves and others. I then compiled the number of the households in each service category at the workers compound at the farm and the results are shown in Table 6-2. Finally to get the load profile for the village the loads for the different appliances used at each hourly period by all households are evaluated. Figure 6-5 shows the load profile curves for the whole farm (a), the farming activity only (b) the total of all the households (c) and one average household. Figure 6-6 shows both the household and farming activities load profiles put together for easier comparison. As can be seen from Figure 5-6, the households load (in yellow) is very small compared to the farm load (in blue). For this analysis, neither seasonal nor weakly variation was considered since the change of consumption pattern through the season and even week is practically not big. This is assumed reasonable since dairy farming activities are almost the same throughout the year, month and week.

Types of services (number of…)	S1	S2	S3	S4	S5	S6
Light	4	4	6	6	6	16
Radio set		1	1	1	1	1
TV set				1	1	1
Fridge 30 litres					1	
Fridge 150 litres						1
Household appliances						1

Table 6-1: Services proposed to the domestic users

Services	S1	S2	S3	S4	S5	S6
No. of households	12	3	2	1	5	3
Totals	26					

Table 6-2: Composition of the village domestic users

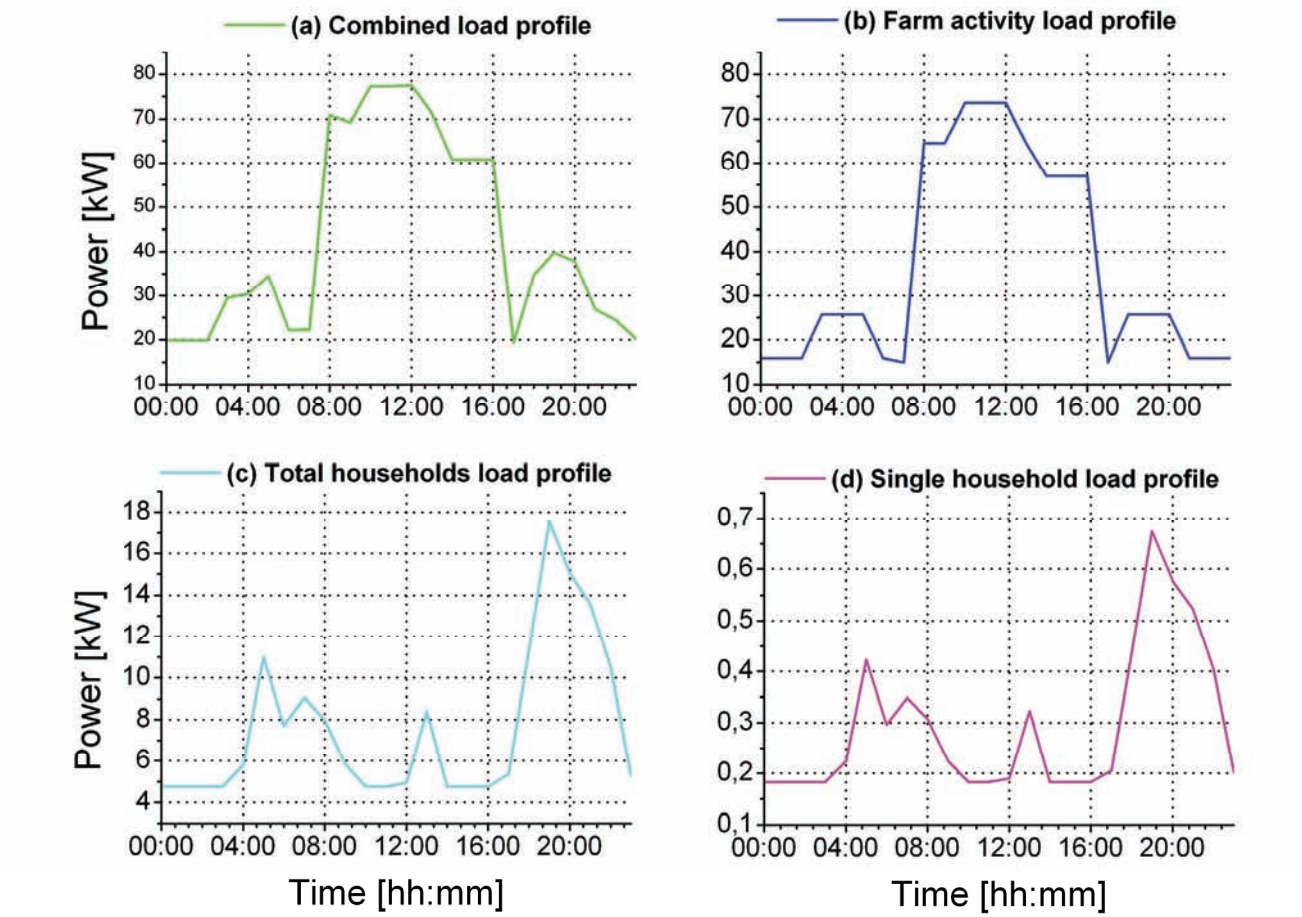

Figure 6-5: The load profiles for (a) combined load profile that encompasses al activities at the farm a workers residence, (b) load profiles for only the farm activities, (c) total households load profile and (d) single household load profile (the average)

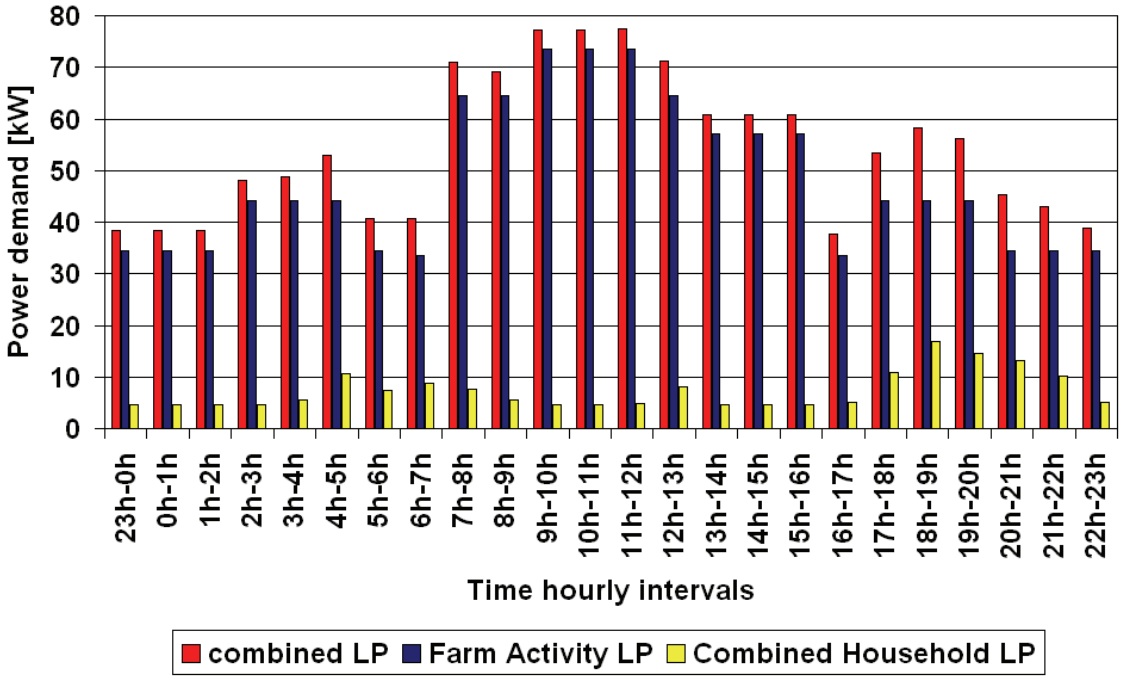

Figure 6-6: Load profiles for Rosenwald Dairy Farm on the highest power demand day

6.3 Biogas and electricity production

Anaerobic digestion of cow manure is a naturally occurring process in which microbes “digest” the organic material in the manure, producing biogas as a by-product. Increasingly, the process is centralized in a “plug-flow,” “mixed,” or other type of man-made digester for odour control and other purposes. The biogas produced in this anaerobic (oxygen-free) environment consists of approximately 60% methane (CH_4, a useful fuel), 40% carbon dioxide (CO_2, a diluting gas), and a small-but-potent dose of hydrogen sulphide (H_2S, a corrosive gas). It is also saturated with water vapour. The lower heating value of biogas at atmospheric pressure is approximately 538 Btu/ft^3 (20,1 MJ/m3). This is significantly lower than the value of 896 Btu/ft^3 (33,4 MJ/m3) for pure methane (the primary component of natural gas) or the value of 2,283 Btu/ft^3 (85,2 MJ/m3) for propane. Nonetheless, the fuel value is significant and the biogas can be recovered to produce heat and electricity. Figure 6-7 shows the chain in the conversion of cow dung to electricity. Besides production of gas, the anaerobic fermentation process produces liquor which can be used as a fertilizer, and a solid residue, which can be used as a soil conditioner. Thus, the anaerobic digester converts waste material into several valuable products. In addition anaerobic digestion processes can be used to treat wastewater.

Digesters can also be classified according to the reactor type. In batch systems, material is digested in lots, often with several vessels in parallel with a staggered start-up to compensate for variation in output. In accumulation continuous flow systems, an essentially batch reactor serves as a manure pit and has material added and removed as needed. However, the most common reactor type is the continuous stirred tank reactor in which material is added regularly and digested material collected via an overflow.

In each case the amount of biogas generated from anaerobic digester depends on the proportion of degradable materials (volatile solids) present on the organic waste. The methane content of biogas varies from 55 to 80 percent with the pure methane heating value at 33.4 MJ/m^3. The biogas energy can be converted to electricity by means of an internal combustion engine, microturbine or fuel cell technologies.

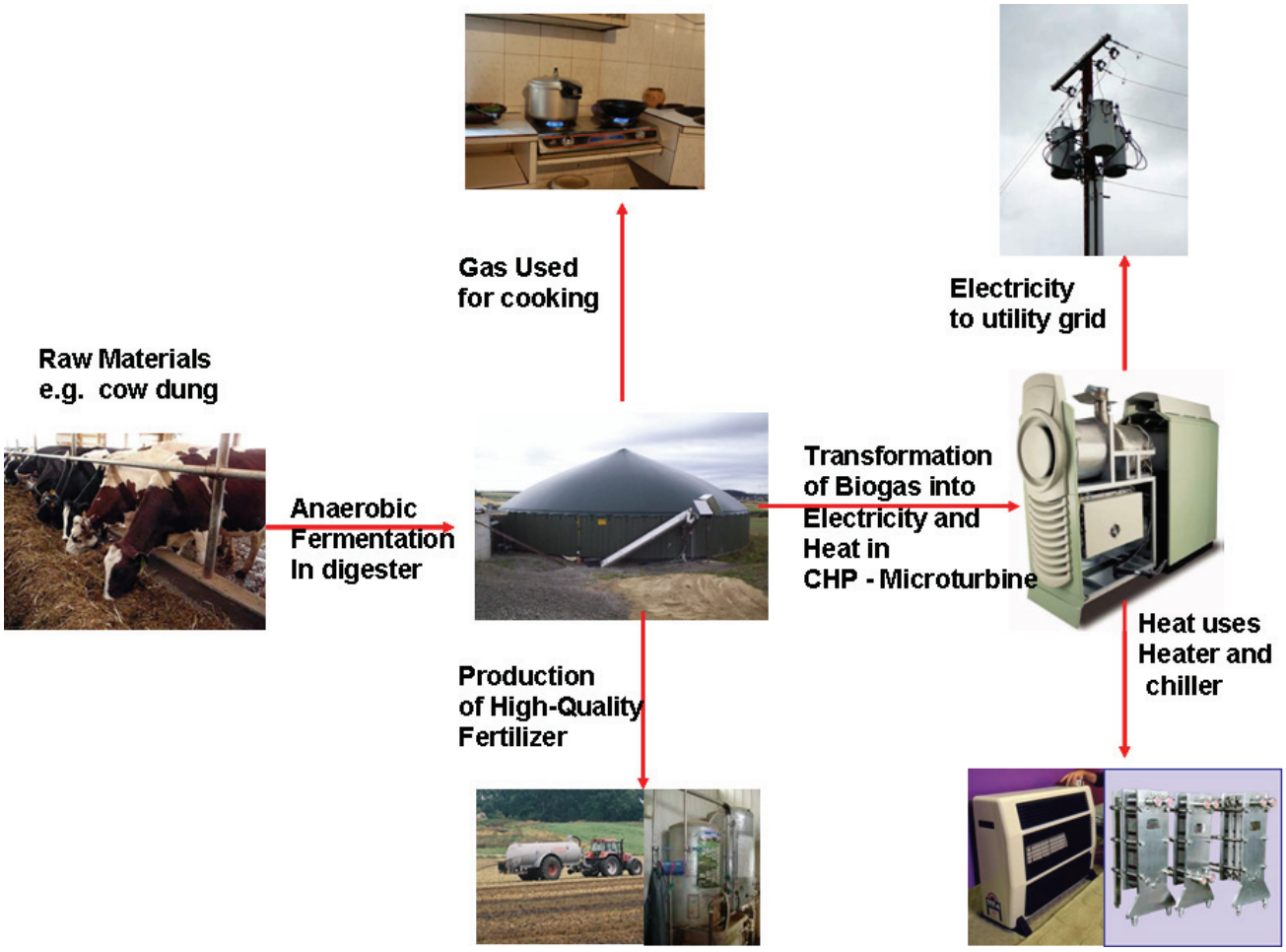

Figure 6-7: Conversion chain from cow dung to electricity

6.4 Microturbine technology description (capstone)

In this thesis microturbine technology was selected for the biogas conversion to electric power and heat. Although microturbines have yet to reach commercial maturity, these are expected to offer numerous potential advantages compared to other technologies for small scale power generation. Advantages include: few moving parts; compact size; light weight; relative high efficiency; and low emissions. West heat recovery can be used with microturbine systems to achieve efficiencies greater than 80%. In this and next sections a detailed description of the microturbine technology and the possible operation mode are given. Results of dynamic operation measurements done on a Capstone 30 kW microturbine operating in grid connected mode are also presented.

Microturbines are gas or liquid-fuel-fired turbine-generator units with an electrical output between 30 and 500 kilowatts. The system incorporates a compressor; recuperator, combustor, turbine and permanent magnet generator (see Figure 6-8 from Capstone Microturbine Corporation). The microturbine engine has only one moving part, basically a shaft. At one end of that shaft is a turbine wheel; at the opposite end of the shaft is a permanent magnet electric generator; and positioned at the midpoint of that shaft is an air impeller wheel (i.e., an air compressor) for drawing in ambient air, compressing it, then pumping it into the combustor (see Figure 6-9). Fuel is then injected into the combustor, where it then mixes with the compressed air. Combustion occurs and the resulting gases expand and rush out through the turbine, spinning it to a very high and varying rpm (96,000 rpm). The shaft on which the rotating components are mounted is supported by air bearings that spin at up to 96,000 rpm. At such high rpm, oil-lubricated bearings are severely challenged [40]. With the air-bearing design used in the Capstone unit, however, the rotating shaft, in effect, is being supported by a film of pressurized air. Ambient air is first drawn into the microturbine system enclosure, filtered, then passed over the electric generator, which is kept cool by this passing air. Next, the air is drawn into the impeller (or compressor), which compresses it before pumping it into the combustor. Now, a part of that compressed-air stream exiting the impeller (compressor) is diverted to the air bearing. The microturbine shaft in effect now rides on a thin film of compressed air—this film being in the thin annular space between the rotating shaft and the stationary bearing housing. The advantage of these air bearings is that they can respond virtually instantaneously to changes in load demands and resulting changes in shaft speeds. As the load demand increases from zero kilowatts on up to 30 or 60 kilowatts, the microturbine shaft can surge from 50,000 rpm up to 96,000 rpm almost

instantaneously. Oil-lubricated bearings introduce viscous drag and can't be as responsive [40]. And that type of heat and variation stress can take quite a toll on lubricants, even the more exotic ones.

6.4.1 Combined Heat and Power (CHP) and / or Combined Cooling, Heat and Power (CCHP) operation of microturbine

In most onsite power installations at commercial and industrial sites, the microturbine system is arranged in a combined heat and power (or cogeneration) configuration. In this configuration the thermal energy (heat) released from the burning of the fuel in the microturbine's combustor will be used not only to spin a turbine-generator to generate electricity, but the heat exiting the turbine will also be captured and used to meet the thermal needs of the site. Not to capture that thermal energy and use it is to waste it to the atmosphere—which would greatly lower the energy efficiency of the microturbine installation, thus greatly reducing its economic attractiveness.

Generally, microturbine systems for any given installation are sized to meet the heating needs, the thermal load, at that site [40], thus leaving in many cases, the electric power generation short to meet 100% of the site's electric power needs. Alternatively if the system is sized for electric needs, then one would usually end up with a larger installation that would waste much heat to the ambient and eventually making the overall system efficiency too low to be economic attractive. Thus it is crucially important, whenever is possible, to be able to link the onsite microturbine to the utility grid so that the power grid could be used to supplement the electric power needs; and to serve as a backup power source when the DG equipment is offline.

The hot turbine flue gases (500°F to 600°F) flowing up the stack pass through a finned heat exchanger near the top of the stack. As the flue gases flow up through the microturbine's heat exchanger, they transfer much of their thermal energy to water circulating through the inside of the heat exchanger. Thus the extracted heat energy from the microturbine exhaust gasses is used to meet thermal loads, such as milk-cooling, water heating in dairy farming, heating water for both space heating and hot water in buildings and apartments, dairy heating swimming pools, etc. Unlike in piston-engine-driven generators, where for CHP purpose one has to siphon off some of the heat from

the engine but not too much, lest the engine run too cold—a delicate balancing act, the simplicity and efficiency of CHP in the case of microturbines, is attributed to the fact that all the thermal energy is contained in the exhaust gases. One of the coolest uses, literally, of microturbine exhaust heat energy is to drive absorption chillers, devices that use heat energy, *instead* of electric energy, to chill air and water.

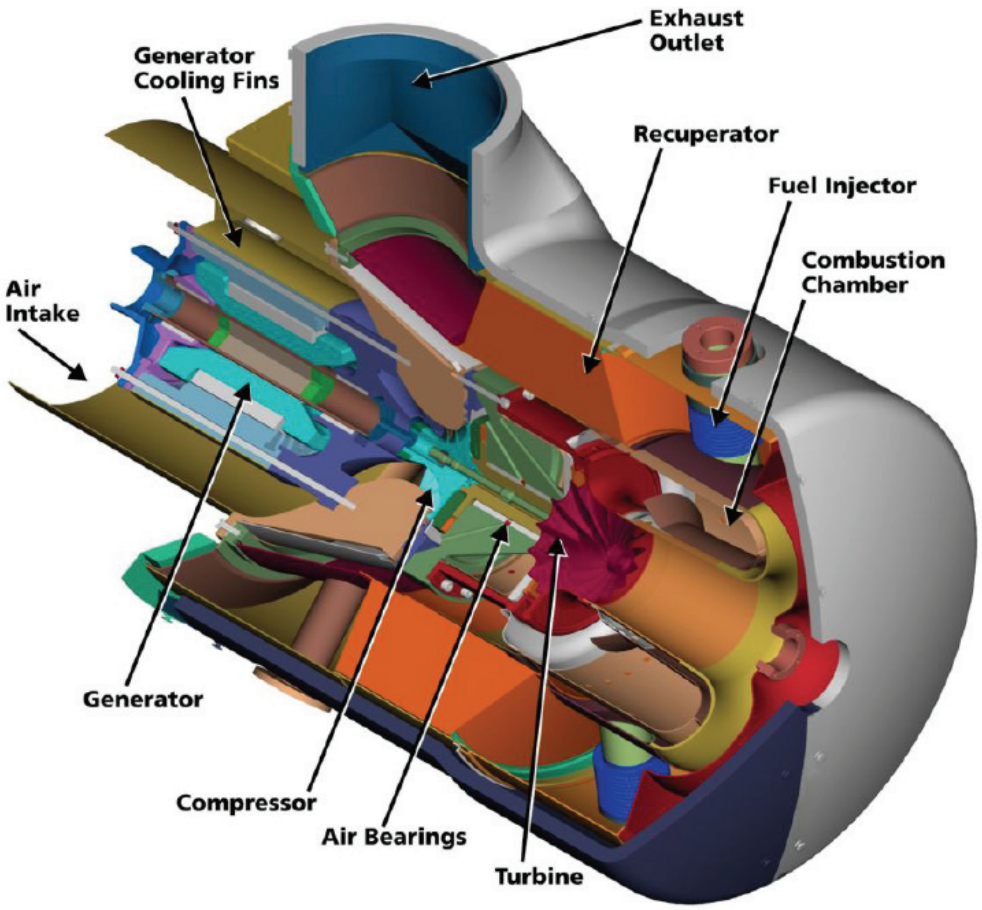

Figure 6-8: A cutaway of a Capstone microturbine
Source: Capstone Turbine Corporation

The technology has the following advantages:

- Low to moderate initial capital cost
- Fuel flexibility, allowing them to burn either gaseous (natural gas, propane, biogases, oil-field flared gas) or liquid fuels (diesel, kerosene)

- Heat released from burning the fuel not only generating electricity, but also providing all heating and cooling needs for a facility through cogeneration, combined heat and power (CHP), and combined cooling, heat and power (CCHP)
- Extremely low air emissions for NOx, CO, and SOx

The ability for a facility to continue operating even during a regional power brownout or blackout, offers greater energy reliability. The system uses no oil, no lubricants, and no coolants and has no pumps, gearbox or other mechanical subsystems. The system achieves ultra-low NOx performance with no post-combustion catalysts or other exhaust cleanup devices. System output is variable frequency (50/60 Hz) 3-phase AC power. This whole microturbine system is packaged in an enclosure not much bigger than a refrigerator—about 2.10 m tall, 0.76 m wide and 1.98 m deep.

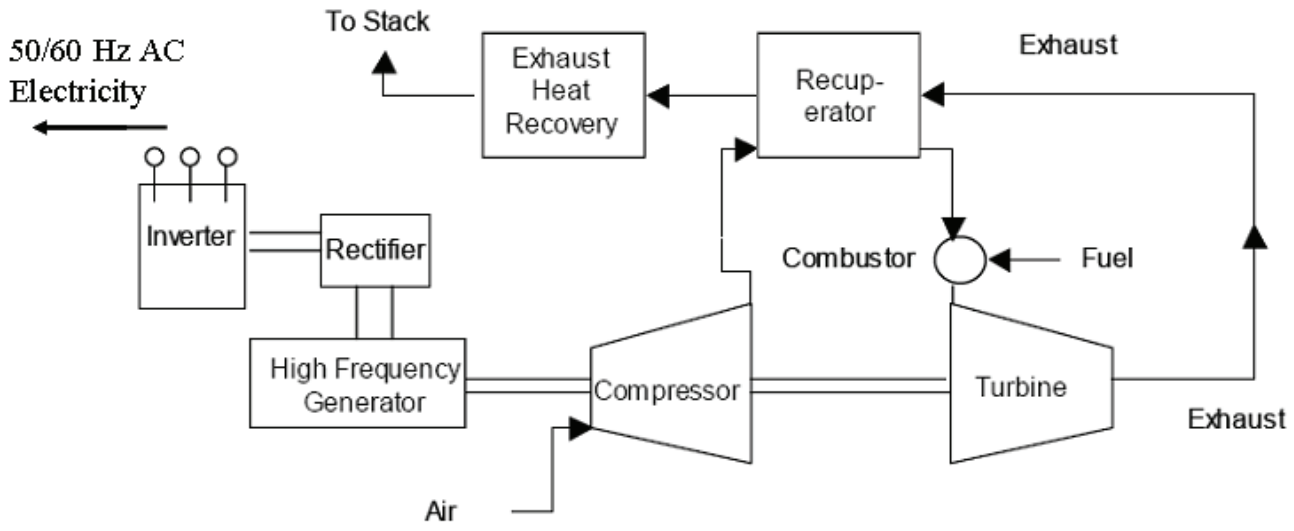

Figure 6-9 Microturbine-Based CHP System (Single-Shaft Design) [41]

6.4.2 Possible operation mode of microturbine

Three modes of operation namely grid connect (live connection to the grid, i.e., the microturbine supplies the base load and operates continuously 24 hours in a day and seven days in a week with a load following function for the load fluctuations), stand alone (with on board battery for start and

transients) see Figure 6-10, and dual mode with the controller shown in Figure 6-11 are possible with the capstone's range of microturbines.

In stand alone option, Capstone Micro Turbines can be used for backup power in two ways:

Dual Mode: Normally operating in Grid Connect mode, the system switches to Stand Alone mode during a grid outage. Switching is done automatically by the Capstone Dual Mode Controller (DMC) as seen in Figure 6-11 that differs from an automatic transfer switch (ATS). An ATS selects between primary (grid) and alternate power sources, while the DMC normally parallels the microturbine(s) to the grid, or, isolates from the grid during a grid outage. When grid is lost the dual mode controller senses this loss of grid and automatically disconnects the microturbine system and the protected loads from the grid and sends a reconfiguration signal (Figure 6-11) to the microturbine to start in Stand Alone mode to supply only the protected loads. The change over time from Grid Connect to Stand Alone is 2 – 4 seconds. At restoration of the grid the dual controller senses this and shuts down the microturbine, reconnects the microturbine and loads to the grid and sends a reconfiguration signal to the microturbine to start in Grid Connect Mode. The connection of the protected loads back to the grid is done within 2 seconds of restoration of the grid and the start-up of the microturbine in the Grid Connect Mode is within seven minutes

Backup Only: By connecting to an ATS on the alternate terminal, the microturbine can be applied as a "backup only" generator, starting when a grid outage occurs and the ATS throws over to the alternate position. ALTERNATE ATS CONFIGURATION: The "backup only" configuration does not take full advantage of microturbine capabilities and cost savings potential from running a large number of hours each year with low maintenance. Alternatively, the turbine can be connected in a "prime power" configuration, on the primary side of the ATS, running full time with the grid as backup.

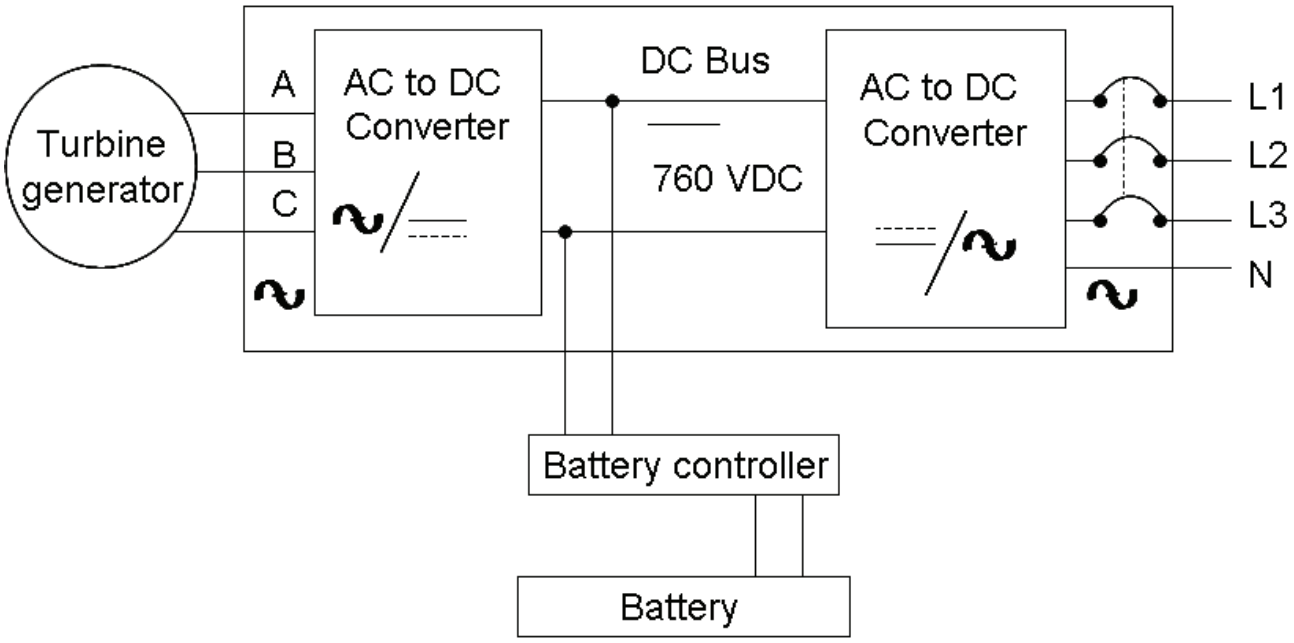

Figure 6-10: Stand alone with battery system

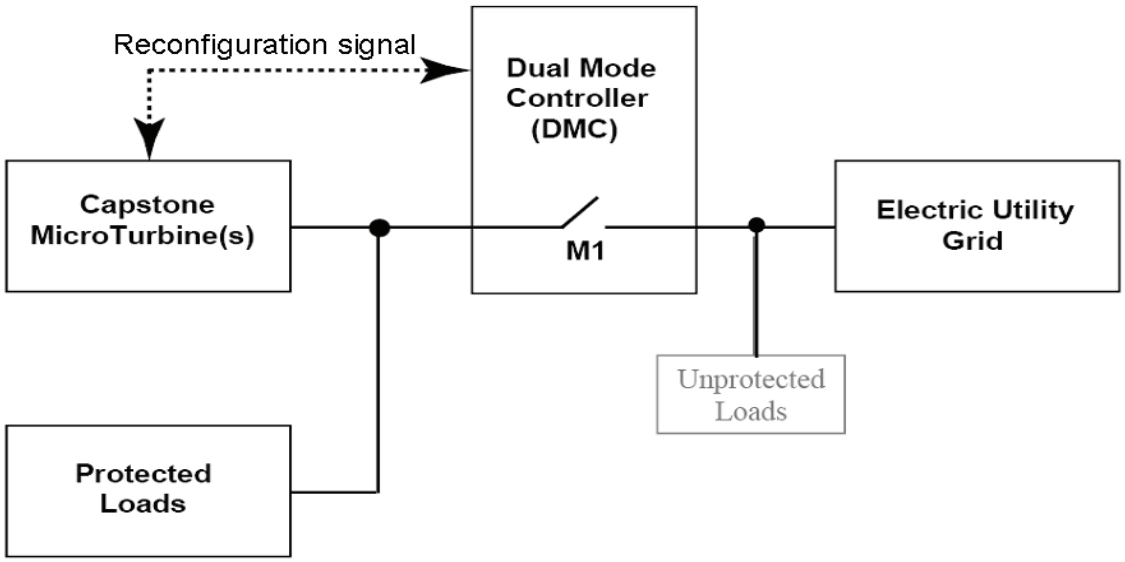

Figure 6-11: Dual mode controller operation

6.4.3 **Microturbine measurement**

To have a better understanding of some of the dynamic operational performance characteristics of a microturbine, the author made some test measurements of a 30 kW biogas-fired microturbine model

C330 from Capstone Corporation installed in April 2005 by ISET at the Landwirtschaftszentrum Eichhof (Eichhof) in Bad Hersfeld as a pilot project to prove the viability of the microturbine technology as working solution for the biogas plants. The farm belongs to the state owned Landesbetrieb and wirtschaft Hesse GmbH. This company is specialized in teaching, training and research around agriculture.

The following parameters were the object of the measurements: start-up time, ramp-up and down, shutdown. This section presents the results of the measurements. Figure 6-12 shows the microturbine under test at Eichhof.

Figure 6-12 The microturbine under test at Eichhof (to the left is the system without the cabin doors and to the right the same system in the closed cabin)

6.4.4 Test method and setup

Microturbine was connected to the utility grid and operated on grid connect mode. The measurements were done by the power analyser combi - quant device from HAAG and monitored and controlled from a laptop computer. The device measures current and voltage and calculates all the other derived quantities like powers. The diagram of Figure 6-13 shows the connections with the Rogowski coils for current measurement and the star connected voltage measurements. The overall measurement setup configuration is shown in Figure 6-14. The several power set points were entered from computer control centre of microturbine. The turbine generated only the selected amount of power regardless of the load on the system. Laptop computer was running with required special software (DAMON software) and data were recorded during the tests.

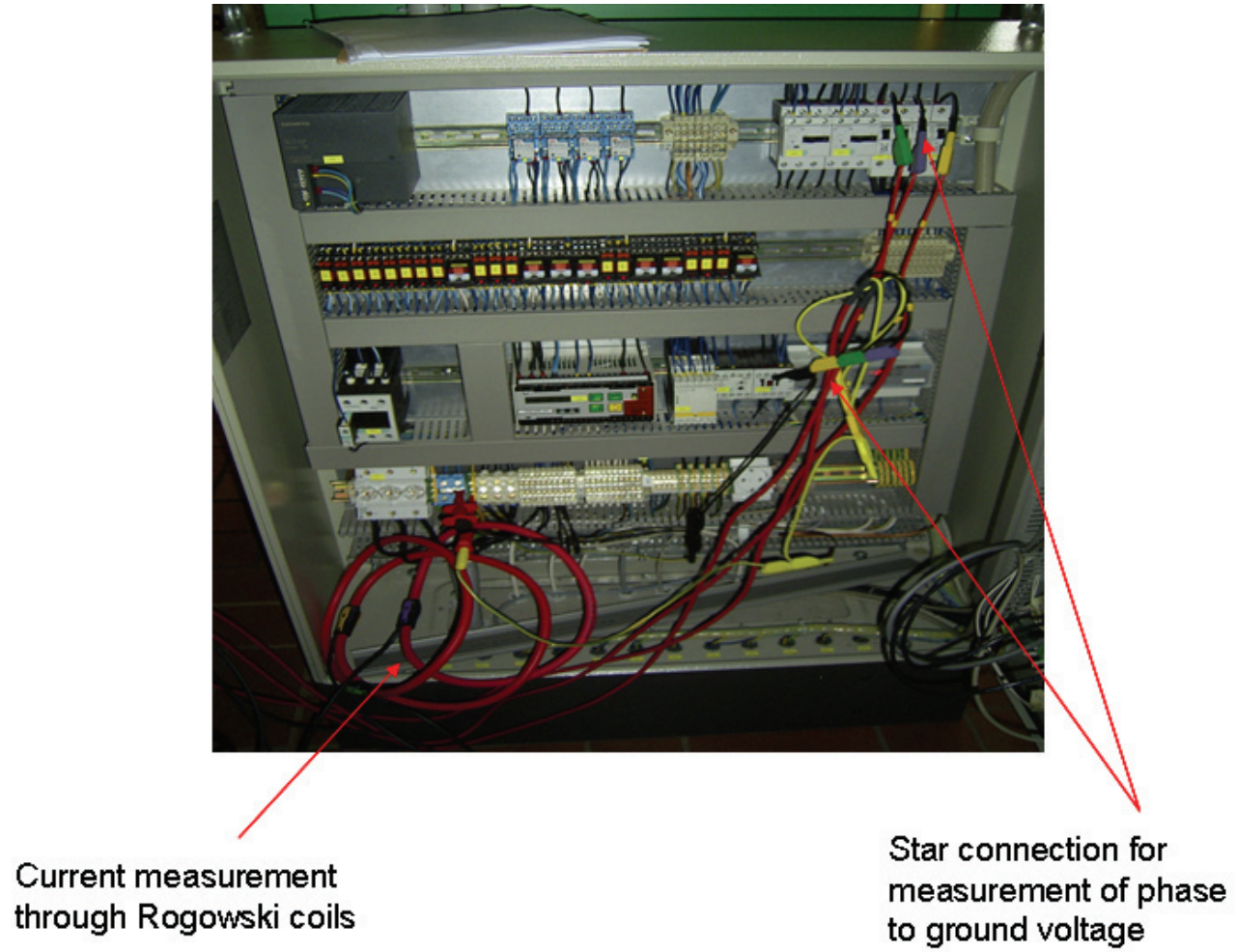

Figure 6-13: The connections for the measurements

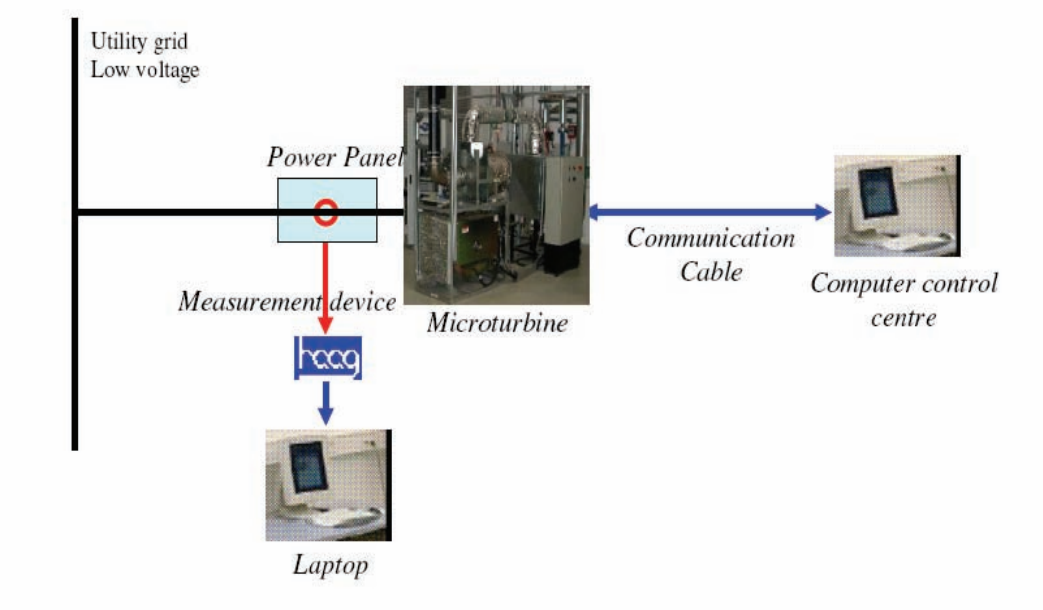

Figure 6-14: Test setup configuration

6.4.5 Results and discussion

The start up operation was measured at one second intervals and the power output was set at full capacity (30 kW). The operation was measured from the moment the microturbine is turned on (at cold start) until each phase of the microturbine started to export power to the utility grid. This process lasted 51 seconds with the amount of power export in phase A, 29.3 W, phase B, 168.7 W and phase C, 206.9 W. The full process (complete start up) from start of the microturbine till full capacity power export lasted 199 seconds with amount power export in phase A, 10.0 kW, phase B, 10.2 kW and phase C, 10.2 kW (Figure 6-15 below).

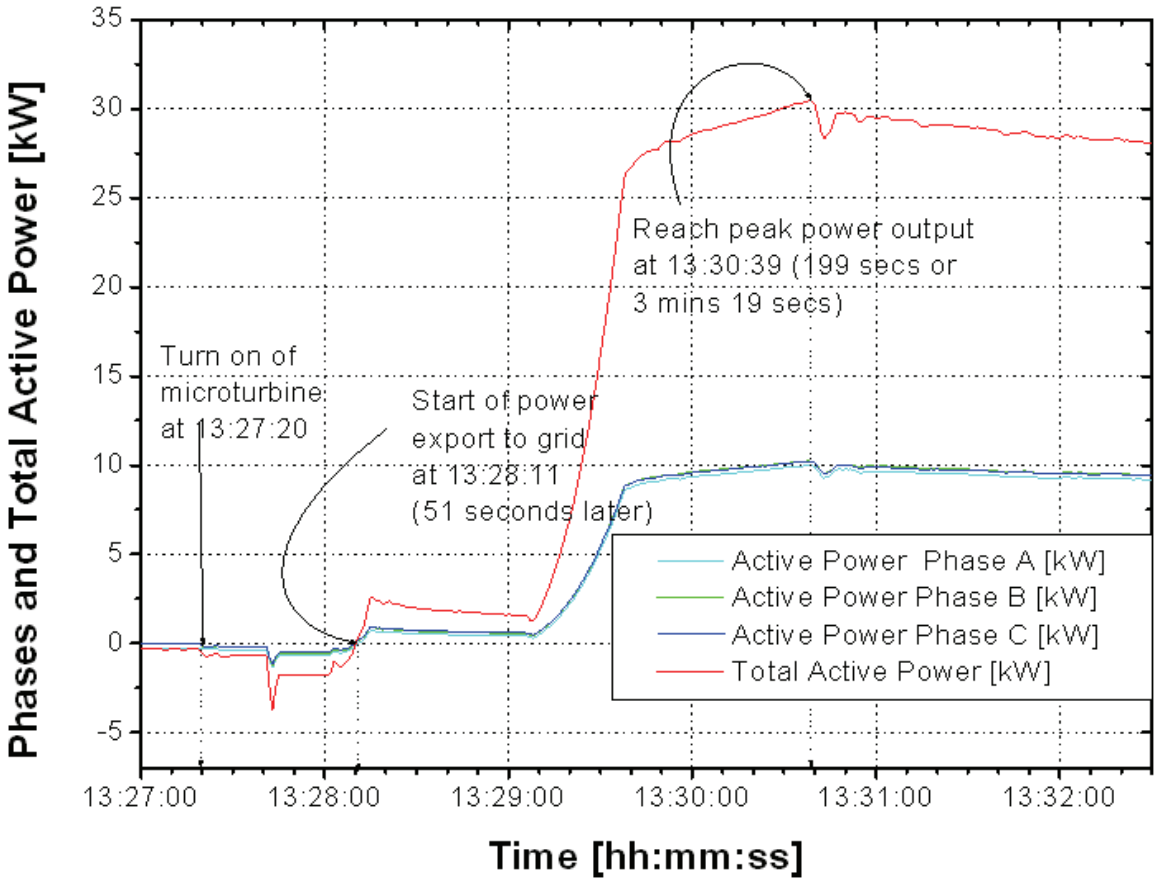

Figure 6-15: Start up time of microturbine showing active power only

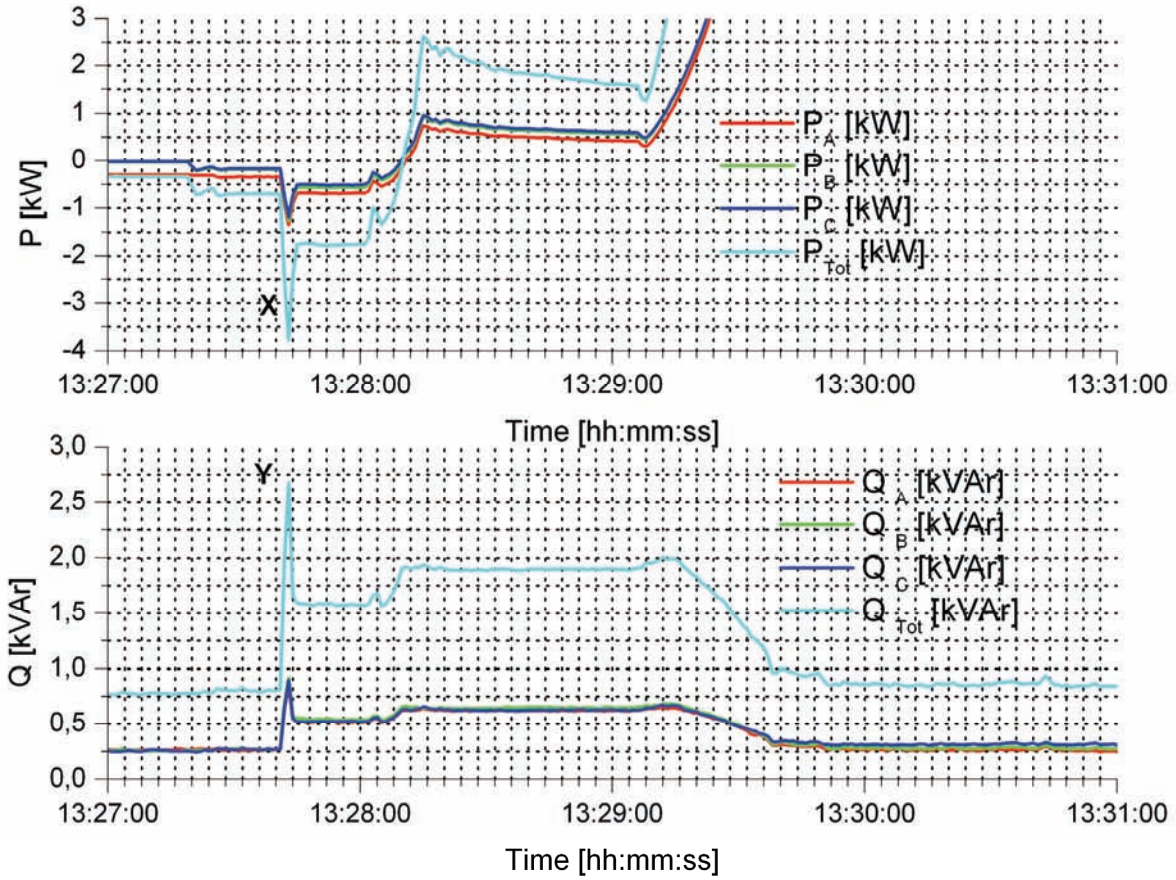

Figure 6-16: Start up process showing both active (zoomed to clearly evaluate the inrush power) and reactive powers

During start up operation, grid power was used to crank and rotate the turbine and it consumed total active power maximum 3.8 kW for this purpose (see Figure 6-15 and point marked X and Y in Figure 6-16). At point X and Y the turbine generator draws an inrush power and as a reaction (electromagnetic induction) the generator supplies reactive power to the grid with a peak of about 2.7 kVAr. From the point marked X the turbine gradually increases its power output in step-like ramps and takes up to 199 seconds to reach the maximum power output. As the turbine approaches the maximum power output the reactive power gradually decrease and becomes almost constant. The above results are important to know if this microturbine is to be use as a backup generator in case of say grid failure. Thus the time of more than 3 minutes for start up may be not short enough to rescue some loads as an uninterrupted power supply (ups). Of importance again is the assessment of the turbine's load following capability. To assess load following capability the power was set to increase

in steps and later decreased in steps and the ramp up and ramp down result are shown below (see Figure 6-17 and Figure 6-18).

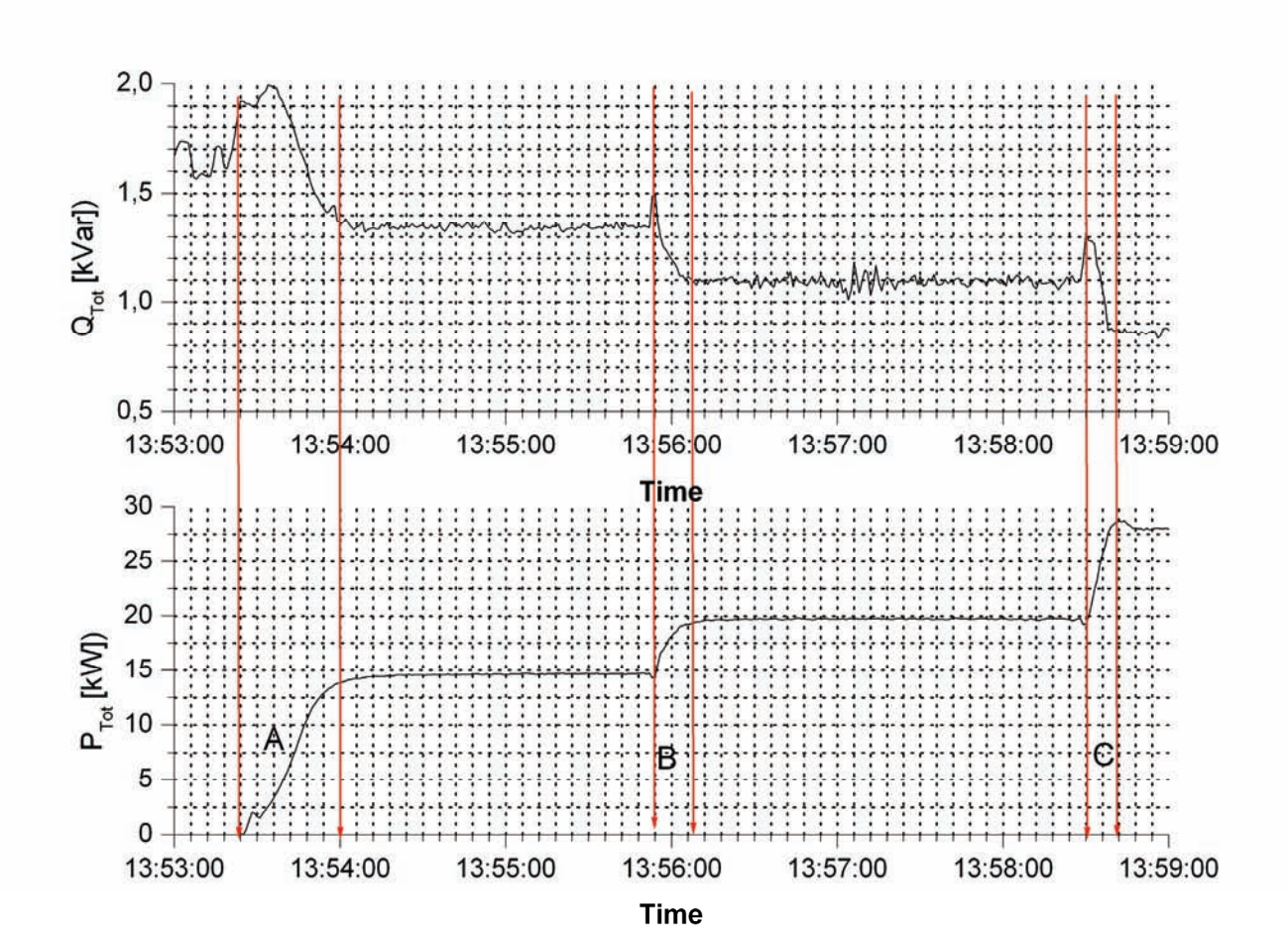

Figure 6-17: Ramp up process of the microturbine

The ramp up process was set to jump from zero power output to 15 kW, 20 kW, and finally to full load of 30 kW. The first ramp from 0 to 15 kW takes about 40 seconds from 15 to 20 kW this takes about 16 seconds and then from 20 to 28 kW the process takes 12 seconds (see time intervals marked A, B and C in Figure 6-17).

In Figure 6-18 the ramp down from an output power of about 26.5 kW to 20 kW, then down to 15 kW and last 10 kW is shown. The last ramp down to 10 kW was not possible as the microturbine could not operate at 10 kW output and below. The ramp down times from 26.5 to 20 kW is 12 seconds, from 20 to 15 kW, 15 seconds and from 15 kW to 10 kW is 15 seconds but the turbine self shuts down.

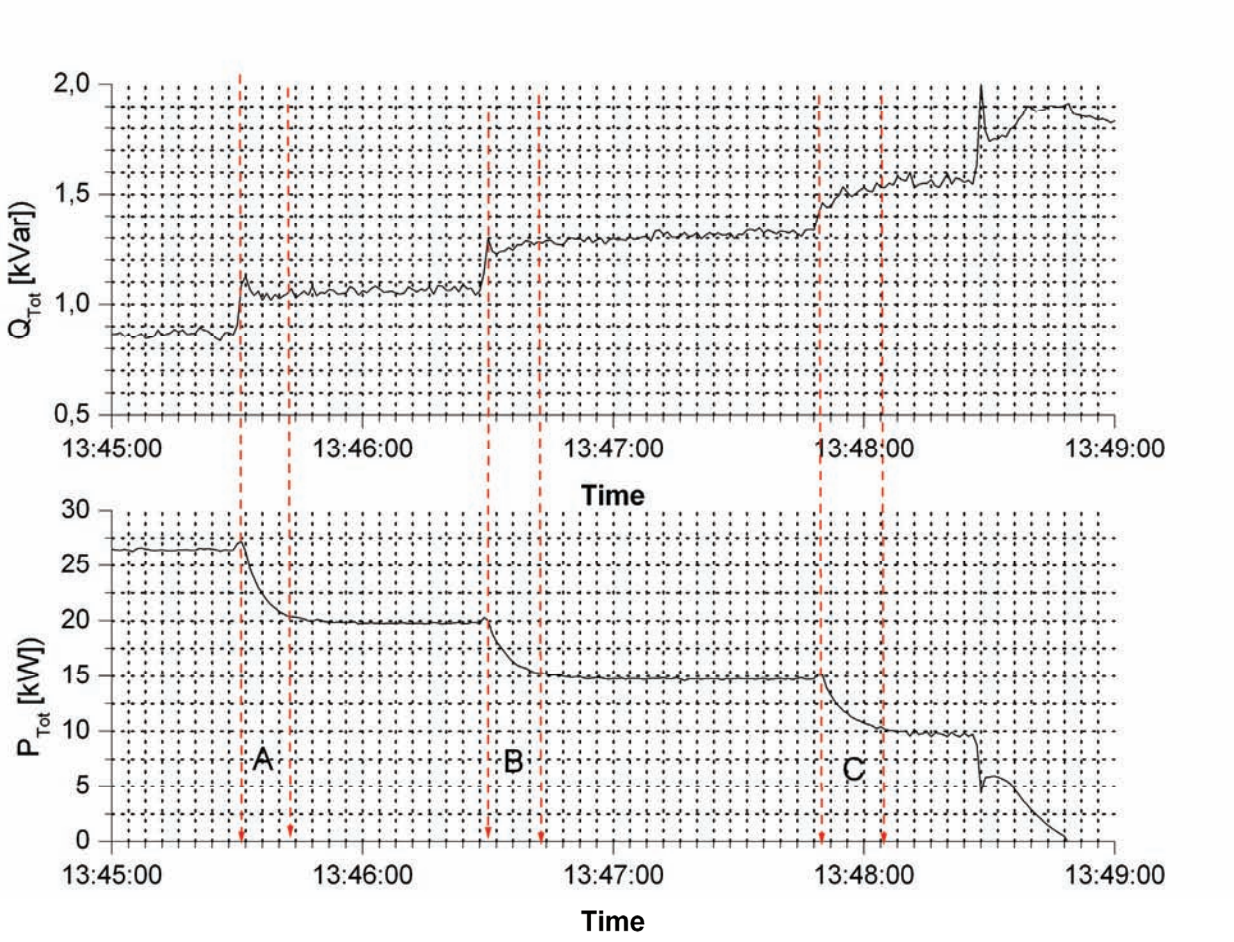

Figure 6-18: Ramp down process of the microturbine

Area	Start power output (kW)	End power output (kW)	Power output changing (kW)	Time to change power output (sec)	Transition time (sec/kW)	Transition power (kW/sec)
A	0.5	15.0	+ 14.5	40.0	2.76	0.35
B	15.0	20.0	+ 5.0	16.0	3.20	0.31
C	20.0	28.0	+ 8.0	12.0	1.50	0.67

Table 6-3: Ramp up process test results

Area	Start power output (kW)	End power output (kW)	Power output change (kW)	Time to change power output (sec)	Transition time (sec/kW)	Transition power (kW/sec)
A	26.5	20	- 6.5	12	1.85	0.54
B	20	15	- 5	15	3.00	0.33
C	15	10	- 5	15	3.00	0.33

Table 6-4: Ramp down process test results

6.4.6 **Conclusions**

From the above measurements it is evident that with a time complete start up, i.e., from start of the microturbine till full capacity power export lasted of more than 3 minutes the microturbine may not be a suitable option for uninterruptible power supply (UPS) function. Also, in this mode the microturbine require relative high power (3.8 kW) to crank and rotate the turbine, thus when applied in Micro-Grids with low nominal power, the micrturbine's start up may affect some connected loads.

The results have also established that the microtubine cannot operate at lower than 50 % load, that is below 15 kW the microturbine ramps down to zero. This information is very crucial when designing the power system in which this is to be applied.

6.5 Design of the power system

6.5.1 Power system technical requirements as per the Grid Code

Rosenwald-Lyondalel Dairy Farm is fed by an 11 kV branch from the main feeder from a substation 20 km from the farm through a 38 kVA (3 x 220/380; 100/5 A) three-phase four-wire transformer. The transformer is connected according to the regulations stipulated in the country grid code [42], that is; distribution system is designed as an effectively grounded system. The interconnecting transformer has a solidly grounded (that is, the neutral of the star connection is pulled out and grounded through very low resistance connection) Wye connected high voltage winding with a Delta connected low voltage winding. To accommodate the modifications on the farm power scenario and to satisfy the grid connection requirements as stipulated in [42], the following protection aspects need to assured:

i. Over current and Earth Fault Protection

Each of the generating components shall be equipped with over-current and earth fault protection to trip off in the event of a fault within the generator or the main breaker trips in the event of a fault on distribution system leaving the system operating in island mode.

ii. Over and under frequency and voltage Protection

In general both under and over-frequency protection (outside the limits 47.5 Hz and 52.5 Hz), and under and over-voltage protection (outside the limits 85% to 115%) would be through the use of the Dual Mode controller correctly set to disconnect whenever the voltage and frequency are out of the range. In a power islanding condition, the Micro-Grid is thus required to be able to maintain the frequency over a range of 49.25 Hz to 50.75 Hz [42]. Since most rural distribution systems apply auto-reclosing to the primary distribution system, to avoid possible damages due to the acceleration that will occur following re-closure the Micro-Grid will be equipped with a no-volts relay that trips the facility off during the re-close dead time.

For the synchronization of the facility to the Distribution System at local level the inverter equipped generators (microturbine) and the Micro-Grid are to be equipped with facilities typically consisting of a synchronizing relays and a sync-check relay with corresponding settings as required by the distribution system operator - ZEDC to insure that they will not adversely affect the operation of the Distribution System.

6.5.2 Presentation of possible power options at Rosenwald-Lyondalel Dairy Farm

Although Rosenwald-Lyondalel Dairy Farm is grid connected, it's the reliability has drastically reduced to extremely low values (sometimes power is available for one or two hours per day or not at all for the whole day) not only to the farm but to many sectors in the country. Thus the concept of grid connected Micro-Grid sounds more suitable for such a situation. The Micro-Grid loads and the micro-sources form an autonomous entity able to control its system voltage and frequency. The power system connects and disconnects automatically to and from the grid when the latter is available and not available respectively. The Micro-Grid imports power from the grid when local generation is lower than consumption and exports when it produces more than it consumes. In case the grid is not available and local generation lower than demand, then some loads are disconnected in order of their least importance. In case more power is generated than the demand and the Micro-Grid is operating in island mode the generators are de-rated to generate according to demand. And if more biogas is produced than required by the generators, then this is vented and burn in the air.

The renewable energy based technologies assessed in this study are solar photovoltaic and biogas generation systems. The wind technology and diesel options have been automatically disqualified due to lower wind speeds (highest monthly average of only 4,5 m/s) and diesel scarcity in the country. The idea is to utilise as much of the renewable energy resources as possible and use the grid as a backup when the system cannot meet the local demand. From a large number of possible options many of them were screened out before any further analysis due to their obvious disadvantages considering the situation at the site. Since the farm is already grid connected, it is more logical to always include the grid in the options, however due to it's very low reliability (the author estimates this to around 16 % in a year given that most days consumers have electricity service for only two or

three hour a day and other days even go without it at all), the power system has to be big enough to cover it's local load for much of the time. In this case the grid can be used as a back up. Due to the obvious high cost of the PV technology, this was not examined neither alone nor with grid, but in combination with biogas and grid. The grid could not also be considered alone given the problem of high unreliability and the country's power crisis. Thus the focus is to demonstrate the viability of an on-farm power generation using the otherwise waste. So the following possible alternatives have been considered for the site:

i. combination of Grid and biogas system,
ii. combination of Grid, PV and biogas and
iii. biogas only (that is, the biogas system cover the full load of the farm and thus avoid bills from the grid)

To select the most suitable technology and optimal configuration from the three options above, a simulation software HOMER, the micro power optimization model, developed by the U.S. National Renewable Energy Laboratory (NREL) was used. This was used to evaluate and compare the cost – effectiveness of installing a biogas system with the conversion technology of microturbine and PV to produce electricity for the unreliable grid-connected facility at Rosenwald-Lyondalel farm.

HOMER's optimization and sensitivity analysis algorithms make it easier to evaluate the many possible system configurations due the variation in technology costs and availability of energy resources that make decisions difficult. This is achieved by simulating the operation of a system making energy balance calculations for each of the 8,760 hours in a year and compares the electric and thermal load in the hour to the energy that the system can supply in that hour. For systems that include batteries or fuel-powered generators, HOMER also decides for each hour how to operate the generators. If the system meets the loads for the entire year, HOMER estimates the lifecycle cost of the system, accounting for the capital, replacement, operation and maintenance, fuel and interest costs. After simulating all of the possible system configurations, HOMER displays a list of feasible systems, sorted by lifecycle cost.

6.6 Assumptions made for the power system simulation input data

6.6.1 Grid tariffs and times of use periods (TOUP)

In Zimbabwe there are many tariffs in place for different categories of consumers and times of use periods (TOUP) are defined for three different typical days as shown in Table 6-5 and Table 6-6 [43], [10], [44]. The assumed electricity tariff are those announce in March of 2006 by the Zimbabwe Electricity Distribution Company [43], and thus all the currency equivalences are of the same time as given in [10], [44]. However due to high increase in the shortage of foreign exchange in the domestic economy of Zimbabwe, since March 2006, the Central Bank introduced a three-tier exchange rate system [44]. Besides the official exchange rate of ZWD 55 / 1 USD, mining firms would use a rate similar to the then "black market" at ZWD 1,350 / 1 USD, while other exporters would use a rate of approximately ZWD 800 / 1 USD. So for the simulations in this study the mining firms rate is adapted (that is, ZWD 1,350 / 1 USD since it reflected the true equivalence).

	Low Voltage	11 kV Supply	33 kV Supply
i. Fixed Monthly charge	ZWD505,600.00 USD 374.52 EUR 311.37	ZWD505,600.00 USD 374.52 EUR 311.37	ZWD505,600.00 USD 374.52 EUR 311.37
ii. A monthly maximum demand charge per unit of demand	n/a	ZWD65,300.00 USD 48.15 EUR 40.03	ZWD47,900.00 USD 34.81 EUR 28.94
iii. An interruptable demand charge	n/a	n/a	n/a
iv. On peak Energy charge per kWh	ZWD 400.00 USD 0.30 EUR 0.25	ZWD 500.00 USD 0.37 EUR 0.31	ZWD 500.00 USD 0.37 EUR 0.31

v. Standard Energy charge per kWh	ZWD 400.00 USD 0.30 EUR 0.25	ZWD 200.00 USD 0.15 EUR 0.12	ZWD 200.00 USD 0.15 EUR 0.12
vi. Off-peak Energy charge per kWh	ZWD 400.00 USD 0.30 EUR 0.25	ZWD 100.00 USD 0.07 EUR 0.06	ZWD 100.00 USD 0.07 EUR 0.06

Table 6-5: Tariffs for Agricultural Customers [43], [10], [44]

In Table 6-5 the Electricity Tariffs for agricultural customers as effective from 1 March, 2006 are shown. Table 6-6 shows the times of use periods for electricity in Zimbabwe. For the simulation of the power system in search for the optimal configuration a number of assumptions were considered. Due to variability of the prices of the technologies and also the site specifics when it comes to installing the system at the site, the costs of the system were assumed from the most appearing costs by many retailers and projects of this nature.

	Hour																							
Day of week	0	1	2	3	4	5	6	7	8	9	10	11	12	13	14	15	16	17	18	19	20	21	22	23
Sunday / Holiday	O	O	O	O	O	O	O	S	S	S	S	S	S	S	S	S	S	P	P	P	S	S	O	O
Week-day	O	O	O	O	O	O	O	P	P	P	P	P	S	S	S	S	S	P	P	P	P	S	O	O
Saturday	O	O	O	O	O	O	O	P	P	P	P	S	S	S	S	S	S	P	P	P	S	S	O	O

Table 6-6: Times of use periods (TOUP) for electricity in Zimbabwe, “O” is the off peak hours, “S” is the standard and “P” is the peak hour [43]

Microturbine technology:

Capstone 30 kW microturbine capital cost EUR 19,042 to EUR 22,215 plus engineering, installation and accessories roughly another EUR 19,042 to EUR 22,215 (thus together EUR 44,430. The bigger sizes were taken to be in proportion to their size (i.e., the 60 kW will considered double the cost of a 30 kW turbine).

PV technology:

The PV technology was considered to have a capital cost of EUR 4,887 / kW installed capacity

The grid:

To take in consideration the unreliability of the grid, on the simulation the grid was given a maximum load share of 16% per year. This is a reasonable guess as is reported by the farm and many other electricity consumers in different places in Zimbabwe on daily grid availability (the author has learned from his informal interviews with some workers from the case study farm that the grid availability is as low as less than three hour per day or even going some days without it at all)

Biogas digester system:

The biogas digester system's capital cost is estimated to be EUR 346,104 for the digester size to digest all the dung from the 627 dairy cows confined the whole day. Thus a cost of EUR 552/dairy cow head for the construction of the biogas digester was adapted from the averaging similar projects reported in [45]. This cost was assumed the fixed capital cost of the project, with a fixed operation and maintenance cost of EUR 36,000 per year (for workers' salaries and other operation cost associated with running the digester). Enough gas is assumed to be produced, (and according to calculations made the raw biogas available per day is 571 m3 / day).

In these simulations all generators (microturbine) are assumed working in their CHP mode to enable the covering of the thermal energy requirements of the dairy activities. Thus a sensitivity analysis is applied on the heat recovery ratio and the minimum primary energy serving percentage. The generators were optimally scheduled to allow HOMER to decide when it is most cost effective to run the generator at the loading ratio depending on the electric power demand and the cost of energy from the grid. The results of the simulations for the most cost effective configuration for each of the options are presented in the next section.

6.6.2 Presentation of power system simulation results

The most cost effective system architecture for each of the three options cases are shown in Figure 6-19. In the figure the sizes of each microturbine generator marked MT is given in brackets. In each case the electrical load scaled peak power is at 112 kW and the deferrable load at 15 kW with

thermal load at 178 kW. In Table 6-7 the results showing the cost summary for each of the three configurations are presented.

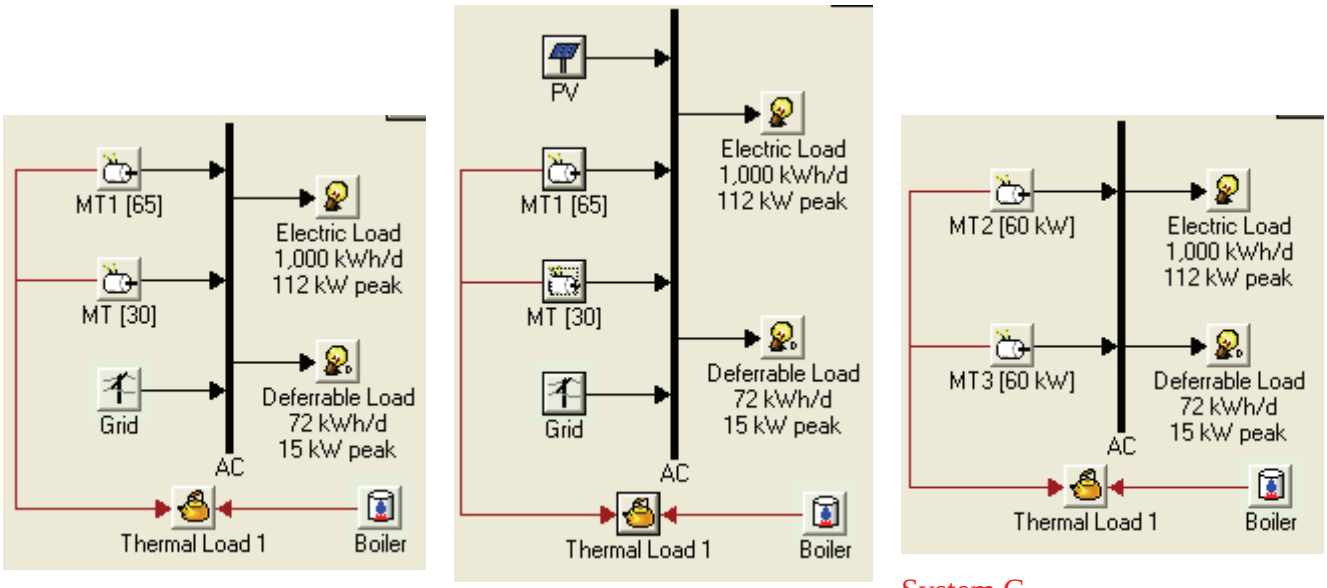

System A

System B

System C

Figure 6-19: The simulated power system configurations, with the generation technologies shown with their corresponding power ratings (MT is microturbine and PV peak power of 5 kW).

	System A Bio_MT+GRID	System B PV+Bio_MT+GRID	System C Bio_MT
Total net present cost	EUR 909,441	EUR 946,234	EUR 1,009,836
Levelized cost of energy per kWh	EUR 0.256/kWh	EUR 0.266/kWh	EUR 0.242/kWh
Operating cost per year	EUR 38,566/yr	EUR 39,093/yr	EUR 36,941/yr

Table 6-7: The cost summary for the three system configurations

	System A Bio_MT+GRID	System B PV+Bio_MT+GRID	System C Bio_MT
Microturbine 2 Heat Recovery Ratio [%]:	75	75	75
Microturbine 3 Heat Recovery Ratio [%]:	65	65	65
Annual Real Interest Rate [%]:	10	10	8
Minimum Primary Energy Savings [%]:	2	2	10

Table 6-8: Sensitivity case applied to the three configurations

Due to the different influence of such parameters like and the heat recovery ratios, annual rate of interest, minimum primary energy savings and many others, it is thus recommended to do a sensitivity analysis to see how the systems total net present cost of the system is affected by these variation of the parameters in question. The choice of range has to be wide but still within reasonable in accordance with the circumstances around the power system under design. In Table 6-8 the sensitivity cases chosen as optimal by the simulation calculations are shown. In each simulated case the range of the sensitive parameters were set the same, for example the heat recovery ratio, 65 %, 70 %, and 75 % were tested. Table 6-9 presents the electrical energy production by each component and the corresponding percentage of the total production together with the consumption by type of load and the system performance parameters and in Table 6-10 the thermal energy production by generating component, the corresponding percentage of the total, thermal energy consumed and the excess is presented. In Figure 6-20 the cash flow analysis for the three configurations are presented in one diagram.

Component	System A Bio_MT+GRID		System B PV+Bio_MT+GRID		System C Bio_MT	
	Production (kWh/yr)	Fraction %	Production (kWh/yr)	Fraction %	Production (kWh/yr)	Fraction %
PV array [5 kW]	-	-	1,107	0	-	-
MT[60 kW, 65 kW]	257,940	66	257,393	66	350,881	90
MT[30 kW, 60 kW]	132,977	34	132,449	34	40,430	10
Grid purchases	372	0	343	0	-	-
Total	391,289	100	391,291	100	391,311	100
Load	Consumption	Fraction	Consumption	Fraction	Consumption	Fraction
AC primary load	364,979	93%	364,981	93%	365,000	93%
Deferrable load	26,309	7%	26,309	7%	26,309	7%
Total	391,288	100%	391,290	100%	391,310	100%
Quantity	Value	Units	Value	Units	Value	Units
Excess electricity	2	kWh/yr	0	kWh/yr	0	kWh/yr
Unmet load	22	kWh/yr	1	kWh/yr	0	kWh/yr
Capacity shortage	276	kWh/yr	256	kWh/yr	6	kWh/yr

Table 6-9: Electrical energy production by each component and the corresponding percentage of the total production, consumption by type of load and performance indicators of the systems

Component	System A Bio_MT+GRID		System B PV+Bio_MT+GRID		System C Bio_MT	
	Production (kWh/yr)	Fraction	Production (kWh/yr)	Fraction	Production (kWh/yr)	Fraction
MT[60 kW, 65 kW]	590,413	61%	589,071	61%	975,939	77%
MT[30 kW, 60 kW]	282,758	29%	282,126	29%	232,783	18%
Boiler	101,765	10%	101,831	10%	53,647	4%
Total	974,936	100%	973,027	100%	1,262,368	100%
Load	Consumption	Fraction	Consumption	Fraction	Consumption	Fraction
Thermal load	547,499	100%	547,499	100%	547,499	100%
Total	547,499	100%	547,499	100%	547,499	100%
Quantity	Value	Units	Value	Units	Value	Units
Excess thermal energy	427,437	kWh/yr	425,529	kWh/yr	714,870	kWh/yr

Table 6-10: Thermal energy production by component in each configuration and the percentage share to the total production and thermal consumption and excess energy produced

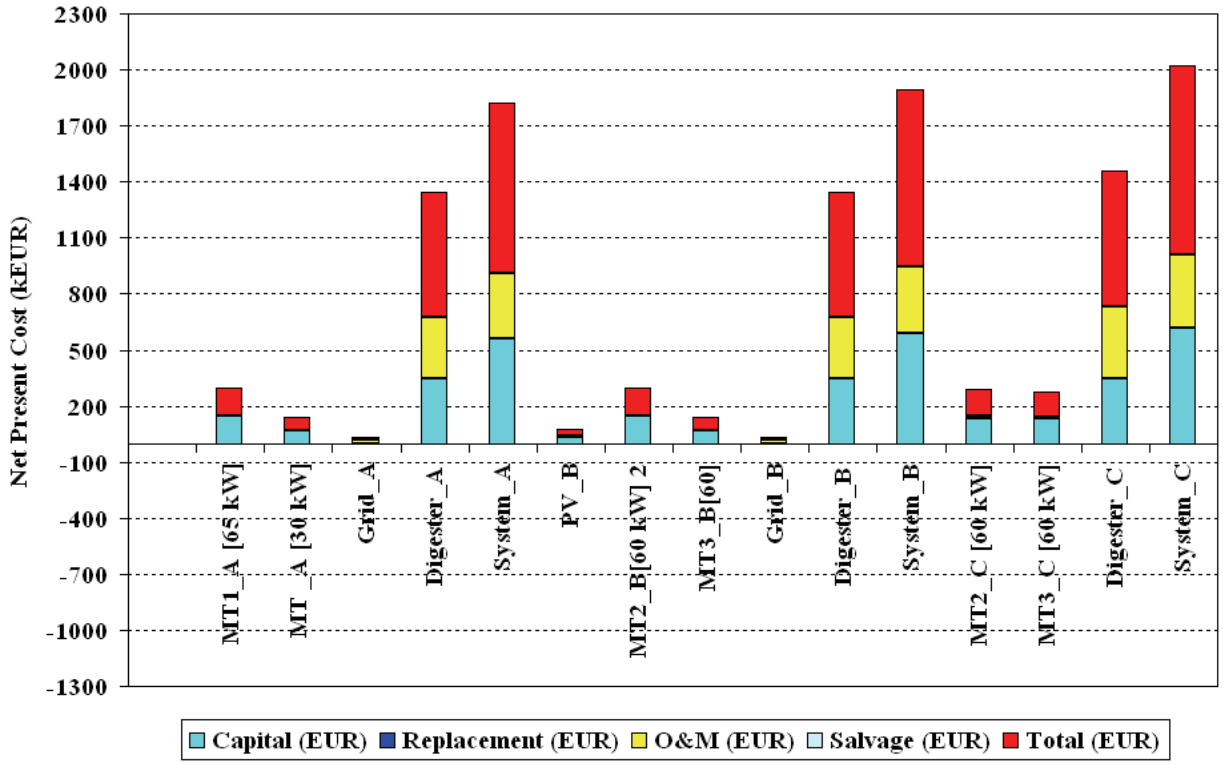

Figure 6-20: The net present cost of the power generating components of the three system architecture

6.6.3 Discussion of simulation results

So judging from the total net present cost, the most cost effective solution to the energy problems of the farm is given by the configuration of system A in Figure 6-19, that is, consisting of two microturbines of 30 kW and 65 kW connected to the grid followed by system B and then C as shown in the figure. The three configurations differ relatively high in their net present cost but the cost of energy as derived from the systems differ only by 1cent/kWh to 2 cents/kWh. The most cost effective system has a total net present cost of EUR 909,441 and a cost of energy at EUR 0.256/kWh. The system which incorporates PV has a net present cost of EUR 946,234 and a cost of energy of EUR 0.266/kWh. Although judging by the net present cost, the biogas only – system C is the most expensive with EUR 1,009,836, however its cost of energy is the lowest with EUR 0.242/kWh due to it's least operational cost (EUR 36,941/yr as compared to EUR 38,566/yr and EUR 39,093/yr of the first and second systems respectively. So the biogas alone option is more expensive for this farm requirements due to the big difference between available microturbine sizes (30 kW, 60 kW, 65 kW,…), otherwise this option would be the most suitable for such a farm given

that the biogas resource is more than enough to meet both the electrical and thermal load demand and the derived benefits like chemical fertilizer replacement for the maize crop for feeding the cows. The mix of technologies would also sound very good, that is, looking at more reliability attached to this option, however the difference of almost one cent per kWh levelized cost of energy erodes it's attractiveness in favour of the option with grid included.

Considering site specifics (like farm is already grid connected but the grid is extremely unreliable) and results of simulations, the system A, that is a combination of biogas fired microturbine connected to the grid is chosen. This system further discussed in the following sections.

6.6.4 System cost benefit analysis

In this section a cost benefit analysis of the chosen system is presented. Here considered is the cost offset generated by using the on farm generated energy instead of buying all the energy from the grid. To calculate this it is assumed that the farm does its energy demand activities in all the three demand periods per day and all year round, that is, peak, off peak and standard and so assuming scaled daily average energy load of 1000 kWh/day, that converts to 365000 kWh/year and this to be consumed in the ratio Peak hours rate : standard hour rate : off-peak hour rate of 2797 : 2678 : 3285 corresponding to the calculations with the time of use periods shown in Table 6-6 hour of tariff and the corresponding tariffs in Table 6-5 (all the hours in each tariff rate are estimated for the whole year). The following breakdown is obtained:

Peak energy cost/yr = EUR 36,128

Standard energy cost/yr = EUR 13,450

Off-Peak energy cost/yr = EUR 8,213

Total /yr = EUR 57,791

In addition to the avoided cost of electricity the farm will also avoid by charcoal for the water heating boiler and assuming the amount of the same range that is the total will be double (EUR 115,582. After digestion, manure has improved nutrient availability, reduced acidity, and reduced odor. By avoiding fertilizer purchases, the farmer can save up to about EUR 34 – EUR 50 per head

per year (from dairy cattle). Thus for this farm with 627 cows that will convert to about EUR 21,318 – EUR 31,350. So it clear that if all the benefits attached to the use of such systems for power generation in farming areas are converted to monetary value, then the cost of energy, and the net present cost of the project will decrease significantly and thus become evidently more attractive. In the next section a sketch diagram of the power system in form of a Micro-Grid is presented and the operational strategy briefly outlined.

6.7 Operation strategy of the power system

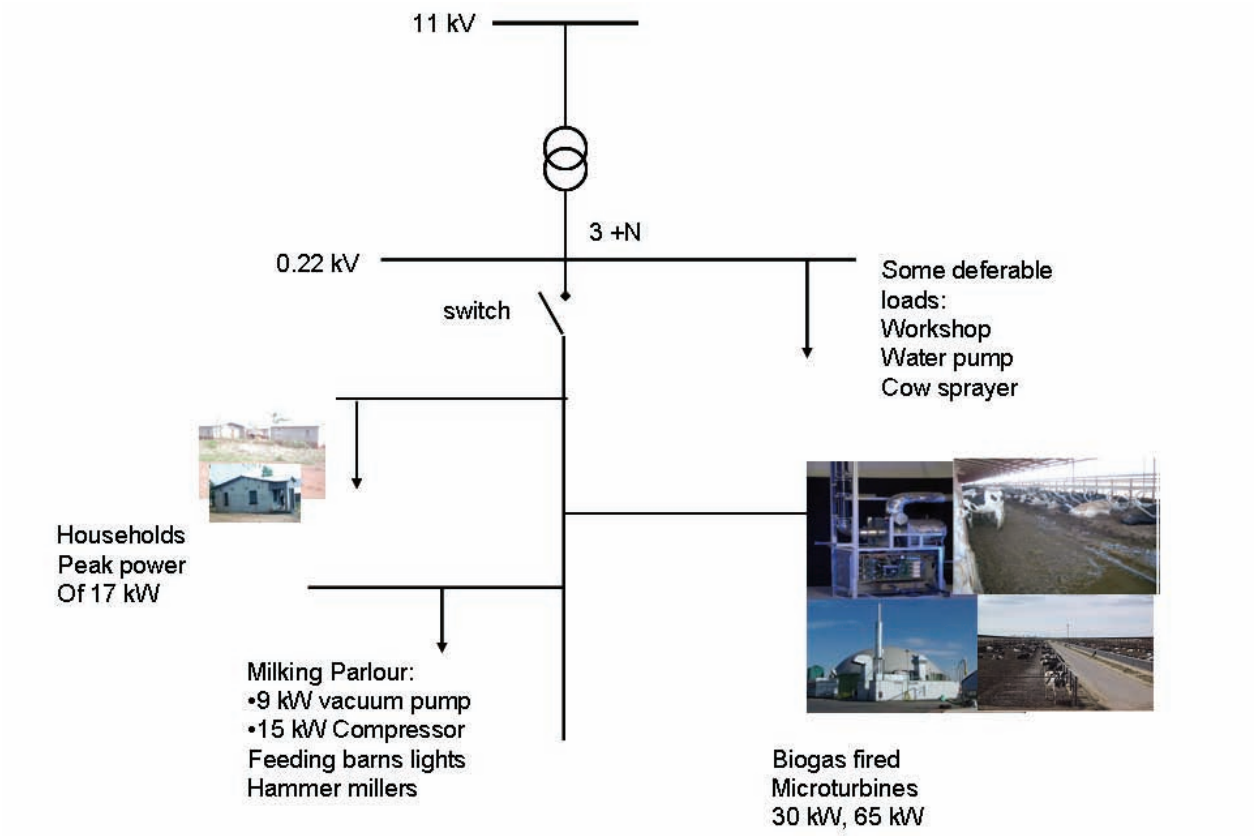

Figure 6-21: The proposed power system diagram

6.8 Dispatch strategy

Here since the aim is to generate as much energy as possible and sell as much as possible to the grid especially during peak hours, the microturbine generators are scheduled to operate during these hours and then optimised during the rest of the time. The power system is in the form of a Micro-Grid and is separated from the main grid by the grid switch. As per the requirement by the international norms regarding these grid connected systems, this Micro-Grid system has capstone microturbines capable of switching themselves to stand alone mode when ever the grid is lost and reconnect once this has been recovered. In this case the Capstone microturbines would be set to operate in Dual Mode, which is, normally operating in Grid Connect Mode allowing the system to switch to Stand Alone mode during a grid outage. Switching is done automatically by the Capstone Dual Mode Controller (DMC)

that differs from an automatic transfer switch (ATS) as explained earlier in this chapter. When grid is lost the dual mode controller senses this loss of grid and automatically disconnects the microturbine system and the protected loads from the grid and sends a reconfiguration signal to the microturbine to start in Stand Alone mode to supply only the protected loads. The change over time from Grid Connect to Stand Alone is about 2 – 4 seconds as explained earlier. The capstone microturbine have load following capability so thus even when the grid is down the whole system will function without problems at change of load in the Micro-Grid..

6.9 **Conclusions**

The study presented on this chapter clearly demonstrate both technical feasibility and economical viability of Micro-Grid power system at Rosenwald dairy farm using the farm wastes as a source of energy. This way a lot of benefits can be derived not only for the farmer but also the surrounding communities and finally the environment by efficiently managing manure. Thus the electricity is generated in a sustainable manner. As could be seen from the energy resource data presented in this thesis Rosenwald farm is one of many such farms in the Zimbabwe that can be self reliant in terms of energy and also the will of the owner of the farm to try the suggested energy options is undoubted as indicated by the support the farmer gave me for the workshop funding and the contributions to the discussions made. The concept of village power system may be the most feasible given the distribution of responsibilities and also sharing of the expenditures among the members of the village. It is therefore my recommendation that Zimbabwean government assist such communities to use these resources and easy the pressure on the national grid. The regulatory authorities may also need to put some incentives on renewable energy fed to the grid in order to promote their use.

While the results of this study clearly show the viability of these systems this can not be taken as very exact especial on the financial matters since a number of assumptions were made especially on prices of the components because the prices are so varied. Thus approximate costs were used based on some projects of similar nature carried out and published in different website and journals.

Chapter 7 **Summary and conclusions**

The widespread application of the concept of village power systems with a mix of energy sources - the hybrid power systems and Micro-Grids to the remote area electrification schemes will become technically and economically feasible only after the development of designs with improved performance that yield a definite solution. Both socio-economic and technical factors contribute to the success or failure of these systems. This work has studied a number of important factors that contribute to the better understanding of some technical and social aspects of power systems suitable for remote villages.

To show the potential of the country Zimbabwe in generating its electricity from renewable energy source, information was collected from different sources through field studies and interviews with different stakeholders. As could be seen from the energy resource data presented in this thesis, Zimbabwe is one of such many developing countries that can benefit a lot from the promotion of appropriate technologies.

The integration of several Micro-Grids in MV operation was also intensively studied by experiment in laboratory and the support in power sharing of these low voltage micro grids was demonstrated. Thus questions concerning the reactive power-exchange and the transient active power sharing of low voltage Micro-Grids via the MV-system were experimentally studied with the Medium-Voltage simulator installed at DeMoTec for inverters which are controlled with the ‘droop concepts’ (f-P and V-Q static control characteristics). For Micro-Grids, which are powered with this kind of inverters, it was experimentally proved, that parallel operation of these inverters is possible, even when the inverters are coupled via a MV network without any dedicated communication. Also demonstrated in this work is work is that reactive loads are shared by the inverters according to the (controllable) voltages at the inverters, while the line parameters are of secondary importance.

On the issue of voltage control in meshed low voltage grids, the work has demonstrated that this could be done by injecting some reactive power at the nearest generator nodes to the load in the low voltage meshed grid. The reactive power can be injected in a continuous way hence control the voltage in the same way unlike the discrete way in most voltage regulation devices in use presently.

Rosenwald farm, the case studied is one of many such farms in the country which can be self reliant in terms of energy and also the will of the owner of the farm to try the suggested energy options is

undoubted as indicated by the support to the workshop funding and the discussions made. The concept of village power system may be the most feasible given the distribution of responsibilities and also sharing of the expenditures among the members of the village. From the assessment done for the case study farm, it was shown that an electricity price of EUR 0.26/kWh is possible from the on – farm energy generation scheme. The results of the simulations showed that the biogas without solar could be most cost effective. In the studied case a great potential of self reliance in terms of energy for the community has been demonstrated.

For the technical viability of the intended system, the results from the measurements carried out on a microturbine operating on biogas and connected to the grid demonstrated the possible operating regimes. The microturbine are not fast enough at cold start up and thus are not suitable for UPS functions or back up for critical loads. However these are good for baseline load and are to be operated at high load.

On the issue of village power systems for the rural electrification in Zimbabwe, it would be of interest to have such a system of the size discussed in this thesis to be installed and used as a pilot project for reference. The author is already engaged in some financial sourcing for the project. It would be of interest to work with the policy make to see if there could be some form of incentives to the promotion of such onsite power generation using renewable energy resources available. So work can be used as a reference for these technologies since a vast number of technical aspects concerning their operations are here summarised.

List of Abbreviations

AC	Alternating Current
APU`s	Auxiliary Power Units
ATP-EMTP	Alternative Transient Program-Electromagnetic Transient Program
BUN	Biomass Users Network
DeMoTec	Design Centre For Modular Supply Technology
DERs	Distributed Energy Resources
DG	Distributed Generation
GMB	Grain Marketing Board
HVDC	High Voltage Direct Current
Hz	Hertz
IPP	Independent Power Production
IEA	International Energy Agency
IEEE	Institute of Electrical and Electronics Engineers
ITDG	Intermediate Development Technology Group
JIEEC	Jornadas Internacionales de Equipos Electricos / (International Electrical Equipment Conference)
LC	Load and Controllers
LCC	Life Cycle Cost
LISN	Line Impedance Simulation Network
LV	Lower Voltage
MGCC	Micro-Grids Central Controller
MIDR	Multifunctional Intelligent Digital Relay
MMO	Multi Master Operation
MS	Micro Sources

MV	Medium Voltage
NPV	Net Present Value
OLTCs	On-Load Tap Changers
Pf	Power frequency
PSCC	Power Systems Computation Conference
PV	Photovoltaic
PWM	Pulse Wave Modulation
PCC	Point of Common Coupling
PIP	Performance Improvement Program
RETs	Renewable Energy Technologies
RPM	Revolution Per Minute
SADAC	Southern Africa Development Community
SMO	Single Master Operation
SOC	State of Charge
SVCs	Static VAr Compensators
VAC	Volts Alternative Current
VSI	Voltage Source Invert
WECS	Wind Energy Conversion System
ZERC	Zimbabwe Electricity Regulatory Commission
ZESA	Zimbabwe Electricity Supply Authority
ZPC	Zimbabwe Power Company
ZDEC	Zimbabwe Electricity Distributed Company

List of figures

List of tables

References

[1] http://www.iea.org/statist/index.htm

[2] Story from BBC NEWS:http://news.bbc.co.uk/go/pr/fr/-/2/hi/africa/7199814.stm Published: 2008/01/21 10:22:28 GMT © BBC MMVII

[3] Ministry of energy and power development Zimbabwe http://www.energy.gov.zw/power/Electricity.htm

[4] http://www.nomaden.gmxhome.de/links/zimbabwe_map.gif

[5] http://www.lib.utexas.edu/maps/africa/south_rhodesia-mine_1979.jpg

[6] *Government Of Zimbabwe Draft Energy Policy*. December 2007

[7] Kayo, D., *Power Sector Reform In Zimbabwe, Proceedings Of A Regional Policy Seminar On Power Reforms In Africa.* African Energy Policy Research Network, Nairobi, 2001

[8] World Bank website: http://www.worldbank.org

[9] Dube, I., *Impact Of Energy Subsidies On Energy Consumption And Supply In Zimbabwe: Do The Urban Poor Really Benefit?* Energy Policy, 31, 2003

[10] http://research.stlouisfed.org/fred2/data/EXUSEU.txt

[11] Mangwengwende, S. E., *Increasing Electricity Access While Ensuring Financial Viability: A Perspective From The African Electricity Industry*. Global Network On Energy For Sustainable Development (Gnesd): Workshop on Electricity and Development, Nairobi, 13-14 July 2005

[12] Mapako, M. C., and Afrane-Okese, Y., *Experiences And Lessons In The Implementation Of Solar Home Systems From Zimbabwe.* Conference Proceedings, Conference on Domestic Use of Electrical Energy, Cape Technicon, Cape Town, April 2002

[13] http://www.uneprisoe.org/RETs/Zimbabwe Country Study/pdf

[14] King, D. E., *Electric Power Micro-Grids: Opportunities And Challenges For An Emerging Distributed Energy Architecture.* Ph.D. Thesis, Department of Engineering and Public Policy, Carnegie Mellon University, Pittsburgh, PA, 2006

[15] Technical Annex Of Contract No.: PL019864 Sixth Framework Programme Priority (More Micro-Grids) 10 June 2005

[16] Jahn, J., *Energiekonditionierung In Niederspannungsnetzen Unter Besonderer Berücksichtigung Der Integration Verteilter Energieerzeuger In Schwachen Netzausläufern.*

Kassel University Press GmbH 2007

[17] Schmid, J., *Visionen Für Die Globale Stromversorgung Mit Einem Hohen Anteil Erneuerbarer Energien.* 1. Internationales Symposium – Verteilte Stromerzeugung und intelligente Netze 2006, 18 - 19. Oktober 2006, www.arsenal.ac.at/downloads/dgtagung/VT/Schmid%20Juergen.pdf, 2006

[18] Pecas Lopes, J. A., Moreira, C. L., Resende, F. O., *Micro-Grids Black Start And Islanded Operation.* 15th PSCC, Liege, 22-26 August 2005

[19] Lopes, J. A., Peças, J., Tomé Saraiva, N., Hatziargyriou, N., *Management of Microgrids.* JIEE Conference 2003, Bilbao, 28-29 October 2003

[20] Akagi, H., Kanazawa, Y., Nabae, A., *Instantaneous Reactive Power Compensators Comprising Switching Devices Without Energy Storage Components.* IEEE Transactions on Industry Applications, vol. IA-20, No. 3, May/June 1984

[21] Engler, A., *Regelung Von Batteriestromrichtern In Modularen Und Erweiterbaren Inselnetzen.* Dissertation.de, Berlin, May 2002, ISBN 3-89825439-9

[22] Weedy, B. M., Cory, B. J., *Electric Power Systems*. John Wiley & Sons, fourth edition, 1998

[23] De Brabandere, K., Bolsens, B., Van den Keybus, J., Woyte, A., Driesen, J. and Belmans, R., *A Voltage And Frequency Droop Control Method For Parallel Inverters.* 35th Annual IEEE Power Electronics Specialists Conference Aachen, Germany, 2004

[24] Laaksonen, H., Saari, P., Komulaienen, R., *Voltage And Frequency Control Of Inverter Based Weak Low Voltage Network Micro-Grid*. IEEE, Future Power Systems, 2005 International Conference on Volume , Issue , 16-18 Nov. 2005

[25] Tuladhar, A., Jin, H., Unger, T., Mauch, K., *Control Of Parallel Inverters In Distributed Ac Power Systems With Consideration Of Line Impedance Effect.* IEEE Transactions on Industry Applications, Vol. 36 No 1, 2000

[26] Engler, A., *Applicability Of Droops In Low Voltage Grids.* International Journal of Distributed Energy Resources, Vol. 1, Number 1, January – March 2005

[27] Piagi, P., Lasseter, R. H., *Autonomous Control Of Micro-Grids.* IEEE, 2006

[28] SMA, *Sunny Island 4500 Bi-Directional Battery Inverter SI4500 For Standalone Applications Installation & Operation.* manual, version 3.1

[29] Lasseter, R., Akhil, A., Marnay, C., Stephens, J., Dagle, J., Guttromson, R., Sakis Meliopoulous, Yinger, A. R., and Eto, J., *White Papers On Integration Of Distributed Energy Resources.* The CERTS Micro-grid Concept, April 2002

[30] Lasseter, R., Piagi, P., *Final Project Report On Control And Design Of Micro-Grid*

Components. Power System Engineering Research Center (PESRC), January 2006

[31] Arulampalam, A., Barnes, M., Engler, A., Goodwin, A. and Jenkins, N., *Control Of Power Electronic Interfaces In Distributed Generation Micro-Grids.* International Journal of Electronics Volume 91, Issue 9 September 2004

[32] Lasseter, R. H., Piagi, P., *Providing Premium Power Through Distributed Resources.* Proceedings of the 33 rd Hawaii International Conference on System Sciences, vol. 4, Maui, Hawaii, 4-7 Jan 2000

[33] Chandorkar, M. C., Divan, D. M., Adapa Adapa, *Control Of Parallel Connected Inverters In Standalone AC Supply Systems.* IEEE Transactions in Industry Applications, vol. 29, No. 1, January/February 1993

[34] Pecas Lopes, J. A., Moreira, C. L., Madureira, A. G., *Defining Control Strategies For Micro-Grids Islanded Operation.* IEEE, Power Systems, IEEE Transactions on Volume 21, Issue 2, May 2006

[35] Braun, M., Degner, T., Vandenbergh, M., *Distributed Generation With High Penetration Of Renewable Energy Sources.* DISPWER Project Deliverable 6.3: Laboratory DG Grid report contract number ENK-CT 2001-00522, March 2006

[36] Osika, O., *Stability Of Micro-Grids With High Share Of Inverter-Dominated And Decentralised Sources*. PhD thesis. Department of Electrical Engineering. Kassel University press, Kassel, Germany, 2005

[37] Engler, A., Osika, O., Barnes, M., Jenkins, N., Rulampalam, A., *DB1: Local Micro Source Controller Strategies And Algorithms.* Large Scale Integration of Micro-Generation to Low Voltage Grids. Work Package B. February 2004

[38] *Product price and information bulletin.,* Zimbabwe Fertilizer Company, 1999

[39] Thirault, D., Besanger, Hadjsaid, N., Dumas, F., and Huard, G., *A Methodology To Design Electric Distribution Infrastructures For Rural Areas.* Power Systems and Communications Infrastructures for the future, Beijing, September 2002

[40] http://www.forester.net/de_0411_microturbines.html *Microturbine Power To The People*. An interview of Keith Field, Capstone's director of corporate communications by Gene Dallaire a frequent contributor to Distribution Energy magazine. DE - November/December 2004 edition

[41] http://www.epa.gov/CHP/documents/microturbines.pdf *Technology Characterization: Microturbines*., Prepared for: Environmental Protection Agency Climate Protection Partnership Division Washington, DC, 2002

[42] Zimbabwe Electricity Regulatory Commission Zimbabwe grid code 2005

[43] http://www.zedc.co.zw/tariffleaflet.pdf

44] http://www.afdb.org/pls/portal/docs/page/adb_admin_pg/documents/financialinformation/zimbabwe.pdf

45] Dennis A., Burke P. E., *Dairy Waste Anaerobic Digestion Handbook: Options For Recovering Beneficial Products From Manure*. Environmental Energy Company, June 2001, www.makingenergy.com

46] Chiang Chi-Yung Yen Kuo-Tsi Chang. *A Frequency-Dependent Droop Scheme for Parallel Control of Ups Inverters*. Journal of the Chinese Institute of Engineers, Vol. 24, No. 6, Hsuang-Chang, 2001

Appendices

Tongai farm

Tongai farm is about 10 km along the Bindura – Harare highway. This is by a prominent farmer Mr Matangira who is in mixed farming. Besides rearing about 314 cattle Mr Matangira has 212 goats/sheep and cultivates 300 hactres for maize which is used for sillage and sell to Grain Marketing Board, 800 hactres for wheat and 15 hactres for potatoes. They use electricity for maize driers, chicken run lighting and heating in cold winter nights, workshop welding, grinding mill for the community, farm house electricity, milling stock-feeds, harmer milling, cow spraying (7.5 kW for 12 hrs per week) and water pumping for irrigation. A short distance from the farm there is a big compound where the workers of the farm reside and a primary school nearby. The farm is grid-connected, however with the present power problems in the country the electricity supply has since been so unreliable. The electric power demand is of the range of also around 100 kW. Most consumption comes from the irrigation of the fields during the dry seasons. If the dung of the cattle and broilers is to be fed in digesters for biogas production, Tongai farm would be capable of producing more than 75 kW of electricity. This is more reliable since it is onsite produced and if the jatropha biodiesel project could be decentralised, to allow individual farmers to onsite produce it, then even standby diesel generators could be easily incorporated and that will even enhance the farm electricity production capacity. The table below shows the approximate electricity generation capacity for Tongai farm.

Type of stock	Quantity	Confined	Approximate genereation capacity
cattle	314	Semi-confined	64 kW_{elec}
chicken	5000	Confined	12 kW_{elec}

Table A 1: Approximate electricity generation capacity for Tongai farm

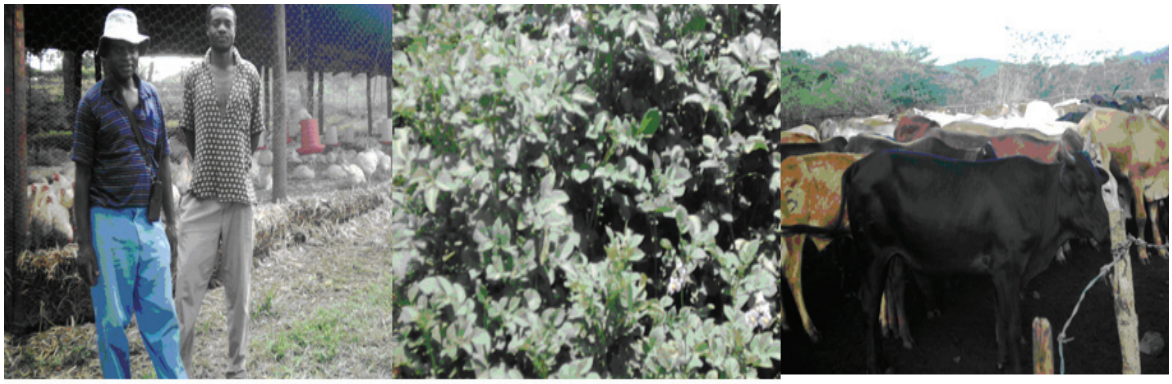

(a) (b) (c)

Figure A 1: (a) Broilers almost ready for slaughter at Tongai Farm, (b) Potato crop at flowering stage at Tongai Farm, (c) Cattle in barbed wire and wood log-fenced kraal

Barton farm

Barton farm is some ten to fifteen kilometres from Bindura town in the Shamva mine direction. This is owned by yet another prominent farmer cum-businessman Mr. Musanhi. Here mixed farming is practised. Mr Mukozho is managing the Farm, in particular on the crop side while his wife Mrs Mukozho is managing the life stock section. On the life stock, the farm concentrates more on beef and chicken. The manager Mr. Mukozho said plans to intensify cattle fattening and construction of an abbartour are at advanced stages. Presently there are 789 cattle with a plan to add 1500 very soon. The cattle fattening project is financed by The Renaissance Bank in Zimbabwe. In addition there are 8000 chicken and 97 goats/sheep. The farm grows wheat, tobacco, soya beans and maize. At full operational the farm requires labour force of around 400 people.

The workers are settled in 3 compounds with 25 to 30 households each. One compound has electricity although not properly connected and the other two are not electrified but the feeder lines pass very close to the compounds. The settlement pattern at Barton farm gives an ideal situation for a weakly meshed Micro-Grid. The three cattle kraals and the planned arbartour constitute generation sites and nearby each of these is a settlement compound, workshop or pump situated and these will constitute the load sites. From each of these generating sites more than one distributed generator (DG) in the form of microturbines, and/or biodiesel generator sets can be put in place. Thus, the

circuit below is a possible configuration for the power system for Barton farm. The situation at the other two farms is slightly different, the animals are kept at a single site. So this a single generation site with many load centres. However the idea of introducing the technology of biogas driven microturbines for generating electricity for the rural electrification is worthwhile.

The load demand is estimated to around 112,5 to 135 kW considering an average power of 1.5 kW for each household. The other farm activities like water pumping (four-125 hp which is about 373 kW) for irrigation, workshop with some lathe machines and welding machines, milling of cattle feeds and abartour services, would raise this power demand to about 400 to 600 kW as peak demand. If Barton farm could make use of its abundantly available biomass resource in the form of cow dung for biogas electricity generation, then it would cover almost 80 %[6] of its electricity peak demand and at non peak can feed excess to the national grid.

Type of stock	Quantity	Confined	Approximate generation capacity
cattle	2289	Semi-confined	463 kW_{elec}
chicken	8000	Confined	18 kW_{elec}

Table A 2: Approximate electricity generation capacity for Barton Farm

Barton farm has even greater potential given the plans of expanding and cattle fattening project. This would change from the semi-confinement to full confinement since the cattle would not be allowed to wonder about in the paddock as is the case presently. Thus to enhance the dung collection some modification in the cattle kraal require to be put in place. Presently the kraal is just a barbed wire or wood log fenced portion (see picture of Fig. 2-9) where the cattle are enclosed during the night for security. The floors are muddy and for easier dung collection the floors may need to be hard concrete sloping to canals in which the dung could be washed into.

[6] Rough calculations show that from the 2289 cattle and 8000 broilers the farm is capable of generating more than 480 kW of electricity.

Figure A 2: Muddy cattle kraal floor at Barton Farm

The dairy activity is very limited at this farm with only less than 30 milking cows. The milking is still done manually and thus practically no much electricity is consumed from this.

As could be seen from the few farms visited, the potential and will of the owners is undoubted. This gives a big challenge to researchers to do a lot of research work in the field of distributed generation with all possible micro/mini grid topologies. The popularities these systems are getting points towards the need for more flexible power supply systems even in the low voltage distribution sector. Aspects like voltage regulation in these low voltage distribution Micro-Grids with meshed topologies are of great interest and thus require some deep investigations.

Assumptions for the power system simulation in Homer

	11kv Supply E3.2.11, E4.2.11	33kv Supply E3.2.33, E4.2.33	Secondary Distribution E6.1
i. Fixed Monthly charge	ZWD 1,393,200.00 USD 1,032.00 EUR 858.00	ZWD 1,393,200.00 USD 1,032.00 EUR 858.00	ZWD 1,515,900.00 USD 1,122.89 EUR 933.56
ii. A monthly maximum demand charge per unit of demand	ZWD136,300.00 USD 100.96 EUR 83.94	ZWD100,000.00 USD 74.07 EUR 61.58	ZWD 64,000.00 USD 47.41 EUR 39.42
iii. An interruptable demand charge	n/a	n/a	ZWD 48,000.00 USD 35.56 EUR 29.56
iv. On peak Energy charge per kWh	ZWD 900.00 USD 0.67 EUR 0.55	ZWD 900.00 USD 0.67 EUR 0.55	ZWD 900.00 USD 0.67 EUR 0.55
v. Standard Energy charge per kWh	ZWD300.00 USD 0.22 EUR 0.18	ZWD300.00 USD 0.22 EUR 0.18	ZWD 300.00 USD 0.22 EUR 0.18
vi. Off-peak Energy charge per kWh	ZWD 200.00 USD 0.15 EUR 0.12	ZWD 200.00 USD 0.15 EUR 0.12	ZWD 200.00 USD 0.15 EUR 0.12

Table A 3: Mining, industrial, commercial & pumping works customers – Maximum Demand